University of Massachusetts Amherst
ScholarWorks@UMass Amherst

Doctoral Dissertations | Dissertations and Theses

July 2016

Enzyme Stabilization in Hierarchical Biocatalytic Food Packaging and Processing Materials

Dana Erin Wong
University of Massachusetts Amherst

Follow this and additional works at: https://scholarworks.umass.edu/dissertations_2

 Part of the Food Biotechnology Commons, Food Chemistry Commons, Food Processing Commons, Nanoscience and Nanotechnology Commons, Other Food Science Commons, and the Other Materials Science and Engineering Commons

Recommended Citation

Wong, Dana Erin, "Enzyme Stabilization in Hierarchical Biocatalytic Food Packaging and Processing Materials" (2016). *Doctoral Dissertations*. 672.
https://scholarworks.umass.edu/dissertations_2/672

This Open Access Dissertation is brought to you for free and open access by the Dissertations and Theses at ScholarWorks@UMass Amherst. It has been accepted for inclusion in Doctoral Dissertations by an authorized administrator of ScholarWorks@UMass Amherst. For more information, please contact scholarworks@library.umass.edu.

ENZYME STABILIZATION IN HIERARCHICAL BIOCATALYTIC FOOD PACKAGING AND PROCESSING MATERIALS

A Dissertation Presented

By

DANA ERIN WONG

Submitted to the Graduate School of the

University of Massachusetts Amherst in partial fulfillment

of the requirements for the degree of

DOCTOR OF PHILOSOPHY

May 2016

Food Science

© Copyright by Dana E. Wong 2016

All Rights Reserved

ENZYME STABILIZATION IN HIERARCHICAL BIOCATALYTIC FOOD PACKAGING AND PROCESSING MATERIALS

A Dissertation Presented

By

DANA ERIN WONG

Approved as to style and content by:

_____

Julie M. Goddard, Chair

_____

Scott C. Garman, Member

_____

D. Julian McClements, Member

_____

Sam R. Nugen, Member

_____

Eric A. Decker, Department Head
Food Science

DEDICATION

First, and most importantly, I would like to dedicate this work to my family – Mom, Dad, and Megan. They are the beacons from whom I derive my focus and drive. Where their encouragement, support, and valuable guidance has kept me steady mentally and emotionally allowing me to take creative risks. Thank you for always believing in me! For all of my family, my grandparents especially, whose sacrifices have meant the betterment of my life, and have emphasized the importance of education in my future.

This work would not have been possible without the positive influence and support of my friends. The old and the new, all life-long, have reminded me to enjoy the ride. To Yen Vuong, Victor Chiu, Edgar Gee, Andrew Yang, Kimberly Fung, Iliana Lopez, Ashley Soldavini, and Carrie Lauer, thank you for reminding me that a great laugh, some sunshine, and an adventure are just a phone call away!

Gianna Spadaro, Lex Minniti, Robin Sarkin, Tori Sbrogna, Hayley Botman, and Kyle Gariepy – thanks for making Amherst and the entire East Coast my home.

To all of those who have had a hand in my educational success; teachers of both school and life, and instructors of sports and art at Project Open Hand, Wah Mei School, Thomas Jefferson Elementary School, Herbert Hoover Middle School, Lowell High School, and the University of California, Davis that have inspired my thirst for information and shaped a solid base for all of my academic endeavors. The most gratitude and admiration goes to Dr. Diane M. Barrett, a true mentor, who has instilled me with scientific research integrity and pragmatism, and has always shown everyone genuine respect.

ACKNOWLEDGMENTS

I would like to thank my advisor, Dr. Julie M. Goddard, where mutual understanding, has paved a way for us to navigate this personal and professional journey together. My committee members, Dr. Sam R. Nugen, Dr. D. Julian McClements, and Dr. Scott C. Garman have been a source of endless knowledge, even in snowstorms.

Former lab mates showed me the ropes and current lab peers made graduate school a blast – Jeffrey Barish, Fang Tian, Kurt Mahoney, Tiphaine Mérian, Kang Huang, Luis Bastarrachea, Anna Denis-Rohr, Maxine Roman, Stephanie Andler, Jason Lin, Paul Castrale, Anne Hung – Fei He, Samuel Alcaine, Angelyca Jackson, Mindy Dai, Charmaine Koo, Juhong Chen, Ziyuan Wang, Troy Hinkley, Danhui Wang – Jay Gilbert, Christina Lincoln! Thanks to Joey Talbert who had answers to all the great questions!

A shout-out to those I will think of always during my time at UMass: Andrea Lo, Theo Ralla, Kyle Landry, David Johnson, Kristin Wong, and Vivian Chong. Cindy Kane, Fran Kostek, Deby Lee, Jean Alamed, Stacy Apostolou, and “Pilot Plant” Dave and Dan have all made my life at Chenoweth easier. I would like to acknowledge all of the individuals and groups who have assisted in the work described herein, including Kris Senecal of the NSRDEC and Louis Raboin of the Electron Microscopy Center.

This work would not have been possible without funding from the following sources: USDA AFRI National Institute of Food and Agriculture Pre-doctoral Fellowship Grant No. 2015-67011-22820, Dairy Management Inc., and Center for Hierarchical Manufacturing at UMass Amherst. The University of Massachusetts has afforded me great opportunities – not only to expand my research capabilities, but also to grow personally by collaborating within the best Department of Food Science

ABSTRACT

ENZYME STABILIZATION IN HIERARCHICAL BIOCATALYTIC FOOD PACKAGING AND PROCESSING MATERIALS

MAY 2016

DANA ERIN WONG, B.S., UNIVERSITY OF CALIFORNIA DAVIS

Ph.D., UNIVERSITY OF MASSACHUSETTS AMHERST

Directed by Julie M. Goddard, Ph.D.

The partnership of biocatalysts and solid support materials provides many opportunities for bioactive packaging and bioprocessing aids beneficial to the agricultural and food industries. Biocatalysis, or reactions modulated by enzymes, allows bioactive materials to assist in bringing a substrate to product. Enzymes are proteins which catalyze reactions by lowering the activation energy required to drive the production of a desired product. Enzymes are commonly utilized in food processing as catalysts with specificity in order to enhance product quality through the production of beneficial food components, and to break down undesirable components that may be harmful or may decrease product quality. Enzymes are proteins with specificity for a substrate, that under the ideal conditions will speed bioprocessing by lowering the activation energy required to create a product.

As the working conditions for biocatalytic materials can be very specific, enzymes are often immobilized and incorporated onto and into solid supports in order extend their thermostability and pH optima as well. Integrating biocatalysts into food packaging also allows for extended use and clean-labeling when non-migratory, which may enable “in-package processing” where food constituents undergo changes to improve quality or shelf-life while in transport and storage. Immobilized enzymes are

more readily recovered, regenerated, and reused – decreasing overall energy, material, and environment costs. Introducing biocatalytic materials to solid polymeric supports requires varied techniques in order to maintain activity. However, disadvantages to immobilizing techniques lead to activity loss and are attributed to denaturation, incorrect orientation, low protein loading, and material incompatibility. Denaturation and incorrect orientation are characteristic of proteins on hydrophobic surfaces. Covalent immobilization allows for food products to interact with non-migratory biocatalytic coatings without incorporating them into the food matrix. Cross-linker compatibility is an essential part of covalent attachment too. Cross-linkers utilize various functional groups to attach active ingredients to solid surfaces and stabilize polymers.

This work progresses through the advantages of covalent and non-covalent enzyme immobilization. First, lactase was immobilized for a bioactive packaging application by Layer by Layer conjugation to low-density polyethylene. Increasing layer deposition increased total protein loading, but did not increase activity per layer. Next, lactase was blended and embedded into polyethylene oxide for an electrospun nanofiber storage and dosing system maintaining up to 92% of free enzyme activity. Embedding and blending is often paired with cross-linking techniques to aid the support material maintain its physical properties. Immobilization of chymotrypsin onto nylon 6,6 demonstrated the benefit of nanoscale materials on retained activity, where the bulk material is water-insoluble. And finally, chymotrypsin was encapsulated by emulsion electrospinning into polycaprolactone with poly(vinyl alcohol) to increase biocompatibility with the solid support. These studies further demonstrate the robustness

of enzymes incorporated into packaging materials is dependent on the processing technique and solid support and tether material.

Food and agriculture have recently turned to nanomaterials in processing and packaging due to the increased surface area to volume ratio, ease of manufacturing scale-up, and maintained or even improved mechanical stability of nanomaterials. Increased surface area provides for more functional surfaces. A combination of the nanoscale and curvature provided by nanofibers allows enzymes to behave like their free enzyme counterparts. Often nanomaterials may be made uniformly, which also benefits increasing processing efficiency for all industries.

The immobilization method must reduce diffusion limitations as well as aid activity retention for increased thermostability and pH stability by taking into account environmental interactions. Herein outlines methods for the incorporation of biocatalytic materials in active packaging by combining the benefits of enzyme immobilization at the nanoscale with complementary material interactions.

TABLE OF CONTENTS

Page

LIST OF TABLES

Page

LIST OF FIGURES

Page

LIST OF EQUATIONS

Page

LIST OF ABBREVIATIONS

ALU	acid lactase units
ANOVA	Analysis of Variance
ASTM	American Society for Testing and Materials
ATR-FTIR	Attenuated Total Reflectance Fourier Transform Infrared Spectroscopy
BCA	bicinchoninic acid
BSA	Bovine Serum Albumin
CLEA	Crosslinked Enzyme Aggregates
CLSM	Confocal Laser Scanning Microscopy
CT	chymotrypsin
Dex	dextran
DMF	dimethylformamide
DMSO	dimethyl sulfoxide
EDC	1-Ethyl-3-(3-dimethylaminopropyl) carbodiimide
F127	Pluronic F-127
FIT-C	fluorescein isothiocyanate isomer I
Gal	galactose
GL	glutaraldehyde
Gluc	glucose
Lac	lactase/lactose
LbL	Layer by Layer
LDPE	low-density polyethylene
NF	nanofiber

NSPN	N-succinyl-ala-ala-pro-phe *p*-nitroanilide
NHS	N-hydroxysulfosuccinimide
ONPG	*o*-nitrophenol-β-D-galactopyranoside
PCL	polycaprolactone
PEI	polyethylenimine
PS	polystyrene
PVA	poly(vinyl alcohol)
PVP	polyvinylpyrrolidone
SEM	Scanning Electron Microscopy
TNBS	picrylsulfonic acid solution

CHAPTER 1

INTRODUCTION

The partnership of biocatalysts and solid support materials provides many opportunities for bioactive packaging and bioprocessing aids beneficial to the agricultural and food industries. Biocatalysis, or reactions modulated by enzymes, allows biocatalysts to assist in bringing a substrate to product. Enzymes are proteins which catalyze reactions by lowering the activation energy required to drive the completion of a reaction and production of a desired product. Enzymes are commonly utilized in food processing as catalysts with specificity in order to enhance product quality through the production of beneficial food components, and to break down undesirable components that may be harmful or may decrease product quality *(1)*. Enzymes are proteins with specificity for a substrate, that under the ideal conditions will speed bioprocessing by lowering the activation energy required to create a product. Enzyme mechanisms and structures have been well studied, and continue to attract attention due to their robustness and usability. Enzyme production has been scaled-up successfully such that they are an economical and widely available in necessary purities. Enzymes have been preferred in food processing due to their specificity, cost, and speed *(2)*. Enzymes are employed in the medical, diagnostic, pharmaceutical, agriculture, and food industries where function is reliant on the folding capability of the protein.

For example, glucose isomerase has been utilized to vary syrup sweeteners by modulating the conversion of glucose to fructose and fructose to glucose. Lactase reduces consumable lactose in lactose-reduced dairy products by hydrolyzing lactose into digestible glucose and galactose *(3-5)*. Proteases and pectinases often tenderize meats and

clarify beverages *(6-8)*. Other enzymes in use debitter beverages and scavenge oxygen to improve food quality *(9, 10)*. Enzymes traditionally have been added batch-wise or applied directly to foods, processed, and then sent out to consumers.

Appropriately, food processing and dosing enzymes into bioprocessing units has moved to reducing material waste. Incorporating enzymes into/onto food contact materials for dosing has expanded the capability of producing bioactive packaging and recoverable enzymes *(11-13)*. As the working conditions for biocatalytic materials can be very specific, enzymes are often immobilized and incorporated onto and into solid supports in order extend their thermostability and pH optima as well. Integrating biocatalysts into food packaging also allows for extended use and clean-labeling when non-migratory which may enable "in-package processing" where food constituents undergo changes to improve quality or shelf-life while in transport and storage. *(14)*. Immobilized enzymes are more readily recovered, regenerated, and reused – decreasing overall energy, material, and environment costs. Introducing biocatalytic materials to solid polymeric supports requires varied techniques in order to maintain activity. Immobilized enzymes can be incorporated into processing plants, as well as facilitate in-package processing where food constituents undergo changes to improve quality or shelf-life while in transport and storage. However, disadvantages to immobilizing techniques lead to activity loss and are attributed to denaturation, incorrect orientation, and low protein loading. Denaturation and incorrect orientation are characteristic of proteins on hydrophobic surfaces, as well as interaction with high temperatures and extreme alkaline and acidic environments.

Immobilized enzyme systems are categorized into covalent and non-covalent binding. Non-covalent attachment incorporates charge interactions and physical adsorption to a surface whereas covalent attachment requires a reactive groups from the enzyme and solid support create a bond *(15, 16)*. Enzyme immobilization has been achieved with a combination of techniques and coating methods. Enzymes have been cross-linked in a carrier free immobilized system, embedded, and attached to solid supports *(17)*.

Non-covalent attachment methods do not require extensive material modification and are less time intensive where enzymes are immobilized in a few steps. Non-covalent attachments that are adsorption driven originate in protein and surface interaction (van der Waals, hydrophobic, electrostatic). Non-covalent immobilization helps to modify surfaces, but often exhibit leaching into the food matrix. Ghasemi et al. compared adsorption of trypsin to covalent immobilization, finding more activity is maintained when using glutaraldehyde tethers *(18)*. The activity loss was attributed to protein loss.

Non-covalent attachments can be charge driven, where positively charged proteins are attracted to negatively functionalized surfaces. The overall charge of an enzyme is determined by the amino acid residues available at the surface while the protein's tertiary and quaternary fold is determined by hydrophilic and hydrophobic interactions *(19-22)*. Different amino acid residues have different functional groups by which they are identified, and therefore have variously associated charges. The overall charge may be influenced by the environment. The solid support's charge is similarly determined by functional groups available at the surface. Functionalized materials may be positively and negatively charged. A common interfacial charge relationship is a

consequence of amine positive charge, and carboxylate negative charge. These natural charge differences determined by the characteristics of the protein and surface, and by the environment allow for opposites to attract proteins to attach to solid supports.

Embedding employs protein incorporation into polymers that are shaped subsequently. Embedding and blending requires the bulk material to be compatible with the bioactive ingredient. This can be achieved by surface functionalization, changing material composition, and bioactive modification. Embedding and blending may simplify commercialization and scale-up as one-pot preparation methods become more available; however, the bioactive material becomes integrated into the food packaging and is susceptible to leaching. The bioactive concentration decreases over time, and therefore the reactivity of the packaging will decrease as well *(23)*. The review by Kong and Hu outlines adsorption techniques on polymers and papers *(24)*. Kong and Hu note that blending techniques may reduce the preparation needed to produce packaging materials. One of the most explored examples of immobilized enzyme systems involves the removal of oxygen for increased food shelf stability. Efforts towards incorporation of an oxygen scavenging package composed of glucose oxidase as a laminate low-density polyethylene layer within paper board have included details for scaled-up production. Various compositions of LDPE, glucose oxidase, and catalase were produced in Tetra Pak's pilot plant, and showed up to 97% activity could initially be achieved even after exposure to 325°C during production. The production parameters were key to maintaining the package's oxygen scavenging capability *(25)*. Johansson et al. worked to improve embedding the glucose oxidase and catalase oxygen scavenging pair by varying combinations of LDPE, polypropylene, and polylactic acid *(10, 26)*. Variations of these

embedding methods for oxygen scavenging by laccase and oxalate oxidase have shown similar results. Work by Talbert *et al.* demonstrates that enzymes may be modified by hydrophobic ion pairing to be soluble and retain activity in solvents used in ink formulations, enabling the preparation of biocatalytic active packaging coatings using existing printing technology *(27)*.

A majority of the work on biocatalytic coatings for food packaging employs covalent immobilization. There has been growth in support for "clean label" foods, where bioactive packaging and bioactive materials have an opportunity to add value to products through materials only regulated by non-migratory contact. Covalent immobilization allows for food products to interact with non-migratory biocatalytic coatings without incorporating them into the food matrix, and therefore do not have to be labeled. Covalent attachments utilize functional end groups from the polymer and the enzyme to create strong attachments. For example, Soares and Hotchkiss developed non-migratory packaging films to de-bitter fruit juices by covalently immobilized fungal naringinase *(9, 28)*. Soares and Hotchkiss K_M were able to maintain naringinase activity after 15 days storage and establish decreased values when compared to free enzyme. Nunes et al. using boric acid for de-bittering *(29)*. Often covalent binding is achieved by amine functionalizing surfaces and introducing aldehyde tethers in order to bind enzymes, here to immobilize β-galactosidase to reduce milk lactose in package *(30)*. UV functionalization of various polymer surfaces, such as low-density polyethylene which may be a part of milk container linings, introduce carboxyl end groups for covalent immobilization *(31)*. Often covalent immobilization methods employ tethers unsuitable for food contact and consumption, including glutaraldehyde. However, moves to utilize

biopolymers and nanocomposites to bind enzymes may make covalent immobilization more suitable for food use. Active packaging commonly attempts to maintain the mechanical properties of the bulk material, which makes non-covalent immobilization an ideal attachment method.

The Layer-by-Layer (LbL) approach allows for increased conjugation of bioactive biocatalysts. This method utilizes differences in charge and available reactive side chain groups for non-covalent and covalent binding from a combination of polymers and cross-linkers. Often there is an increase in total protein content with each additional functional layer. For example lactase bioactive films for milk processing increased total protein content with every additional layer composed of polyethylenamine, glutaraldehyde, and lactase *(31, 32)*. However, no significant change in activity is a common observation as the contact frequency between substrate and enzyme may not be constant or decrease when materials are layered. Although the LbL technique has been shown to increase protein loading, diffusion of substrate to enzyme can become difficult. Substrate must be able to navigate through formed layers to increase the contact required to increase catalytic efficiency. Non-covalent immobilization often requires fewer steps and no functional tethers or cross-linkers when compared to covalent immobilization. Often biocatalytic materials are attached to solid supports by adsorption and electrostatic interaction.

The cross-linker is an essential part of covalent attachment. Cross-linkers utilize various functional groups to attach active ingredients to solid surfaces and stabilize polymers. Zero-length, heterofiunctional, and homobifuntional are the three primary types of cross-linkers used in this capacity *(33)*. Zero-length cross-linkers, like

EDC/NHS, are often not consumed during the crosslinking process, and therefore provide a linkage that does not increase distance between the two bonded substances. Homobifuntional cross-linkers, like glutaraldehyde, have the same reactive group facilitate attachment to an active ingredient and solid support *(31, 34, 35)*. Heterobifunctional cross-linkers bring substances together by using different functional groups on each of its ends *(34, 36, 37)*.

There has been an increase in nanomaterials research in the medical, diagnostic, and electronic industries. All of these areas rely on similar surface modification in order to control the loading or release properties of the nanomaterials. Food and agriculture have recently turned to nanomaterials in processing and packaging due to the increased surface area to volume ratio, ease of manufacturing scale-up, and maintained or even improved mechanical stability of nanomaterials. Increased surface area provides for more functional surfaces. Often nanomaterials may be made uniformly, which also benefits increasing processing efficiency for all industries. The National Nanotechnology Initiative supported by the United States Federal Government is a representation of the effort and commitment to growing nanomaterials in various fields.

Electrospinning is a method by which enzymes and bioactive materials can be incorporated into a nanoscale bulk material, decreasing the preparation needed to fabricate packaging materials. Lactase blended into polyethylene oxide nanofibers was found to maintain up to 93% of free enzyme activity *(38)*. The medical, pharmaceutical, and textile industries have begun processes to scale-up production of modified non-woven electrospun mats. Incorporation of glucose oxidase in polymer solutions was favored to reduce preparation of the biocatalytic material *(39)*. Drug delivery with

controlled release has excited new interest in various fiber morphologies. Similar functionalization techniques have been applied to micro and nanoparticles and hydrogels. Embedding and blending is often paired with cross-linking techniques to aid the support material in maintaining its physical properties. These studies further demonstrate the robustness of enzymes incorporated into packaging materials is dependent on the processing technique.

Biocatalytic packaging can be achieved by various coating means. Previous applications of immobilized enzymes for food packaging have favored embedding and covalent attachment. The immobilization method must reduce diffusion limitations as well as aid activity retention for increased thermostability and pH stability. The overall stability of the bound enzyme determines the success of the coating method. Herein outlines methods for the incorporation of biocatalytic materials in active packaging, and works which have the potential for application in food packaging.

CHAPTER 2

LAYER BY LAYER ASSEMBLY OF A BIOCATALYTIC PACKAGING FILM: LACTASE COVALENTLY BOUND TO LOW-DENSITY POLYETHYLENE *(32)*

2.1 Abstract

Active packaging is utilized to overcome limitations of traditional processing to enhance the health, safety, economics, and shelf-life of foods. Active packaging employs active components to interact with food constituents to give a desired effect. Herein we describe the development of an active package in which lactase is covalently attached to low-density polyethylene (LDPE) for in-package production of lactose-free dairy products. The specific goal of this work is to increase the total protein content loading onto LDPE using Layer by Layer (LbL) deposition, alternating polyethylenimine, glutaraldehyde (GL), and lactase, to enhance the overall activity of covalently attached lactase. The films were successfully oxidized via ultraviolet light, functionalized with polyethylenimine and glutaraldehyde, and layered with immobilized purified lactase. The total protein content increased with each additional layer of conjugated lactase, the 5 layer sample reaching up to 1.3 μg/cm^2. However, the increase in total protein did not lend to an increase in overall lactase activity. Calculated apparent K_m indicated the affinity of immobilized lactase to substrate remains unchanged when compared to free lactase. Calculated apparent turnover numbers (k_{cat}) showed with each layer of attached lactase, a decrease in substrate turnover was experienced when compared to free lactase; with a decrease from 128.43 sec^{-1} to 4.76 sec^{-1} for a 5 layer conjugation. Our results

This chapter has been published – Wong, D.E.; Talbert, J.N.; Goddard, J.M. Layer by layer assembly of a biocatalytic packaging film: lactase covalently bound to low-density polyethylene. *J. Food Sci.* **2013**, *78*, E853-E860.

indicate that while LbL attachment of lactase to LDPE successfully increases total protein mass of the bulk material, the adverse impact in enzyme efficiency may limit the application of LbL immobilization chemistry for bioactive packaging use.

Practical Application: Immobilization of the enzyme lactase on polyethylene enables development of an active packaging film to produce lactose-free milk products. Using layer by layer immobilization chemistry increases the amount of enzyme that can be immobilized per unit area of packaging film.

2.2 Introduction

Many adults suffer from lactose intolerance, the inability to digest lactose due to a lack of natural production of the enzyme, lactase, in the small intestine *(40-42)*. Lactose intolerance may result in gut symptoms of variable severity including abdominal cramps, diarrhea, and gas *(43, 44)*. Lactose intolerance has been connected to other systemic symptoms including eczema and asthma *(45)*. Modern methods have been designed to remove lactose by use of free enzyme as β-galactosidase isolated from the *Aspergillus* or *Kluyveromyces* yeast and mold. Currently lactose-free and reduced-lactose dairy products are processed in batch operations, where free lactase is added to pasteurized fluid milk to hydrolyze lactose, followed by a secondary heat treatment to deactivate the enzyme and inactivate any microorganisms that may have been present in the enzyme preparation. The modern batch method is effective, but not ideal to consumers who have an aversion to the final sensory characteristics of a twice heat treated product, which tends to be sweeter and more viscous than a normal milk product *(46-48)*. Also, batch production requires inefficiently high concentrations of lactase to be added to achieve the desired activity as well as additional processing equipment and time *(49)*.

Immobilized enzymes are enzymes which are entrapped within or attached onto bulk materials. Immobilized enzyme reactors allow for more efficient use of the biocatalyst due to recovery and reuse of the enzyme as well as continuous processing *(1, 50)*. Lactase has been immobilized on various bulk materials including polymer beads, cotton, aluminum, and activated glass for use in processing and biosensors *(16, 51-53)*. However, immobilized lactase processes are limited by equipment cost, implementation of non-traditional unit operations, loss of enzyme activity and stability, and cleaning which can lead to enzyme inactivation.

Active packaging, packaging that provides some design function beyond the inherent passive properties of the material, can be utilized to overcome limitations of traditional processing and packaging to enhance the health, safety, economics, and shelf-life of foods. Active packaging allows for active components to interact with food product constituents, and has been used to scavenge excess oxygen and ethylene, to chelate trace metal catalysts of oxidation, to reduce moisture, and to create controlled release of antimicrobial components *(11, 54)*. Common methods of incorporating active agents into active packaging include entrapment into bulk material and attachment onto the food contact surface by coating or covalent immobilization *(39, 55)*. Entrapment is a straightforward technique for loading active agents into the material, and entrapped enzymes have been found to withstand high physical stress. However, entrapment can result in reduced availability of substrates due to diffusional constraints, and entrapped bioactives (e.g. enzymes) often suffer activity losses following packaging conversion processes. *(56-58)*. Surface attachment requires that the material have inherent surface functionality or undergo surface modification to provide an activated interface for ionic,

hydrophobic, affinity, or covalent attachment of the active component. Surface attachment allows for direct food contact and may offer a regulatory benefit if covalent attachments are used.

Using enzymes in active packaging systems allows for in-package processing of the product during transport, which may reduce the amount of enzyme needed. Surface immobilized enzymes have been researched towards development of active packaging materials *(59)*. Lactase has previously been attached to packaging surfaces as a means to reduce lactose in packaged dairy products *(30, 31)*. One of the limitations of surface attachment is the lowered surface area available for conjugation of active agents, thus limiting overall activity. Layer by Layer (LbL) deposition is a surface modification method used in which an active component is layered between successive, molecularly thin layers of polymers which are often charged, creating a multilayered film *(60-62)*. Additional layers provide for greater surface area to attach increasing amounts of bioactive components. Previous works on homogeneous and heterogeneous bioactive component systems have shown increases in overall activity by using a layer by layer deposition process for immobilization of enzymes and other bioactives *(62-64)*. These layers can be produced by spraying or dip-coating, and the multilayers can be stabilized by electrostatic interactions or covalent bonds *(64, 65)*. Patterned LbL surface modification techniques enable an increased protein loading over a fixed surface area, and a range of polymers with varying reactive end groups are available for LbL deposition. There are a number of reports of enzyme immobilization via LbL deposition including glucose oxidase for blood glucose sensors, catalase for hydrogen peroxide

removal, and for multiple enzyme systems *(66)*. LbL deposition has also been used for development of antibacterial and oxygen scavengers and medical grade films *(63, 67)*.

While LbL deposition has been explored for immobilization of enzymes in biomedical and sensing applications, it has not been explored towards the development of active packaging materials. The goal of this work was to utilize LbL deposition of polyethylenimine, glutaraldehyde (GL), and lactase to increase the amount, and therefore activity, of enzyme (lactase) that can be immobilized onto low-density polyethylene (LDPE) films compared to prior work *(30, 31)*. The impact of LbL deposition on total protein content, overall immobilized enzyme activity, and enzyme kinetics were also explored.

2.3 Experimental Materials and Methods

2.3.1 Materials

Additive-free low-density polyethylene (LDPE) pellets were purchased from Scientific Polymer Products (Ontario, NY). Anhydrous potassium phosphate dibasic, anhydrous potassium phosphate monobasic, anhydrous sodium bicarbonate, anhydrous sodium carbonate, anhydrous sodium acetate trihydrate, glacial acetic acid, hydrochloric acid, sodium hydroxide, acetone (99.8%), isopropanol (99.9%), and PTFE filter units (0.2 μm) were purchased from Fisher Scientific (Fairlawn, NJ). 1-Ethyl-3-(3-dimethylaminopropyl) carbodiimide hydrochloride (EDC - HCl) was purchased from Proteo-Chem (Denver, CO). N-hydroxysuccinimide (NHS), Orange II (acid orange 7 [AO7]), and ortho-nitrophenol (99%) were purchased from Acros Organics (Geel, Antwerp, Belgium). Glutaraldehyde (25%) was purchased from Alfa Aesar (Ward Hill, MA). *o*-nitrophenol-β-D-galactopyranoside (ONPG), bicinchoninic acid (BCA) assay

reagents, and bovine serum albumin (BSA) were purchased from Thermo Scientific (Rockford, IL). Branched polyethylenimine (PEI, M_w 25 kDa) was purchased from Sigma-Aldrich (St. Louis, MO). ‘‘Amicon Ultra’’ (50k MWCO) centrifugal filter devices were purchased from Millipore Ireland (Carrigtwohill, Co. Cork, Ireland). Syringe filters were purchased from Whatman (Florham Park, NJ). Dried lactase preparation from *Aspergillus oryzae* was donated by Enzyme Development Corporation (New York, NY).

2.3.2.1 Lactase Purification

The lactase was prepared in a 0.1 M, pH 5.0 acetate buffer and filtered through a 0.2 μm PTFE syringe filter before centrifugal filtration (50k MWCO) at 6500 rpm for 30 min. The filter pore size allowed lactase to be trapped in the membrane and then later flushed out with equal volumes of 0.1 M, pH 5.0 acetate buffer. The purified free enzyme lactase solution was stored at 4°C.

2.3.2.2 Preparation and Functionalization of PE Films

2.3.2.2.1 Production of PE Films

LDPE pellets were cleaned in isopropanol, acetone, and deionized water. Pellets were sonicated in two repetitions of each solvent at 10min intervals. Cleaned LDPE pellets were dried overnight, and were pressed into sheets 294 +/- 17 μm thick with a Carver Laboratory Press (Fred S. Carver Inc., Summit, NJ). LDPE sheets were cut into 2×1 cm rectangular films and cleaned as described above for LDPE pellets. Clean films were dried overnight on a bed of cleaned LDPE pellets and then stored dry in covered petri dishes at room temperature.

2.3.2.2.2 Functionalization of Films

Clean LDPE films were arranged as a monolayer in uncovered glass petri dishes and were exposed to 28 mW/cm^2 ultraviolet (UV) light at 254 nm. Each film was placed 2 cm from the light source and was treated for 15 minutes per side to create a total of 4 cm^2 activated surface area *(68)*. Oxidized PE films (PE-Ox) were sonicated for 5 minutes in DI water to remove water soluble oligomers and stored in DI water at 4°C.

2.3.2.2.3 Layer by Layer Deposition

A sequential LbL deposition technique was employed to immobilize the enzyme lactase onto UV functionalized polyethylene films. Each layer was comprised of polyethylenimine (PEI), glutaraldehyde (GL), and lactase (LAC) (**Fig. 2.1**). Ultraviolet light functionalized polyethylene films are denoted PE-Ox. PE-Ox films to which PEI has been covalently conjugated are denoted PE-PEI. PE-PEI films to which GL has been covalently conjugated are denoted PE-GL. PE-GL films to which lactase has been covalently conjugated are denoted PE-LAC. Covalent conjugation of a single layer (up to five layers were evaluated herein) is described below.

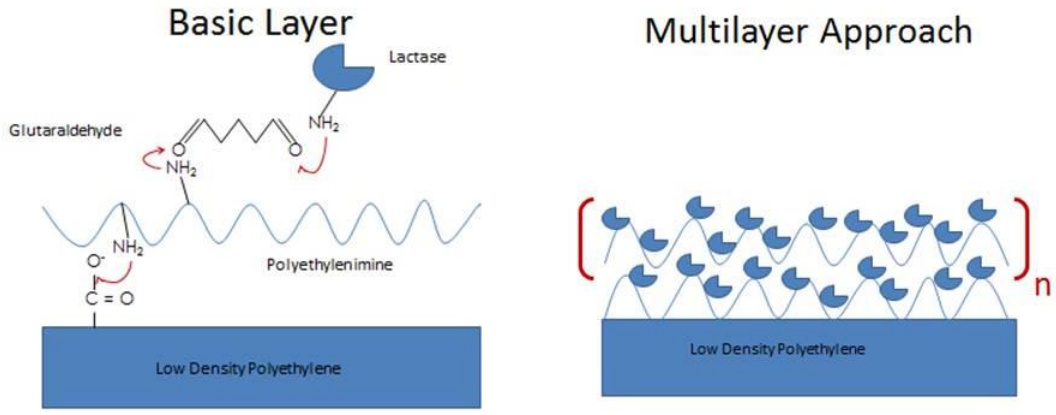

Figure 2.1. Schematic of layer by layer enzyme immobilization chemistry. Left, components of each individual multilayer. Right, illustration of multilayer strategy.

Attachment of polyethylenimine (PEI) to PE-Ox by amide bonds allows a surface composed of primary amines to later be attached to aldehyde tethers *(69)*. By using a previously established procedure for amide bond formation and lactase immobilization, PE-Ox films were stirred in a conjugation buffer composed of 0.1 M sodium carbonate at pH 9.6, 30 mg/mL PEI, 5×10^{-2} M EDC-HCl, and 5×10^{-3} M NHS for 2 hrs at room temperature *(31, 70, 71)*. The PE-PEI films were rinsed three times in DI water and kept in 0.1 M, pH 7.8 potassium phosphate buffer at 4°C until GL conjugation.

PE-PEI films were further modified to possess aldehyde surface functionality by conjugation of glutaraldehyde (GL) using an altered one-step method as described by Hermanson *(33)*. PE-PEI films were stirred for 1 hour in a conjugation buffer of 0.1 M, pH 7.8 potassium phosphate buffer containing 10 times molar excess GL (25%) to primary amine sites. The PE-GL films were rinsed three times in 0.1 M, pH 7.8 potassium phosphate buffer and stored in 0.1 M, pH 7.8 potassium phosphate buffer at 4°C until lactase conjugation.

Washed PE-GL films were placed in a conjugation buffer of 0.1 M, pH 7.8 phosphate buffer with lactase from the purified free enzyme solution to a final concentration of 2×10^{-2} mg/mL. The films were stirred for 30 minutes at room temperature. After conjugation, the PE-LAC films were rinsed three times in 0.1 M, pH 7.8 phosphate buffer and stored at 4°C in 0.1 M, pH 5.0 acetate buffer. Primary amines from lysine residues of the lactase covalently attach to free aldehydes at the ends of the GL on the PE-GL films forming amide bonds *(31)*.

Additional lactase was covalently added to PE-LAC using LbL deposition (PEI → GL → LAC) using concentrations and reaction times as described in creation of the

initial layer, above. Up to five covalently attached layers of PEI, GL, and LAC were created on the same films by repeating the three conjugation steps for the desired number of layers.

2.3.2.3 Film Surface Analysis

2.3.2.3.1 Attenuated Total Reflectance Fourier Transform Infrared Spectroscopy (ATR-FTIR)

ATR-FTIR spectra were obtained using an IR Prestige 21 spectrometer (Shimadzu Corporation, Kyoto, Japan) with a diamond ATR crystal. IR solution (v. 1.3, Shimadzu Corporation) was the software used to collect the information. Each absorbance spectrum represents 32 scans at 4.0 cm^{-1} resolution using Happ-Genzel apodization on an acetone cleaned ATR crystal exposed to the ambient atmosphere as a background. KnowItAll software (v. 8.1, Biorad Laboratories, Philadelphia, PA) was used for spectral analysis. ATR-FTIR was used to confirm modification of the PE film surfaces. Spectra were collected for native PE and PE-Ox, and for every layer of PE-PEI, PE-GL, and PE-LAC.

2.3.2.3.2 Surface Primary Amine Analysis

The number of primary amines on the film surface was quantified by the Acid Orange 7 (AO7) dye assay in order to determine the necessary concentration of GL for PE-GL production and to quantify the effect of multilayer deposition on amine functionality. Acid Orange 7 dye prepared to 1×10^{-3} M in pH 3 water adjusted using HCl, was allowed to adsorb to the film surface by shaking for 3 hrs at room temperature. After three hours, the films were washed in three consecutive pH 3 water baths to remove any non-complexed dye. The dye was desorbed off of the films using water adjusted with

NaOH to pH 12 for 15 minutes. The absorbance of the desorbed dye was measured at 455 nm using clean PE films as a control. The absorbances were compared to a standard curve of known concentrations of AO7 prepared in pH 12, DI water to calculate the concentration of primary amines per unit area.

2.3.2.3.3 Quantifying Total Amount of Protein

The total protein content of the free lactase enzyme solution and modified films was quantified using a modified bicinchoninic acid (BCA) assay. The BCA assay is a colorimetric test that quantifies protein by detecting a color change caused by the reduction of Cu^{2+} contained in the working reagent to Cu^{1+} *(72, 73)*. For the measurement of free enzyme protein concentration, an aliquot of 10 µL free lactase enzyme solution was reacted in 2 mL of BCA working reagent for 30 minutes at 37°C. Films were shaken in 3 mL of BCA working reagent for 1 hr at 60°C. All samples were read at 562 nm for comparison against a standard curve created from known concentrations of Bovine Serum Albumin (BSA). In order to eliminate any interference associated with the PEI-GL conjugation, protein content of an individual multilayer was calculated by subtracting the apparent protein content of a given multilayer's PE-GL layer from that of the same multilayer's PE-LAC. Total protein per unit area, as reported in the results and figures, represents the sum of each individual multilayer's protein content as determined by the following equation

Equation 2.1: Total protein per unit area

$$protein\ content\ = \sum_{j=1}^{k=5} \frac{[(PE\text{-}LAC)_j - (PE\text{-}GL)_j]}{A_s}$$

Where A_s represents film surface area (4 cm^2 per film) and the total protein content was calculated for every layer, j, for up to 5 layers, k.

2.3.2.3.4 Lactase Activity Quantification

Lactase activity was determined for both free lactase enzyme and lactase bound to PE films using the *o*-nitrophenol-β-D-galactopyranoside (ONPG) assay as outlined in the Foods Chemical Codex for *A.oryzae (74)*. Free lactase from *A.oryzae* has an optimum activity at 50°C and pH 5.0. Our prior work has demonstrated that the chemistry used herein for lactase immobilization does not alter optimum pH or temperature for activity; we therefore used these conditions for enzyme activity assays in this work *(30)*. The samples were compared to a blank sample containing only an equal aliquot of buffer. The lactase activity was calculated using an experimentally determined extinction coefficient (ε) of 4.05 μmol/mL. The extinction coefficient was calculated by measuring the absorbance of O-nitrophenol (99%) and 1% (wt/vol) sodium carbonate aqueous solution at varying concentrations. O-nitrophenol is the end product of the lactase hydrolysis reaction on the synthetic substrate, ONPG, which is measured at 420 nm. The resulting data was fit to a line from which the slope represented ε. The resulting lactase activity calculations are represented in ALU defined as cleavage of 1 μmol ONPG per minute.

A solution consisting of 10 μL of a 10% (vol/vol) solution of the purified free lactase enzyme solution was added to 2 mL of 3.7 mg/mL ONPG in 0.1 M, pH 5.0 acetate buffer, pre-warmed to 50°C. After shaking for 15 minutes, 2.5 mL of 10% (wt/vol) sodium carbonate solution in water was added to stop the reaction as the activity is dependent on time. The samples were diluted with DI water to reach a final volume of 25 mL.

To measure the activity of bound lactase, films were placed in 3 mL of 3.7 mg/mL ONPG in 0.1 M, pH 5.0 acetate buffer for 1hr of shaking at 50°C. The reaction

was stopped with 4 mL of 10% (wt/vol) sodium carbonate solution in water. DI water was added to make the final sample volume 10 mL. Activity values were determined by subtracting the control value determined by subjecting clean PE films to the same assay.

2.3.2.3.5 Enzyme Kinetics

Kinetics studies of both free and bound lactase were done using the modified ONPG assay described previously. ONPG solutions in 0.1 M, pH 5.0 acetate buffer for optimal enzyme activity were prepared at varying concentrations: 1 mM, 2 mM, 4 mM, and 6 mM *(74)*. The data was plotted for calculations of apparent k_{cat}, K_m, *and* k_{cat}/K_m. The turnover number, k_{cat}, is calculated by dividing the velocity by the total protein concentration. K_m refers to the concentration needed to reach half of the velocity maximum. A ratio of k_{cat} and K_m is a measure of the kinetic efficiency of the enzyme system *(75)*. Michaelis- Menten enzyme kinetics were calculated using Graphpad Prism software with n = 3 films for each layered treatment at each ONPG concentration analyzed once.

For free enzyme kinetics, 1 μg free lactase solution in 0.1 M, pH 5.0 acetate buffer was added to 3mL of the ONPG. Reactions were stopped with 10% (wt/vol) sodium carbonate aqueous solution at intervals of 30 seconds between 0-5 minutes.

For LbL kinetics of multilayer films, one multilayer film (2×1 cm^2) was added to the ONPG and stirred according to the modified ONPG assay. Total lactase content added to the sample was determined using the BCA assay as described above per layer using correlating layers of PE-GL as controls. Each sample reaction was stopped with 10% (wt/vol) sodium carbonate aqueous solution at 0 min, 1 min, 2.5 min, 5 min, 10 min, 15 min, 30 min, 45 min, 60 min, and 75 min.

2.3.2.4 Statistical Analysis

One-way analysis of variance (ANOVA) was done using Graphpad Prism software (v. 5.04, Graphpad Software, La Jolla, CA) with Tukey's pairwise comparison for the identification of statistical differences between samples within a 95% confidence interval, $P<0.05$. Results are the means of data collected during three independent experiments conducted on different days with n=12 individual films prepared for each of the separate chemical surface analysis techniques (ie: 4 independent films were prepared for each analytical method on each of the three experimental replications).

2.4 Results and Discussion

2.4.1 Surface Functionalization of Film

Modification of the film surface was determined at each step in the LbL deposition process through both physical and chemical analyses. Absorbance bands at 700, 1480, 2700, and 2800 cm^{-1} represent stretching at carbon-carbon double bonds and carbon-hydrogen bonds respectively, which indicate the native LDPE surface is clean. These bands appear in each subsequent sub-layer as the peaks are characteristic of all LDPE.

PE-Ox was created by UV treatment of native LDPE surface. Exposing PE to short wavelength UV light creates carboxylic acid groups *(68)* which are negatively charged as carboxylates and available for interaction with positively charged species. The extent of film oxidation was determined with FTIR analysis as seen in **Figure 2.2**. The band between 1650 and 1800 cm^{-1} is indicative of an O-H vibration from carboxylic acid groups.

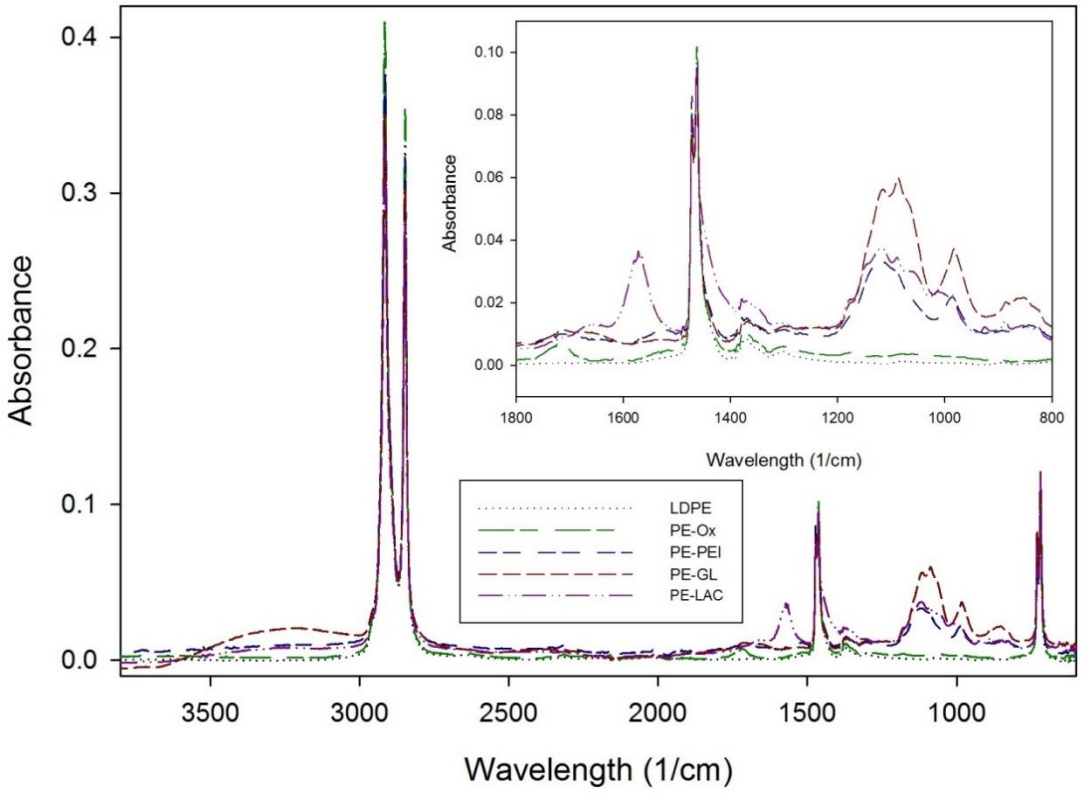

Figure 2.2. ATR-FTIR spectra overlay of each component of the first multilayer. Includes native LDPE, PE-Ox, PE-PEI, PE-GL, and PE-LAC with inset of wavelength range 1800 cm-1 to 800 cm-1.

2.4.2 Attachment of PEI to Film

PE-PEI films were created by attaching PEI to PE-Ox films by amide bonds. PEI provides the surface with an excess of primary amine sites that can be utilized for further covalent attachments. Functionalization by PEI was analyzed both qualitatively and quantitatively. As seen in Figure 2, FTIR analysis shows a vibration between the carbon and nitrogen in a straight chain at around 1100 cm^{-1}. The nitrogen – hydrogen bond bends at 1600 cm^{-1} in addition to primary amines stretching around 3300 cm^{-1}.

The number of available primary amines on each multilayer's PE-PEI film surface was quantified using the AO7 dye assay (**Fig. 2.4**). Values reported represent the total number of primary amines available with clean PE serving as a control (n=12).

Despite the fact that the standard deviations are relatively large in comparison to total reported values, such scatter is consistent with other reports using dye assays of this type *(68)*. Nevertheless, statistical analysis enables us to conclude that with each subsequent layer there is no significant difference except for primary amine quantity between the first and last layer. One would expect that the immobilization of each additional layer of lactase would increase the number of primary amines present due to lysine and terminal amines of the protein. It is possible that steric hindrance prevented complete diffusion of the relatively large, aromatic AO7 dye to underlying multilayers, thus underestimating the total number of amines present. It is also likely that GL conjugation quenched available amines in previous layer conjugations preventing site availability to AO7 dye, allowing only the top-most layer of primary amines to be quantified. These results suggest that while a layer by layer approach may be suitable for increasing the amount of bound protein (described below) it may be ineffective in increasing the total number of available reactive functional groups.

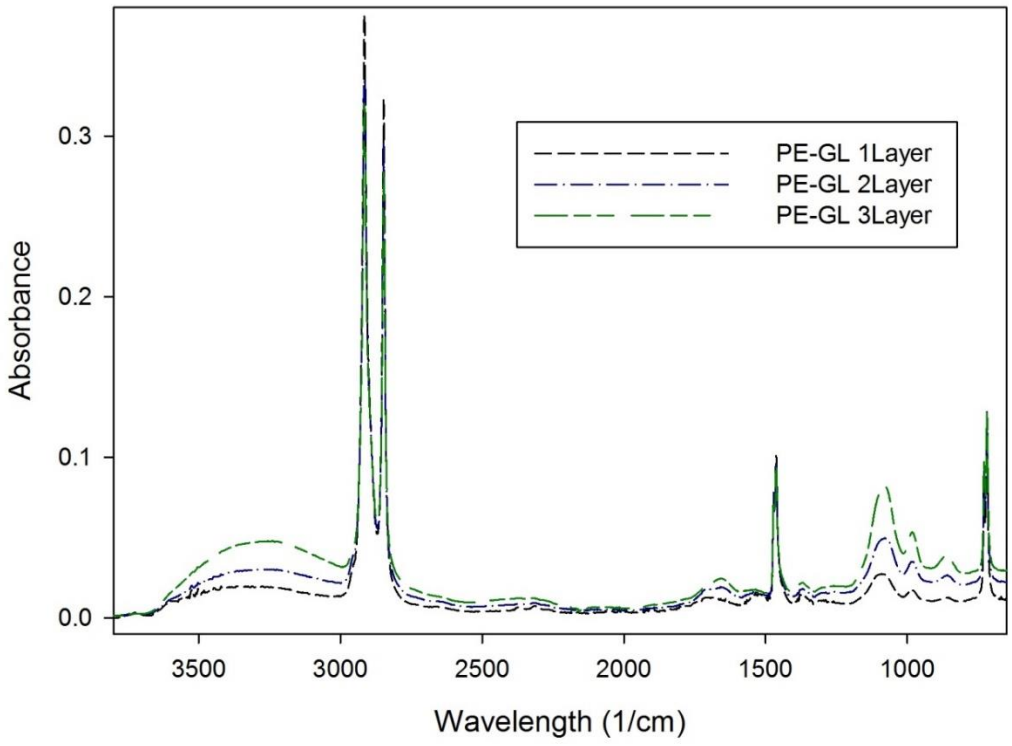

Figure 2. 3. ATR-FTIR spectra overlay of 1, 2, and 3 PE-GL layers.

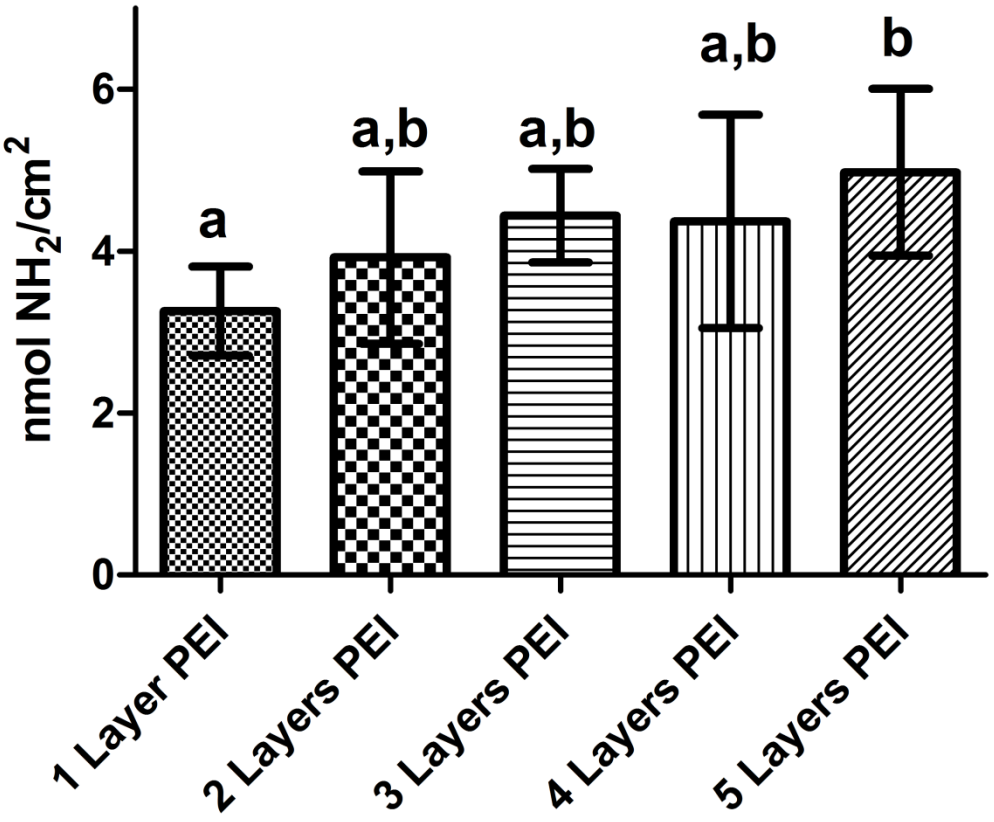

Figure 2. 4. Number of total available primary amine sites per unit area with each additional multilayer as quantified by AO7 assay. Clean PE served as a control. Different letters indicate statistically significant differences ($p<0.05$). Values are means ($n = 12$) with error bars representing standard deviations.

2.4.3 Attachment of GL to Film

PE-GL films were produced by attaching GL to PE-PEI films by nucleophilic addition to create an amide bond *(33)*. ATR-FTIR analysis confirmed successful conjugation of GL (**Figures 2.2, 2.3**). The broad absorbance between 3000 cm^{-1} and 3700 cm^{-1} is typical for the stretching of the bond between a nitrogen and carbon with hydrogen, as is present in an amide bond. The peak around 1150 cm^{-1} suggests a stretching of a carbon-carbon bond next to a ketone with a peak between 1630 cm^{-1} and 1695 cm^{-1} representing the carbonyl group of an amide bond. **Figure 2.3** shows an

increase in these key absorbances with each additional layer of GL when compared to previous PE-GL layers confirming successful LbL deposition (**Fig. 2.3**).

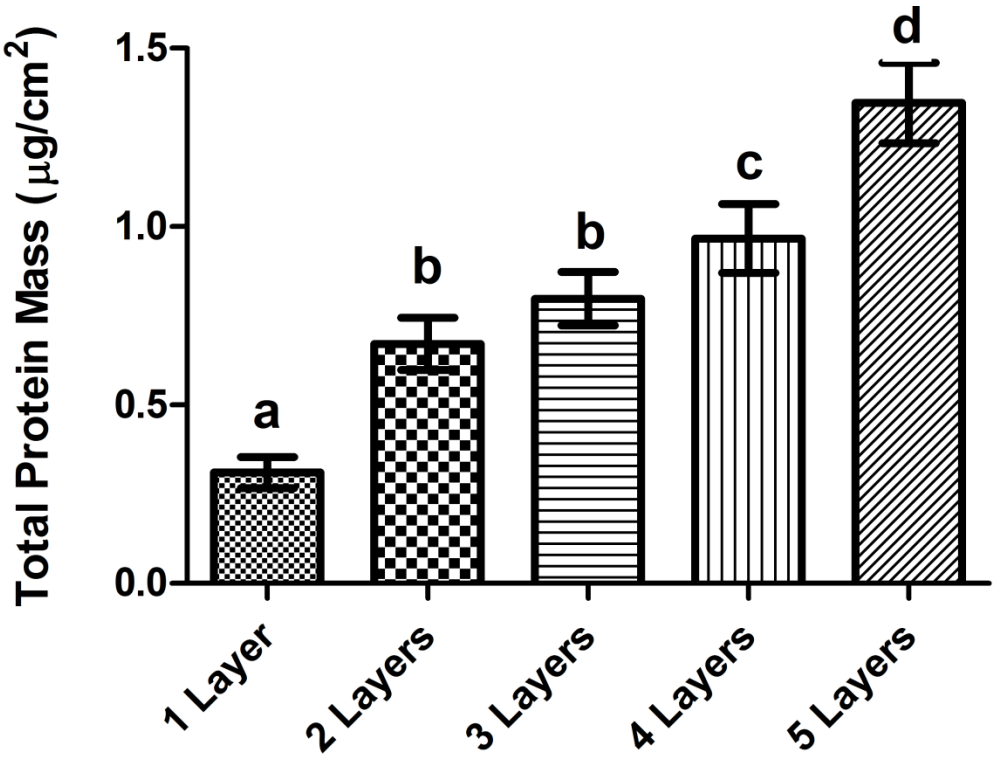

Figure 2. 5. Total protein content of films as mass per unit area of film with each additional multilayer as quantified by BCA protein assay. Different letters indicate statistically significant differences ($p<0.05$). Values are means (n = 12) with error bars representing standard deviations.

2.4.4 Total Protein Loading on Film (BCA) by layer

The goal of the LbL lactase immobilization technique was to increase total protein content with the ultimate goal of increasing total lactase activity for a set film surface area. The total protein content on the film surface was quantified by using the BCA assay after every layer of lactase addition. As noted in the methods, protein content of an individual multilayer was calculated by subtracting the apparent protein content of a given multilayer's PE-GL layer from that of the same multilayer's PE-LAC. Total

protein per unit area, as reported in the results and figures, therefore represents the sum of each individual multilayer's protein content. An increase in total protein content was observed with the addition of each subsequent multilayer (**Fig. 2.5**). This indicates that amount of lactase immobilized on a given surface area of film increased with the conjugation of each subsequent multilayer, suggesting that the LbL deposition technique is successful in increasing the amount of bound enzyme onto polymer supports per unit area.

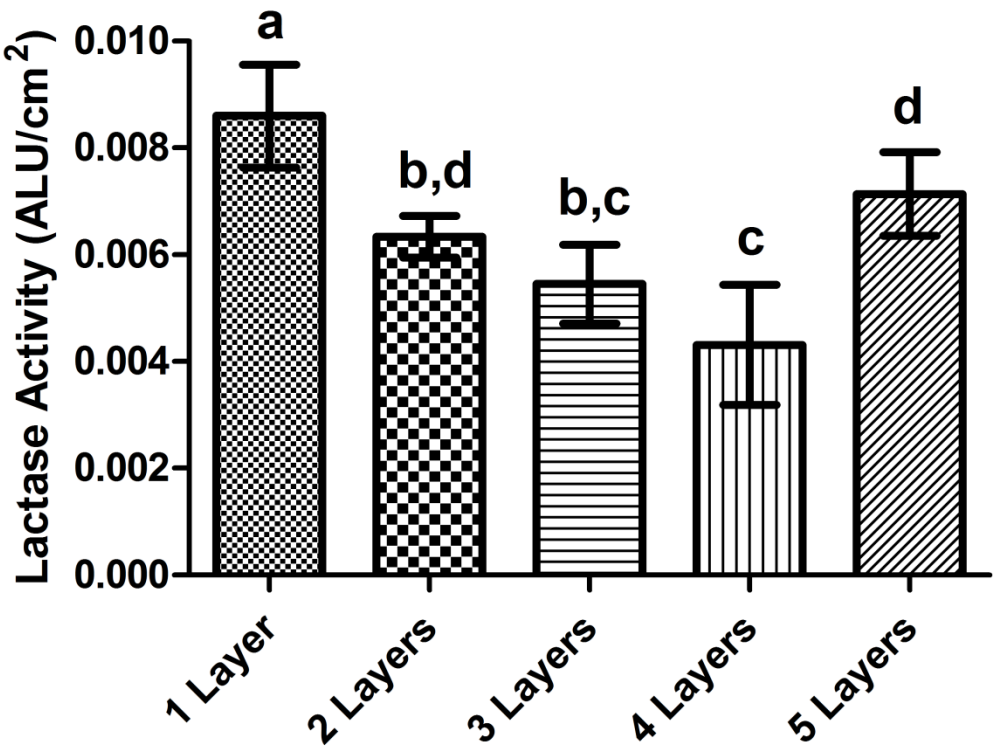

Figure 2.6. Total immobilized lactase activity per unit area with each additional multilayer. Clean PE served as a control. Different letters indicate statistically significant differences ($p<0.05$). Values are means ($n = 12$) with error bars representing standard deviations.

2.4.5 Effect of Layer by Layer Protein Attachment Approach to Activity

Lactase activity was measured by the ONPG assay and is reported both as activity per unit area of film (**Fig. 2.6**) and normalized to activity per gram protein (**Fig. 2.7**), with clean PE serving as a control (n=12). Statistically significant, but negligible,

differences were found in lactase activity per unit area of film with no apparent correlation or trend between activity and number of multilayers immobilized (**Fig. 2.6**). This is the most basic representation of overall film activity. There is slight decrease in activity per unit area with the exception of an increase from the fourth to fifth layers. While parameters of our statistical analysis indicate significant differences, the practical differences are inconsequential for overall activity. Division of ALU/cm^2 (as reported in **Fig. 2.6**) by $\mu g/cm^2$ (as determined by BCA and reported in **Fig. 2.5**) enables evaluation of activity per mass of lactase immobilized (**Fig. 2.7**). Despite the increase in amount of lactase immobilized with each additional multilayer, as concluded by Figure 5, the activity per gram enzyme actually decreased as additional multilayers were deposited. This suggests that with deposition of additional lactase layers, the enzyme maintains constant activity with each layer, but the increase in total protein mass creates a downward trend. Therefore, dividing a constant activity value (**Fig. 2.6**) by an increasing protein mass (**Fig. 2.5**) results in a trend of decreasing activity per gram with each layer.

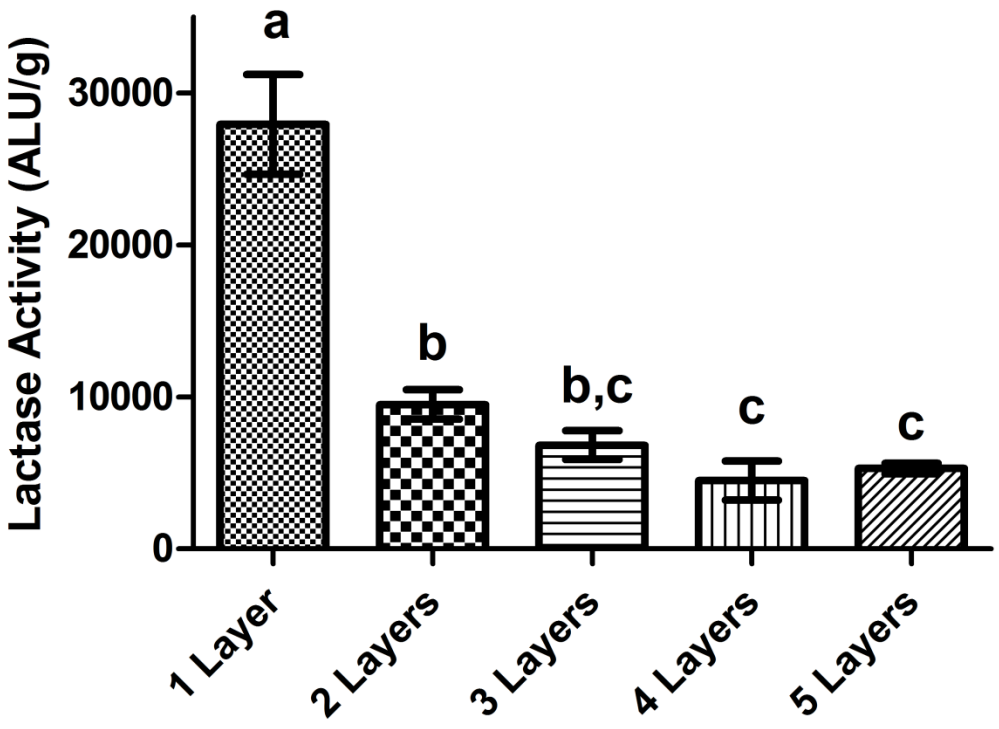

Figure 2.7. Total immobilized lactase activity per gram of protein with each additional multilayer. Different letters indicate statistically significant differences ($p<0.05$). Values are means ($n = 12$) with error bars representing standard deviations.

The observed decrease in activity per gram lactase with each additional multilayer may be due to a number of factors including diffusional constraints imparted by the multilayers, denatured protein or morphology change with additional layers, or substrate accessibility due to blocked active sites. A common complication of immobilized enzyme systems is the lack of access to substrate due to diffusion restrictions which depends on tortuosity of the substrate pathway to the enzyme. Substrate may be unable to pass by the immobilized lactase readily even if the enzyme maintains full activity after covalent attachment. It has been established by the determination of total protein loading (**Fig. 2.5**) that lactase exists on the surface of the bulk material, but the morphology of lactase cannot be proven. A misfolded enzyme may be fashioned following additional GL and

PEI attachment which will make the protein non-functional and would not contribute to the activity calculation of the films. If the active site is blocked when additional layers of PEI and GL are added, no substrate will be able to access the binding or catalysis site. Loss of activity of the immobilized lactase relative to the free enzyme has been seen previously, and has been attributed to surface denaturation, protein orientation, and substrate diffusion to the surface of the film *(16, 31)*. The BCA protein quantification method is unable to distinguish between active and inactive lactase.

2.4.6 Lactase Kinetics

Kinetic studies using varying concentrations of ONPG at different time points for the reaction help to determine the k_{cat} and K_m value *(75)*. Observing a change in these values when compared to the same values attributed to free lactase indicates there is a reduced substrate access and catalytic activity loss following conjugation. All lactase kinetics were calculated with n = 3 and LDPE controls (**Table 2.1**).

Table 2.1. Lactase Michaelis-Menten kinetic constants. Values are means (n = 3) with error bars representing standard deviations.

	V_{max} (10^{-5} mM/s)	K_m Apparent (mM)	k_{cat} Apparent (1/s)	k_{cat}/K_m (1/mM s)
Free Lactase	40.8 ± 6.33 [a]	1.31± 0.41[a]	128.43± 19.94 [a]	103.41± 18.80 [a]
1Layer	4.89± 1.67[b]	0.68± 0.24 [a]	9.72± 3.44 [b]	14.34± 0.47 [b]
3Layer	7.46± 6.03[b]	1.25± 1.05 [a]	6.73 ± 5.44 [b]	7.57± 4.10 [b]
5Layer	11.4± 4.75[b]	1.20± 0.30 [a]	4.76± 0.20 [b]	4.16± 0.84 [b]

V_{max} indicates that all subsequent layers were significantly different from free lactase. V_{max} is a measurement of the theoretical maximum working rate, and is an extensive property of an enzyme. Extensive properties change with enzyme concentration; the more enzyme is conjugated to the film surface, the faster the theoretical enzyme speed. As seen in **Table 2.1**, with increasing layers comes an increase in V_{max}; however, when determining k_{cat}, which is calculated using the enzyme concentration, a decrease is seen with increasing layers. This result suggests that while additional layers may increase the activity of the films on a per unit area basis, it comes with a loss in the activity of the population of enzymes. For the development of active packaging films, this is an important parameter when considering the economic value of adding additional layers.

The Michaelis-Menten constant (K_m) represents the lactase concentration needed to reach half of the enzyme's maximum speed, and is referred to as a measure of the affinity between enzyme and substrate. K_m is an intensive property of an enzyme, one that does not change with enzyme concentration. The apparent K_m of immobilized enzymes has been shown to increase with the size of material, which has been attributed to mass transfer limitations and collisions between the enzyme and substrate *(76)*.The apparent K_m values with increased layer conjugation were not significantly different from that of free enzyme. This indicates that the system as tested is not limited by interactions between the substrate and the film.

The specificity constant (k_{cat}/K_m) is an indicator of enzyme efficiency. Because different rate steps of catalysis towards a final product cannot be separated, k_{cat}/K_m combines all constants. Since this system is of an immobilized enzyme, the catalytic

constants are all valued to be “apparent” observations. Statistical analysis shows each additional layer creates a decrease in catalytic efficiency when compared to free lactase. This is expected as K_m remained unchanged and the apparent k_{cat} decreased with increasing enzyme layers.

2.5 Conclusion

In this work, we utilized a LbL immobilization technique to develop an immobilized enzyme active packaging film. LbL attachment of lactase to LDPE increased total protein mass bound per unit surface area of polymer film. UV oxidation of the film surface initially activated the film, allowing the attachment of PEI for primary amine functionalization. GL acted as a tether for which aldehyde groups reacted with amine groups of lactase purified from *Aspergillus oryzae*. Activity measurements using the synthetic substrate, ONPG, indicated that additional multilayers containing lactase do not increase the overall activity per unit area, despite the increase in bound lactase as concluded by protein analysis. It is difficult to attribute overall activity to separate multilayers. Michaelis-Menten kinetic constant analysis indicated that the system was not mass transfer limited and the maximum velocity of the films on a per unit area basis could be increased with increasing layers but at the expense of catalytic efficiency. The results suggest that LbL approach to immobilize lactase to packaging films is useful in increasing bioactive material bound, but should be weighed against considerations of enzyme efficiency. Alternative polymers may be more suitable for use in retaining enzyme activity after LbL immobilization. Additional studies are being pursued to evaluate alternative conjugation layers as well as immobilization of cross-linked enzyme aggregates to enhance protein loading and film effectiveness.

CHAPTER 3

BIOCATALYTIC POLYMER NANOFIBERS FOR STABILIZATION AND DELIVERY OF ENZYMES *(38)*

3.1 Abstract

Electrospun water-soluble nanofibers as enzyme supports have potential to overcome limitations of traditional immobilization by increasing the surface area-to-volume ratio, reducing diffusional limitations, and improving storage stability. In this study, galactosidase (lactase, *Aspergillus oryzae*) was electrospun into polyethylene oxide (PEO) nanofibers with Pluronic F-127 (F127) (polyethylene oxide/polypropylene [1]oxide block copolymer) to enable dry storage stability and subsequent rapid dissolution upon use in applications such as sensing, bioactive packaging, and bioprocessing. Nanofibers were cylindrical (average diameter ~300 nm) and exhibited no beading after spinning or storage. After electrospinning, enzymes retained up to 92% of their native activity. After 4 weeks storage, the immobilized enzyme fiber retained up to 44% of the activity of the original fiber. These results suggest that co-spinning enzymes in a polymer nanofiber matrix can improve activity retention and dry storage stability compared to traditional immobilization methods and enables rapid dissolution for ease of use.

3.2 Introduction

Enzyme encapsulation and delivery systems facilitate commercial applications of enzyme catalyzed reactions (e.g. sensing, bioprocessing, active packaging) *(16, 77-80)*. Incorporation of enzymes into/onto nanoscale materials takes advantage of the uniquely

This chapter has been published: Wong, D.E.; Dai, M.; Talbert, J.N.; Nugen, S.R.; Goddard, J.M. Biocatalytic polymer nanofibers for stabilization and delivery of enzymes. *J. Mol. Catal. B: Enzym.***2014**, *110*, 16-22.

high surface area to volume ratio of nanomaterials, increasing surface area available for protein loading and improving catalytic efficiency *(81, 82)*. Electrospun nanofibers represent an emerging, commercially scalable technology in nanomaterial fabrication with surface areas of ~100-1000 m^2/g *(83-85)*. Non-woven nanofiber mats are produced by application of a high positive voltage to a polymer solution through a capillary moving towards a grounded collector *(84, 86)*. Nanofiber size and morphology can be controlled by adjusting processing parameters such as polymer matrix composition, solvent, flow rate, etc. *(87-90)*. Interest in electrospinning has grown in biological applications such as tissue scaffolding, drug delivery, electronics, and diagnostics fields, in which biocatalytic components can be incorporated into or onto the fibers during electrospinning or in material post-processing *(91-95)*.

Incorporation of enzymes into/onto nanofibers has been shown to improve catalytic efficiency and broaden the working pH and temperature optimum ranges of enzymes *(96, 97)*. In one report, both increased operational pH and thermal stabilities of up to one pH unit and 7°C were observed in post-electrospinning immobilization of the enzyme acetylcholinesterase to polyacrylonitrile nanofiber mats when compared to free enzyme *(97)*. Sathishkumar et al. attributed increased thermal stability of laccase immobilized onto poly (lactic-co-glycolic acid) nanofibers to covalent bonds formed and decreased diffusion limitations experienced at higher temperatures *(98)*. Further Zeng et al. found a linear increase in luciferase activity over one day due to the slow addition of protein to the test environment, which demonstrated that coated poly (vinyl alcohol) nanofibers were capable of controlled protein release while maintaining enzyme activity *(99)*.

Indeed, enzyme immobilization onto nanofibers has shown potential to improve enzyme stability under operational conditions of bioprocessing systems; however, previous studies often require multi-step synthesis strategies (e.g. additional surface functionalization steps or post-processing cross-linking). For example, initial explorations into enzyme immobilization onto nanofibers include lipase adsorption after electrospinning *(100)*. Further developments in enzyme immobilization onto nanofibers have focused on material surface modification after electrospinning, and have focused on addition of enzyme by functionalized end groups and zero-length cross linkers. One study by El-Aassar treated poly (An-*co*-MMA) nanofibers with polyethylenimine before immobilizing β-galactosidase with glutaraldehyde *(101)*. Li et al. utilized amidination, or the functionalization of nitrile groups, on the surface of polyacrylonitrile nanofibers to in turn attach lipase using amine side chains *(102, 103)*. The goal of this work was to demonstrate an enzyme stabilization and delivery technique in which enzyme is directly electrospun in polymer nanofibers by a one-step synthesis method that enabled increased enzyme storage stability, and rapid enzyme release for controlled dosing.

In this work, lactase, an enzyme important in diagnostic and bioprocessing applications, was electrospun in polyethylene oxide (PEO) nanofibers with Pluronic F-127 (F127) [polyethylene oxide / polypropylene oxide block copolymer] to enable dry storage with high retained catalytic activity, for subsequent rapid enzyme release upon usage. A one-step electrospinning method was used to streamline nanofiber synthesis, increase the enzyme incorporation efficiency, and to minimize enzyme denaturation commonly associated with secondary chemical cross-linking *(104)*. Exploration by Qu et al. found that trypsin and collagenase electrospun into PEO as a part of a complex

PEO/polycaprolactone composite non-woven mat had the potential to aid meniscus tissue repair *(105)*. PEO and F127 were selected as nanofiber matrix polymers due to their hydrophilic, biocompatible natures, supportive of both protecting the enzyme during spinning and storage, and enabling rapid dissolution upon exposure to aqueous solutions *(100, 105)*. PEO is also readily electrospun from water that allows for ease of enzyme incorporation and quick release into bioprocessing systems. Electrospun nanofibers with and without incorporated lactase (Lac-NF and NF, respectively) were characterized for morphology, protein loading (quantity and uniformity), activity, and storage stability.

3.3 Experimental

3.3.1 Materials

Polyethylene oxide (PEO) [300,000 MW], Pluronic® F-127 (F127), Bradford Reagent, fluorescein isothiocyanate isomer I (FITC), dimethyl sulfoxide (DMSO), and α-D-glucose were purchased from Sigma-Aldrich (St. Louis, MO). Anhydrous potassium phosphate dibasic, anhydrous potassium phosphate monobasic, anhydrous sodium acetate trihydrate, anhydrous sodium bicarbonate, anhydrous sodium carbonate, D-lactose monohydrate, glacial acetic acid, , and sodium chloride were purchased from Fisher Scientific (Fair Lawn, NJ). Dried β-galactosidase (lactase, *Aspergillus oryzae*) was donated by Enzyme Development Corporation (New York, NY). *o-nitrophenol-β-D-galactopyranoside* (ONPG) and bovine serum albumin (BSA) were purchased from Thermo Scientific (Rockford, IL). Syringes were purchased from BD Syringe (Franklin Lakes, NJ) and blunt stainless steel 22 gauge, 1.5 in needles were purchased from Component Supply Co. (Fort Meade, FL). ‘‘Amicon® Ultra’’ (50k MWCO) centrifugal filter devices and “Amicon® Ultra” (10k MWCO) centrifugal filter devices were

obtained from Millipore Ireland (Carrigtwohill, Co. Cork, Ireland). Syringe filters were purchased from Whatman (Florham Park, NJ). OneTouch® Ultra® Blue blood glucose meter strips, lot 3480648, were purchased from LifeScan, Inc. (Milpitas, CA). Hershey's® UHT skim milk was purchased from Diversified Foods Inc. (Metairie, LA), and liquid food dye was purchased from McCormick® (Sparks, MD).

3.3.2 Methods

3.3.2.1 Lactase Purification

The lactase was rehydrated in a 0.1 M, pH 5.0 acetate buffer and filtered through a 0.2 μm PTFE syringe filter. The filtrate was subject to centrifugal filtration (50k MWCO) at 6500 rpm for 30 min. The lactase was trapped in the filter membrane, and was flushed out and collected with equal volumes of 0.1 M acetate buffer, pH 5.0. The purified free enzyme lactase solution was stored at 4°C for further use.

3.3.2.2 Polymer Matrix Preparation

PEO and F127 polymers were dissolved in water overnight (12 wt. % PEO, 5 wt. % F127) with stirring, after which 1000 μg/mL purified free lactase solution was added and stirred for 20 min prior to electrospinning. Polymer weight percentages were determined by adaptations of prior reports of electrospun nanofibers produced from PEO, and the authors' own preliminary studies *(106, 107)*. Mixtures of enzyme and polymers not used immediately for electrospinning were stored at 4°C for up to 1 week.

3.3.2.3 Electrospinning Nanofibers

The electrospinning set-up (**Fig. 3.1**) was composed of a grounded high voltage supply from Gamma High Voltage Research (Ormond Beach, FL) connected to the needle of a polymer matrix filled syringe. A syringe pump regulated the polymer flow at

0.2 mL/hr. As the polymer matrix flowed through the syringe, 22 kV was applied to form a Taylor Cone which dried the polymer enzyme fiber. Nanofiber mats formed as fiber was collected on a grounded copper plate covered in heavy duty aluminum foil, located 16 cm from the needle tip. The entire system was enclosed in a Lucite box in which humidity was maintained below 25%. The resulting nanofiber produced after 5 min of spinning is referred to as a nanofiber mat herein.

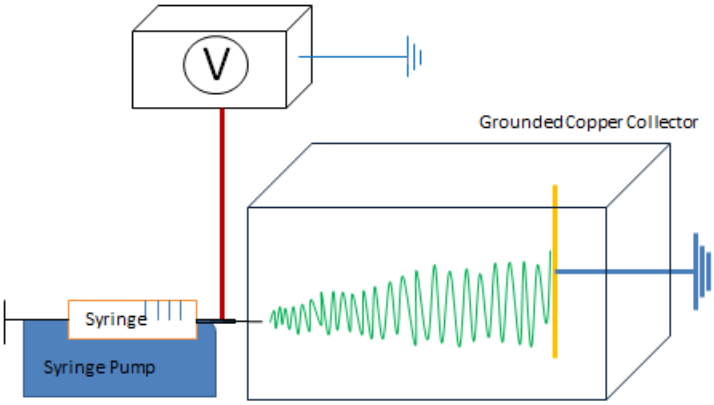

Figure 3.1. Schematic of electrospinning apparatus. A high voltage source is connected to a capillary from which an extruded polymer matrix travels to a grounded collector.

3.3.2.4 Attenuated Total Reflectance Fourier Transform Infrared Spectroscopy (FTIR)

FTIR spectra were collected on an IR Prestige 21 spectrometer (Shimadzu Corporation, Kyoto, Japan) using a diamond ATR crystal. Spectra were collected using IR Solution (v. 1.3, Shimadzu Corporation) in which 32 scans were collected at 4.0 cm^{-1} resolution using Happ-Genzel apodization. The exposed crystal cleaned with reagent grade acetone served as a background. KnowItAll software (v. 8.1, Bio-Rad Laboratories,

Philadelphia, Pa., U.S.A.) was used for spectral analysis. Nanofiber mats were removed from the foil collector, and placed on the exposed crystal for analysis.

3.3.2.5 Scanning Electron Microscope (SEM)

All samples were coated in gold in a Cressington Sputter Coater 108auto (Watford, U.K.) before SEM analysis. All micrographs were taken on a JEOL Neoscope JCM 5000 Benchtop SEM from Nikon Instruments, Inc. (Melville, NY). The SEM operated at a voltage of 10kV. The micrographs were analyzed with ImageJ (NIH) to determine the diameter mean and distribution. The diameter distribution was determined from 75 measurements, as 25 measurements taken from 3 micrographs of NF and Lac-NF.

3.3.2.6 Confocal Laser Scanning Microscopy

Lactase was tagged with FITC as a 1:1 molar ratio to lysine residues as determined by the protein primary amino acid sequence *(108)*. FITC was rehydrated in DMSO at 1 mg/mL, added to purified lactase in 0.1M sodium carbonate buffer, pH 9.0, and stirred for 2 hrs at room temperature *(109)*. The resulting tagged lactase was further purified through a filter unit (10k MWCO) by microcentrifugation at 14,000 g for 15 min, and repeated until the mixture appeared transparent (5 times). The tagged lactase was stored at 4°C in an amber vial and covered in aluminum foil to prevent photo bleaching. The fluorescently tagged lactase was blended into the PEO/F127 polymer matrix and spun as described above. Nanofiber mats were removed from the foil collectors, placed on glass microscope slides, and protected by coverslips. The nanofiber was imaged by confocal laser scanning microscopy (CLSM) [Nikon D-Eclipse C1 80i, Nikon, Melville,

NY, U.S.] using a 10x eyepiece, a 40x objective, and an excitation and an emission wavelength 495 nm and 525 nm, respectively.

3.3.2.7 Dissolution

The rate of dissolution is an important measurement in delivery system characterization. Reported techniques quantifying gel tablet swelling and other drug delivery methods often characterize water intake by mass or volume, imaging techniques, and porosity calculations *(18, 110, 111)*. Due to the rapid dissolution rate of the nanofiber mats, direct imaging was selected to quantify dissolution. Videos were taken to quantify rate of fiber dissolution in water using fibers prepared with the addition of red food color. Nanofiber mats electrospun with dye in place of lactase were shown to be representative of nanofiber mats produced with lactase for this measurement. Additional tests supported that the use of nanofiber mats electrospun with dye were the same to Lac-NF in dissolution measurements. The nanofiber mats were cut into 1.5 cm diameter rounds using a die-cut and placed on a glass Petri dish to which 50 μL of water was added by pipette to dissolve the mat. Videos were analyzed by time lapse imagery by Windows Live Movie Maker.

3.3.2.8 Total Protein Quantification

The amount of protein in the purified free lactase solution was determined by the Bradford assay in which 0.1 mL of 50% purified free lactase solution was added to 3 mL of Bradford Reagent and shaken at 25°C for 45 min. The total protein of the nanofiber was determined by the Micro-Bradford assay where an entire nanofiber mat was dissolved in 1 mL of 0.1M sodium acetate buffer, pH 5.0 and mixed with 1 mL Bradford Reagent and shaken at 25°C for 45 min. The working range of the Micro-Bradford assay

has been reported at 0.5 μg/mL to 20 μg/mL. *(112)*. The samples were read at 595 nm and compared to a standard curve produced from BSA.

3.3.2.9 Activity and Storage Stability of Lactase Nanofibers

In this work, lactase activity was measured in three ways: glucose production in a neat solution of lactose in buffer, glucose production in a complex matrix (skim milk), and hydrolysis of a synthetic substrate (ONPG, O-nitrophenol-β-D-galactopyranoside). Details and specific objectives of each method of measurement are described in the following. Activity of free lactase was quantified by direct quantification of glucose production in a neat solution of lactose in buffer, using an OneTouch® Ultra® Mini blood glucose meter from LifeScan, Inc. (Milpitas, CA). Free lactase was incorporated into a 0.18 M lactose solution in 0.1 M phosphate buffer, pH 6.8, and incubated at 50°C for 15 min. Lactase activity was determined by comparison to a standard curve of glucose in 0.1M phosphate buffer, pH 6.8; a new standard curve was prepared for each lot of blood glucose strips. Free lactase activity was measured in pH 6.8 in order to mimic the natural buffered environment of milk *(113)*. Incubation times for activity measurements were pre-determined optimums for use with free lactase and surface immobilized lactase *(32)*. To quantify the effective enzyme activity of the nanofiber mats in a complex media typical of diagnostic and bioprocessing applications, the protocol described above was similarly performed after dissolving nanofiber mats in UHT skim milk. Briefly, freshly prepared nanofiber mats were dissolved in milk dilutions as outlined by Amamcharla and Metzger, and incubated at 50°C for 120 min *(114)*. Activities were calculated from the meter readings within the blood glucose testing strips' working range (20-600 mg/dL) as provided by the manufacturer. The calculated values determined in skim milk of the Lac-

NF were then compared against values for free lactase at pH 6.8 (**Table 3.1**), and have been presented as overall activity and % activity. These values represent the as-spun activity of the lactase nanofibers in biological (neutral) conditions using direction quantification.

Table 3.1. Protein content and activity retention of freshly electrospun nanofiber mats (average of n=12 ± standard deviation). Activity retention expressed as % activity was calculated by comparison of activity of Lac-NF to that of free lactase under the same test conditions.

Sample	Test Condition	Protein Content (µg)	Activity (10^3 ALU/g)	% Activity
Free Lactase	ONPG in pH 5.0 buffer	2.75	190.4 ± 11.3	-
Free Lactase	Lactose in pH 6.8 buffer	2.75	60.8 ± 4.2	-
Lac-NF	ONPG in pH 5.0 buffer	8.83 ± 4.3	174.0 ± 20.8	91.37%
Lac-NF	Lactose in pH 6.8 milk (complex matrix)	7.30 ± 2.0	41.5 ±11.9	68.33%

Storage stability of the lactase nanofibers was determined by measuring the activity of the lactase nanofiber mat after refrigerated storage (4°C) under both dry (15% relative humidity maintained by storage with calcium sulfate desiccant) and humid (70% relative humidity maintained by storage over saturated NaCl solution) conditions for up to 4 weeks. Nanofiber mats were kept in vacuum sealed laminated low-density polyethylene bags during storage before activity measurements were made. Lactase activity during storage was determined using the O-nitrophenol-β-D-galactopyranoside (ONPG) assay for *A.oryzae (74)* at 50°C and pH 5.0. A synthetic substrate and optimal enzyme working pH 5.0 were used to quantify activity in the storage stability study to improve assay sensitivity. Activity was calculated using an experimentally determined extinction coefficient (ε) of 4.05 μmol/mL calculated from a standard curve of O-nitrophenol (99%) and 1% (wt. /vol.) sodium carbonate aqueous solution *(32)*. Lactase activity is reported as the acid lactase unit (ALU), in which one ALU is equivalent to the amount of cleaved ONPG in μmol/min. Entire fiber mats were dissolved in 1.5 mL 0.1M sodium acetate buffer, pH 5.0, to which 1.5 mL of 7.4 mg/mL ONPG in 0.1 M sodium acetate buffer, pH 5.0, was added. For free purified lactase samples, 10 μL was added to 3 mL of 3.7 mg/mL ONPG in 0.1M sodium acetate buffer, pH 5.0. Samples were incubated for 15 min with shaking at 50°C. The reaction was stopped by addition of 4 mL of 10% (wt. /vol.) sodium carbonate solution in water; samples were further diluted with deionized water to a final volume of 12 mL and absorbances were quantified at 420 nm. All measurements described above were taken in sets of four samples (n = 4).

3.4 Results and Discussion

3.4.1 Electrospinning Technique and Fiber Morphology

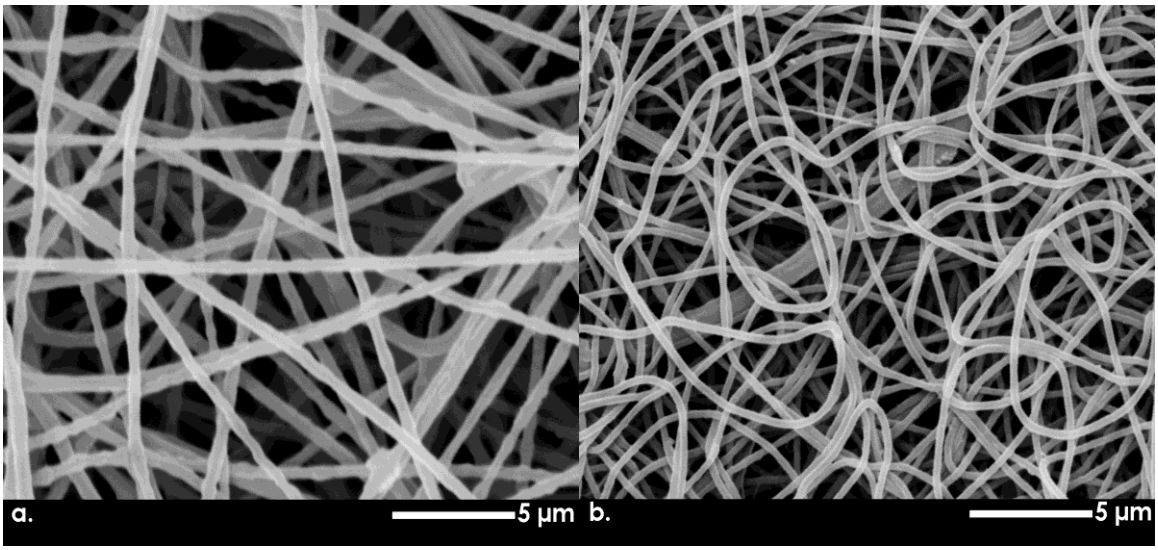

Figure 3.2. SEM micrographs of freshly spun a) NF, b) Lac-NF. Micrographs were taken at 5000x magnification and 10 kV accelerating voltage.

In this work, the food grade, hydrophilic, biocompatible polymers PEO and Pluronic-F127 were used to stabilize lactase in an electrospun nanofiber suitable for dry storage and rapid enzyme delivery. Preliminary studies (data not shown) indicated that a polymer matrix of 12% PEO and 5% F127 resulted in continuous, cylindrical nanofibers of uniform morphology, without beading or spraying, as confirmed by SEM (**Fig. 3.2**). Fibers were formed for both the polymer matrix without (**Fig. 3.2a**) and with the inclusion of the enzyme lactase (**Fig. 3.2b**). Some "necking" of the fiber, in which there are variations in diameter within a fiber, was observed, most notably on the nanofibers prepared without enzyme. This effect was likely a result of the polymer matrix concentration and interactions between PEO and F127 causing wavering at the capillary

tip, did not have an effect on the final enzyme nanofiber application, and was not considered a defect as continuous fibers were nevertheless formed.

Image analysis was performed on SEM micrographs to generate diameter distributions of fibers with and without incorporated lactase (**Fig. 3.3**). Without incorporated lactase, nanofibers had an average diameter of 305 ± 129 nm (average ± standard deviation). Lac-NF had a diameter of 292 ± 55 nm (average ± standard deviation). The diameter distribution was wider, and less uniform, for fibers produced without lactase (**Fig. 3.3a**) than those produced with lactase (**Fig. 3.3b**). F127 is a nonionic block copolymer composed of hydrophobic polypropylene glycol and hydrophilic polyethylene glycol which has been reported to protect enzyme conformation against surface induced hydrophobic denaturation by association of hydrophobic blocks to hydrophobic amino acid residues and against dehydration induced denaturation by association with hydrophilic blocks *(115, 116).* It is possible that such interaction also improves uniformity of size distribution of the nanofibers. Further, addition of a surfactant to a polymer matrix has been shown to reduce polymer solution viscosity, which may further influence electrospun fiber morphology *(117-120).* Interestingly, fibers produced with lactase were also easier to remove from the aluminum foil collection than those produced with PEO and F127 alone. These observations may therefore be a result of the interaction between the F127 and lactase.

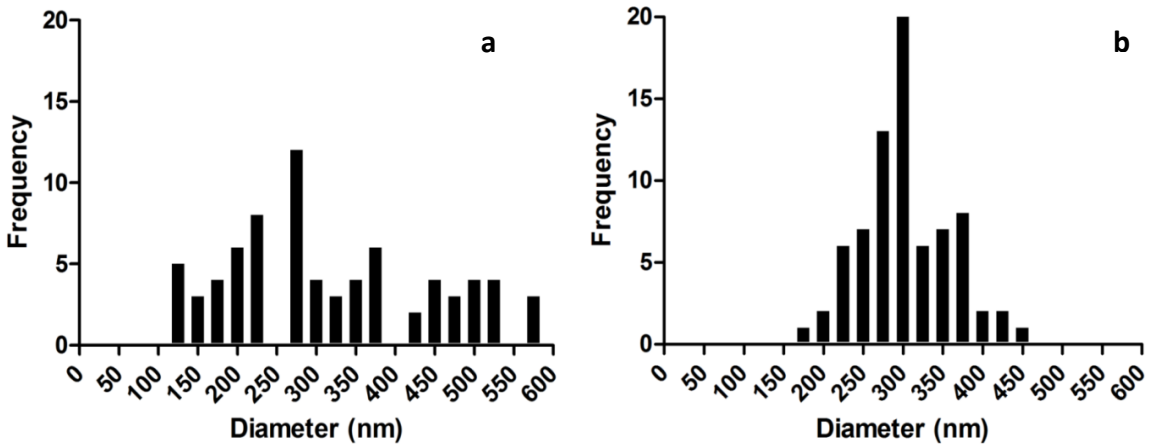

Figure 3. 3. The diameter distribution as determined by analysis of SEM micrographs using ImageJ. Each distribution is composed of 25 measurements taken from 3 micrographs for both a) NF and b) Lac-NF (n = 75). Nanofiber diameters range from 114 nm to 562 nm.

3.4.2 Lactase Nanofiber Characterization

Chemistry of native and lactase incorporated electrospun nanofibers was analyzed by FTIR. Spectra are reported in **Fig. 3.4** as native (NF) and lactase incorporated (Lac-NF), with an inset highlighting absorbances characteristic of proteins (**Fig. 3.4**). Strong absorbances characteristic of the alkyl and ether present in PEO and F127 were observed at 2800 and in the range of 1300-1000 cm^{-1}, respectively *(121)*. Additional absorbances characteristic of the methyl group in the polypropylene oxide block of F127 were observed at 1450 cm^{-1}. Absorbances characteristic of the peptide bonds present in enzymes were expected around 3500-3100 cm^{-1} for N-H stretch, ~1650 cm^{-1} for carbonyl stretch, and ~1600 cm^{-1} for amide bend. Only subtle differences, with low absorbance intensity, were observed between NF and Lac-NF in regions characteristic of peptide bonds. This low intensity is likely due to the relatively low percentage of protein (0.052 wt. % of nanofiber mat) present in the lactase incorporated nanofibers *(122)*. Nevertheless, absorbances characteristic of N-H bending of the peptide bond were observed at ~1630-1570 cm^{-1} for Lac-NF spectra. The absorbance at ~1650 cm^{-1} in the

NF spectra could be attributed to deformations of O-H from hydration of the PEO/F127 polymers. *(123-125)*. The reduction of this absorbance intensity in Lac-NF spectra may be a result of molecular reorientation of the PEO/F127 polymers in which polymers associate around the lactase instead of water.

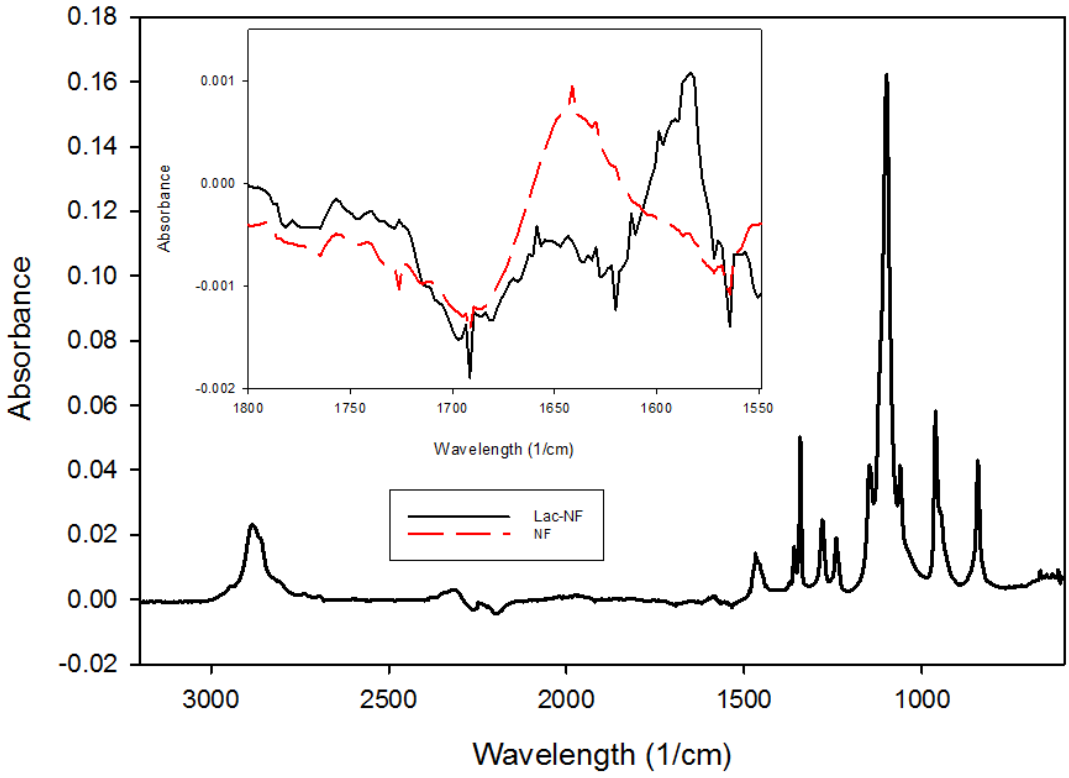

Figure 3.4.FTIR spectra of native and lactase incorporated nanofibers (NF, LacNF). Inset: FTIR spectra of the range 1800-1550 cm^{-1}, characteristic of protein absorbances.

Confocal microscopy was performed to confirm that lactase was uniformly distributed throughout the PEO/F127 nanofibers. An overlay of light and fluorescent micrographs of the same magnification at the same location indicates the uniform fiber morphology and lactase distribution within the biocatalytic nanofibers (**Figure 3.5**). Fluorescence microscopy revealed possible localized aggregation of enzyme: polymer clusters. Nevertheless, the overall uniformity in enzyme distribution supports the findings

of the enzyme activity assays in concluding that uniform biocatalytic nanofibers can be prepared by the method described herein.

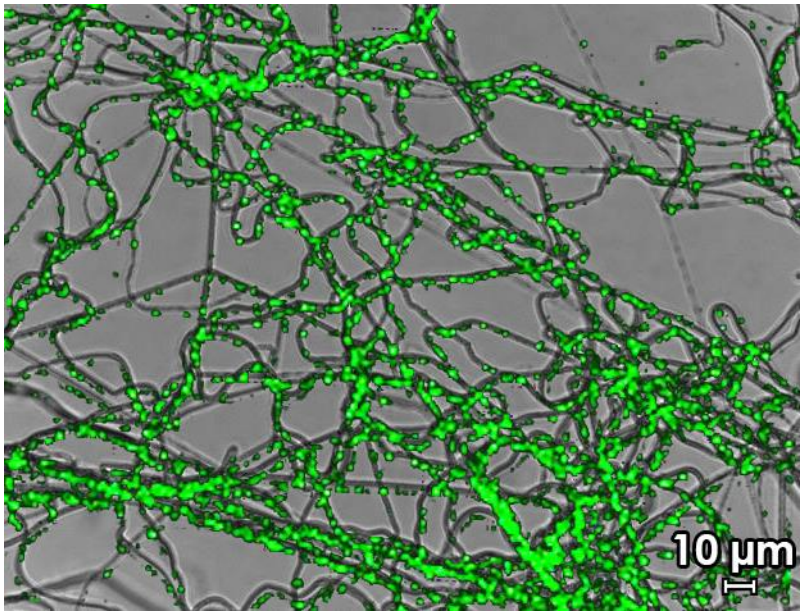

Figure 3.5. Confocal micrograph of FITC tagged lactase electrospun onto nanofiber overlaid onto optical micrograph of the same nanofiber mat, where green indicates lactase placement. The sample excitation and emission were 495 nm and 525 nm respectively. Images were taken at 40x magnification with a 10x eye lens. Adobe Photoshop was used to overlay the optical and confocal micrographs.

The effectiveness of the lactase nanofibers in rapid enzyme delivery upon rehydration was quantified by video time lapse analysis. Water (50 µL) was added to a nanofiber mat prepared with the addition of food dye, and images were captured every 2.5 s until complete dissolution. Dissolution rate was quantified to be 0.14 cm^2/s without mechanical agitation, which qualitatively was observed as being instantaneous. The ability of the nanofibers to dissolve instantaneously supports their potential application as enzyme delivery systems in on-chip reagent delivery, dosing, and bioprocessing applications (**Fig. 3.6**).

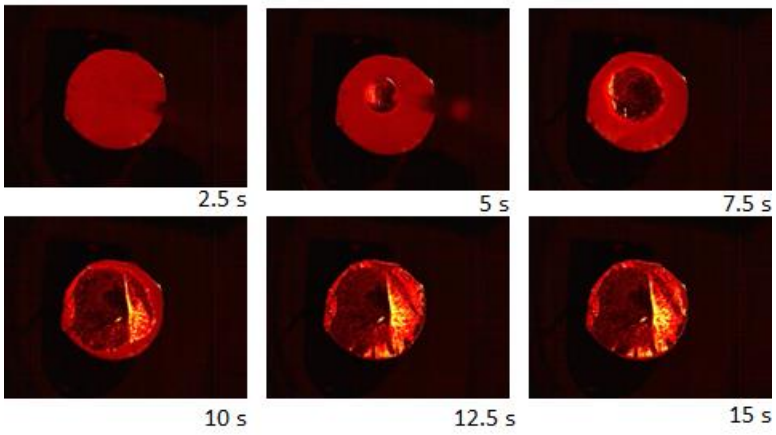

Figure 3. 6. Video time lapse with the rate of dissolution determined to be 0.14 cm2/s for a 1.5 cm diameter round nanofiber mat electrospun without lactase. Stop-motion photographs were captured every 2.5 s.

3.4.3 Total Protein Loading

The protein content of each nanofiber mat (expressed as wt. % enzyme in polymer) was calculated by the Micro-Bradford assay; free lactase protein concentration (used to calculate percent activity retention) was calculated using the Bradford assay (**Table 3.1**). Nanofiber mats prepared without the addition of lactase (NF) served as negative control. Total protein content per mat was quantified to be up to 8.832 ± 4.28 (average ± standard deviation of 4 measurements on 3 independent days). The observed variability between separate sample preparations is likely a result of varying grounding efficiency with increasing electrospinning time due to the loss of conductivity of the grounded plate through insulation by building collected fiber on the collector plate surface, however can be mitigated by controlling other electrospinning parameters and changing electrospinning times. Lac-NF reached up to about 2.5 μg/cm^2 (equivalent to 0.530 mg/mL and 0.052% wt. %) enzyme in nanofiber. In comparison, a previous study showed that the common layer by layer immobilization of lactase on a planar polymer

film yielded 1.5 μg/cm^2 of lactase by a 5 bilayer attachment *(32)*. In other work, β-D-galactosidase immobilized onto Fe_3O_4-chitosan nanoparticles by Pan et al. reached an immobilization maximum of 0.5 mg/mL *(126)*. Whereas Talbert and Goddard found β-D-galactosidase onto magnetic particles activated by to achieve up to 0.38 μg/cm^2 (reported as 3.8 mg/m^2) *(82)*. It has also been reported that lactase immobilized onto alginate-carboxymethyl cellulose gels had up to 60% protein loading efficiency of a 50 mg/L solution or 0.03 mg/mL *(127)*. These results support the hypothesis that using nanomaterials like nanofibers as enzyme carriers for delivery systems can improve protein loading efficiency.

3.4.4 Activity and Storage Stability of Lactase Nanofibers

In order to report enzyme activity under both optimal conditions and in a complex matrix typical of diagnostic and bioprocessing applications, the overall activity of free enzyme and electrospun nanofibers was quantified in a solution of synthetic substrate (ONPG) at the optimal working pH of lactase produced by *Aspergillus oryzae* (pH 5.0) as well as in skim milk, by direct measurement of glucose generation. For nanofiber characterization, measurements were made on entire Lac-NF mats compared to control NF mats. Activity of free lactase at pH 6.8 was ~40% of the activity of free lactase at the optimum condition of pH 5.0. Under optimal pH conditions, using synthetic substrate, as-spun lactase nanofibers had an activity retention of 91.37% compared to free enzyme under the same conditions. Activity of lactase nanofiber mats in milk (pH 6.8) was 68.33% compared to free enzyme. These results suggest that significant activity retention is achieved by electrospinning lactase in PEO/F127 nanofibers.

In order to demonstrate the storage stability of lactase incorporated into polymer nanofibers, enzyme activity was measured for up to 4 weeks at both 15% relative humidity and 70% relative humidity (**Fig. 3.7**). Under both high (70% RH) and low (15% RH) relative humidity conditions, Lac-NF retained significant activity compared to both as-spun Lac-NF and free enzyme. After one week, Lac-NF presented 86% and 72% of free lactase activity at high and low relative humidity, respectively. Both conditions exhibited a drop in activity of Lac-NF after 2 weeks, which plateaued after 4 weeks storage at 22% and 44% activity under high and low relative humidity, respectively. The difference in overall activity between weeks 2 and 4 for both high and low humidity is not significant. These results suggest that electrospinning lactase in PEO/F127 nanofibers may improve dry storage stability in enzyme delivery systems.

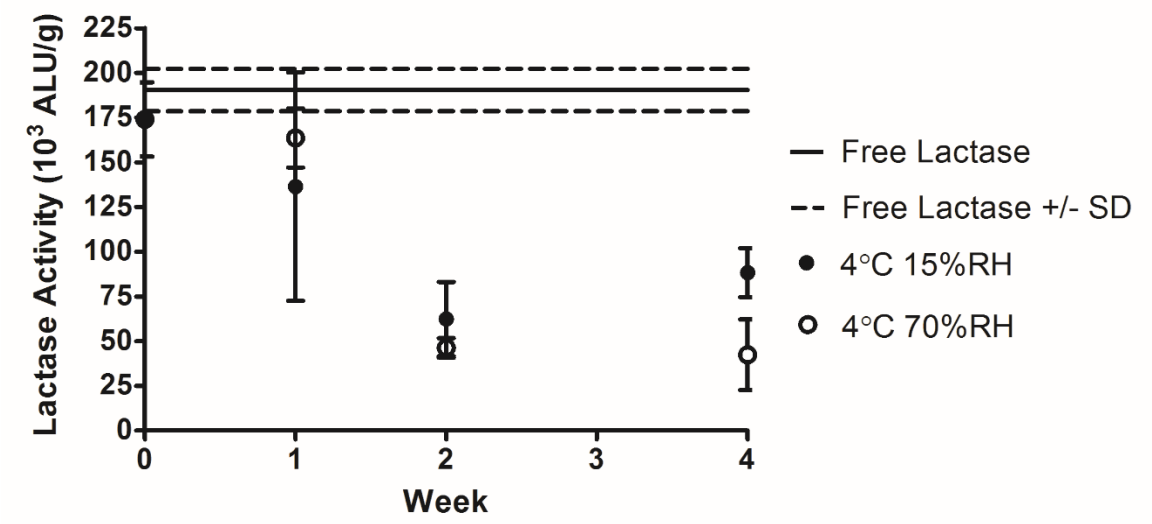

Figure 3.7. Storage stability over 4 weeks at 4°C, 15% and 70% relative humidity. Nanofiber mats were stored in vacuum sealed bags with n = 4. Activity is expressed as ALU/g from measurements taken in ONPG at 50°C and pH 5.

Morphology of lactase nanofibers after 4 weeks storage at both low and high relative humidity conditions were compared to that of as-spun nanofibers by electron

microscopy (**Fig. 3.8**). At higher relative humidity, fiber morphology exhibited some loss in uniform cylindrical structure, however retained overall fiber integrity. These results suggest that lactase nanofibers prepared as described herein would retain sufficient mechanical integrity for storage, handling, and use in delivery systems.

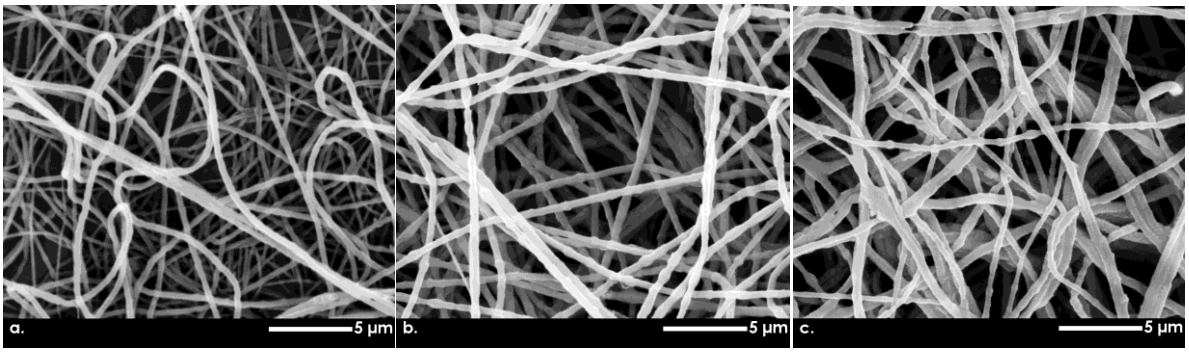

Figure 3.8. SEM micrographs of a) freshly electrospun Lac-NF b) Lac-NF stored at 4°C, 15% relative humidity for 4 weeks, and c) Lac-NF stored at 4°C, 70% relative humidity for 4 weeks. The micrographs were captured at 5000x magnification and 10 kV accelerating voltage.

3.5 Conclusions

In this work, the enzyme lactase was stabilized in electrospun polymer nanofibers for use in enzyme delivery systems. Utilization of nanofibers enabled increases in total protein loading (both per unit area and per volume), in agreement with other published work on immobilizing enzymes in/on nanomaterials. Activity retention after spinning was significant, at up to 92% and 68% when characterized using synthetic substrate at optimal pH and direct glucose measurement from hydrolysis in milk, respectively. Use of PEO and F127 polymers to prepare the nanofibers effectively stabilized enzyme activity over time in both dry and humid storage conditions for up to 4 weeks. It is hypothesized that the Pluronic-F127 block copolymer protected the enzyme against surface induced hydrophobic denaturation during spinning and against disassociation of protective water

molecules during storage. Fluorescence microscopy and image analysis confirmed uniform enzyme distribution within uniformly cylindrical nanofibers. Nanofibers were also determined to have a dissolution rate of 0.14 cm^2/s by dissolving the nanofiber mats in water. The dissolution time was comparable to dissolution and swelling rates of water soluble polymers and drug delivery systems, which supports their utilization in enzyme stabilization and delivery systems.

CHAPTER 4

IMMOBILIZATION OF CHYMOTRYPSIN ON HIERARCHICAL NYLON 6,6 NANOFIBER IMPROVES ENZYME PERFORMANCE

4.1 Abstract

Immobilized enzymes enable advances in bioprocessing efficiency and bioactive packaging. Enzyme immobilization onto macroscale solid supports is often limited by low protein loading, inadequate access to substrate, and non-ideal orientation to the solid support; immobilization on nanomaterials has improved activity retention and enabled improved performance in extreme environments, yet has practical limitations including handling, recovery, and unknown toxicological risks. This work describes the immobilization of chymotrypsin to nylon 6,6 in two formats: electrospun nanofibers and planar films. Protein loading and enzyme activity were compared to that of a commercially available system (chymotrypsin on agarose beads). Electrospun nylon 6,6 nanofibers had an average fiber diameter of 161 ± 73 nm, improving protein loading compared to its planar macroscale counterpart. Chymotrypsin immobilized onto nylon nanofibers exhibited shifts in both working optimum pH and temperature with an increase from pH 7.8 to pH 9, and increased optimum temperature by 10°C compared to free enzyme. The nanofibers also improved activity retention and enhanced thermostability compared to native enzyme, enzyme on planar films, and the commercial standard. This work demonstrates the potential of hierarchical nanomaterials in improving enzyme performance, leveraging benefits of both nano and macroscale supports.

This chapter has been submitted for publication – Wong, D.E.; Senecal, K.J.; Goddard, J.M. Immobilization of chymotrypsin on hierarchical nylon 6,6 nanofiber improves enzyme performance. *Process Biochemistry*. **2016**.

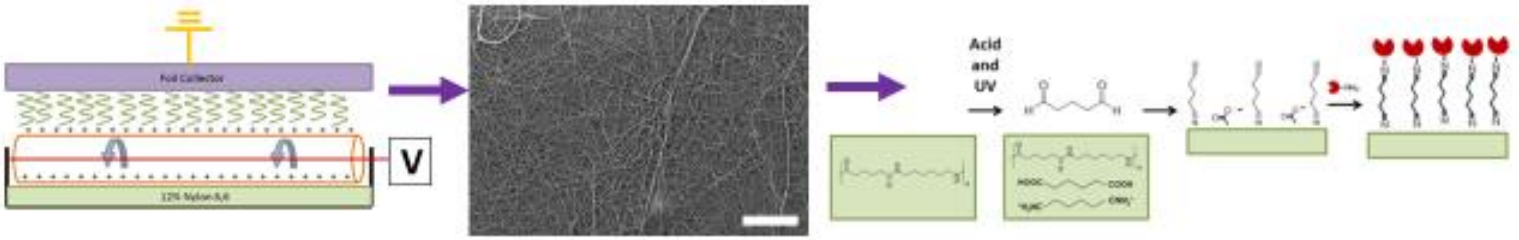

Figure 4.1. Graphical abstract

4.2 Introduction

Enzymes are highly specific biological catalysts, capable of improving specificity and efficiency in a range of bioprocessing applications. Often enzymes reacted batch-wise to food processing systems must be added in excess increasing material waste, and must be deactivated before the product is packaged. Immobilized enzymes take advantage of various attachment and coating schemes in order to allow for recovery, regeneration, reuse, and appropriate dosing of enzymes. Enzyme immobilization has also been shown to increase the thermostability, pH stability, and overall storage stability of the enzyme *(128-130)*. However, immobilization often adversely impacts enzyme performance due to denaturation and incorrect protein orientation during attachment *(131-133)*. Methods to increase activity include achieving higher protein loading and increasing retention of enzyme activity after immobilization to the solid support.

The chemical and physical attributes of the solid support in an immobilized enzyme system influence the success of enzyme immobilization. When creating biocatalytic materials, the biocompatibility, mechanical resistance, and chemical structure of the solid support must be considered. One physical characteristic that influences both protein loading and retained enzyme activity is solid support size. Decreasing the dimension of the solid support to the nanoscale results in substantial increases the total surface area per mass as well as unique physiochemical characteristics of the material. These unique properties of nanomaterials have enabled advances in their research for applications in electronics, sensors, medical devices, drug delivery, and food and agriculture *(134-139)*. Indeed, nanomaterials exhibit a significantly higher surface area to volume ratio than their macroscale counterparts, and are often able to maintain and even

improve tensile, mechanical, and wetting properties of the bulk material *(140-143)*. Increased surface area enables increased enzyme immobilization and has been shown to influence activity retention of immobilized enzyme by affecting protein-protein and protein-material interactions *(16, 144)*. Immobilization to nanoscale materials has also been shown to increase enzyme thermostability and pH stability *(144-146)* and enables improved performance due to fewer diffusion limitations, creating a microenvironment that mimics that of free enzyme *(128, 144)*. Indeed, much of the research on improving immobilized enzyme performance on nanomaterials has focused on nanoparticles. Klein *et al.* explored the effect of chitosan nanoparticle size on immobilized β-galactosidase for lactose hydrolysis. B-galactosidase on nanoparticles were found to have higher activity retention, but lower thermostability *(147)*. In one work, performance of β-galactosidase on magnetic core nanoparticles improved with reducing nanoparticle diameter, yet with decreasing diameter came a corresponding increase in recovery time to commercially impractical timeframes (17 hours for 18 nm nanoparticles) *(82)*. Further, the size of the nanoparticles makes it difficult to verify that 100% of all material has been recovered. There has therefore been a motivation to explore immobilization of enzymes on hierarchically structured materials in which both nano and macroscale size domains enable the performance retention of nanomaterials but the improved handling and recovery of macroscale supports.

Electrospinning is an emerging method for nanomaterial production that is applicable to many polymer solutions, and can be scaled-up. Electrospinning produces nanoscale fibers as non-woven fiber mats by the application of a high voltage to liquid polymer solutions as it passes through a tight capillary. The polymer solution builds

positive charge at its surface, and is drawn to a grounded collector by the formation of a Taylor Cone *(84)*. The drawn polymer dries by the whipping action and movement during collection. By using the same charge build-up and drying principles, needle-less electrospinning uses a charged rotating wire to produce large (up to 1.6 m wide, roll-to-roll) non-woven nanofiber sheets commercially **(Fig. 4.2)** *(148-152)*. Polymer nanofibers represent a commercially scalable hierarchical material, with nanofibers of dimensions ranging from <100 to 800 nm, and webs of material formed on a much larger (centimeters to meters) scale.

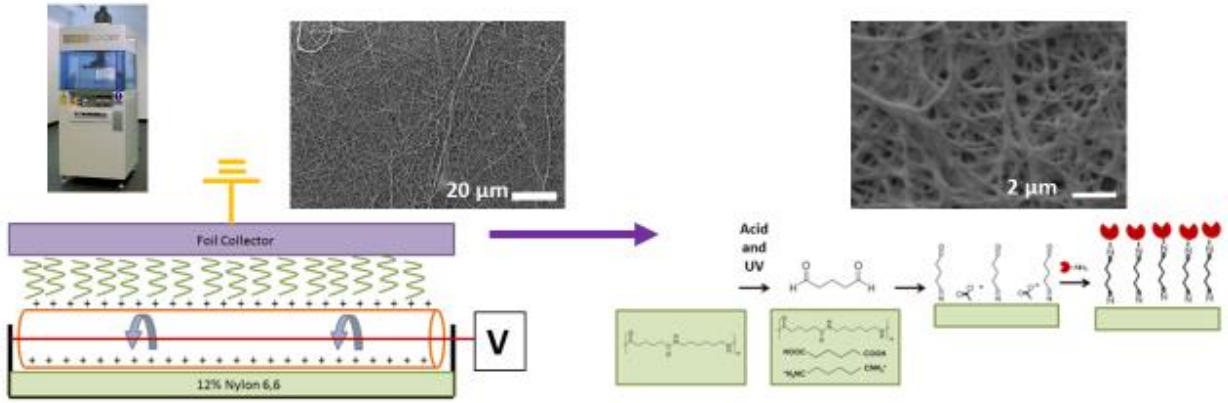

Figure 4.2. Schematic of material production and material functionalization. Immobilized chymotrypsin on electrospun nylon 6,6 nanofiber mats, planar nylon 6,6 films (NF-CT, Film-CT)., and agarose beads were compared.

Nanofibers can be readily functionalized and have served as enzyme supports in biosensors, drug delivery, active packaging and tissue regeneration applications *(153-156).* Work by Ge *et al.* tested the antimicrobial ability of glucose oxidase immobilized onto polymer composite nanofibers in order to increase shelf-life *(39).* A study conducted by Campbell *et al.* evaluated enzyme-enzyme interactions and nonspecific attachments of peroxidases and glucose oxidase immobilized to carbon nano-supports. They found maximizing activity on a nano-support was dependent on enzyme-material compatibility and solid support characteristics such as curvature and chemical make-up *(157).* While previous works have demonstrated improvements in enzyme performance after immobilization on nanofibers, there remains an opportunity to explicitly demonstrate the influence of immobilization on nanoscale and macro-scale materials of the same composition on enzyme performance.

In this work, chymotrypsin, an enzyme used in the food industry for beverage clarification and protein digestion, was immobilized onto amine functionalized nylon 6,6 nanofibers and planar films via glutaraldehyde. Enzyme performance was characterized by protein loading, activity retention, determination of kinetic parameters, and both pH and thermostability. Performance was further compared to that of free chymotrypsin.

4.3 Experimental

4.3.1 Materials

Sodium phosphate monobasic monohydrate, sodium phosphate dibasic heptahydrate, potassium phosphate monobasic, potassium phosphate dibasic, sodium dodecyl sulfate, formic acid (88%), and dimethylformamide were purchased from Fisher Scientific (Fairlawn, N.J., U.S.A.). Glutaraldehyde (25%) was purchased from Alfa Aesar

(Ward Hill, Mass., U.S.A). Type II lyophilized α-chymotrypsin (BRENDA *Bos taurus* UniProt P00767 pBLAST, E.C. 3.4.21.1) from bovine pancreas (40 units/mg), nylon 6,6, N-Succinyl-Ala-Ala-Pro-Phe *p*-nitroanilide (NSPN), L-lysine (>98%), and picrylsulfonic acid solution (TNBS) (5% wt./vol) were purchased from Sigma-Aldrich (St. Louis, Mo., U.S.A.). The Pierce BCA Protein Kit was purchased from Thermo Scientific (Waltham, MA., U.S.A.).

4.3.2 Methods

4.3.2.1 Purification of Commercial Chymotrypsin on Agarose Beads (ProteoChem Bead-CT)

Chymotrypsin immobilized agarose beads were purified before use. Equal amounts of ProteoChem Bead-CT and 0.1M, pH 7.8 potassium phosphate buffer were mixed and centrifuged at 6000 rpm (2000 x g). The resulting supernatant was removed and replaced with additional buffer. ProteoChem Bead-CT beads were washed three times with buffer and stored at 4°C in buffer for further use. The total protein on ProteoChem Bead-CT was determined by the BCA assay, where 2mL of working reagent was reacted for 30 min at 37 ^{o}C with 0.1 mL of sample, followed by reading absorbance at 562 nm and comparison to a standard curve of BSA in potassium phosphate buffer.

4.3.2.2 Immobilization of Chymotrypsin on Nylon 6,6 Planar Films (Film-CT) and Nanofibers (NF-CT)

To characterize the influence of support topography on immobilized enzyme performance, chymotrypsin was immobilized onto amine-functionalized nylon 6,6 via glutaraldehyde cross-linking in the formats of both planar films and electrospun nanofibers **(Fig. 4.1)**. Chymotrypsin was purified by passing rehydrated protein through

a 0.22 μm PTFE syringe filter, and subsequent separation using centrifugal filtration (MWCO 10,000). Purified α-chymotrypsin was rehydrated in 0.1M, pH 7.8 potassium phosphate buffer, and stored at 4°C until further use. Nylon 6,6 films (2 x 2 cm) were washed prior to surface modification in isopropanol, acetone, and water. Cleaned films were subjected to surface acid hydrolysis in 3M HCl for 30 min, followed by rinsing for 5 min in deionized H_2O. Washed films were stored dry at room temperature for further analysis. Both sides of the films were exposed to 30 min UV-ozone treatment, at 3 cm from the light source (JeLite, FL) to generate primary amine groups on the film surface. Film surfaces were exposed to 28 mW/cm^2 UV light at 254 nm. Films were reacted in 5% (v/v) glutaraldehyde in 0.1M, pH 7.8 potassium phosphate buffer for 1 hr prior to chymotrypsin conjugation for 1 hr in 1000 μg/mL α-chymotrypsin (0.1M, pH 7.8 potassium phosphate buffer). All assay solutions were prepared at volumes of 1 mL/cm^2 material.

Nanofiber mats were prepared by electrospinning a solution of nylon 6,6 in formic acid (12 w/v%). Nanofiber mats were produced by needle-less electrospinning in an Elmarco Nanospider (NS Lab 1WS500) running between 45 and 47 kV to an aluminum foil covered flat collector 14 cm from the polymer source **(Fig. 4.1)**. Positively charged taught wires move through a trough filled with polymer solution, forming droplet nodes along the wire surface. Nanofibers are drawn to a grounded collector directly above the rotating wires, generating a 45 × 20 cm mat of nanofibers. Nanofiber mats were collected after 1 hr of electrospinning, and cut into 1.5 cm diameter circular nanofiber mats by a circular die. Nanofiber mats were removed from the collector foil and subjected to 20 min UV-ozone treatment to introduce primary and secondary amines

to the fiber surface *(158, 159)*. Amine functionalized nanofiber mats were then reacted in 5% (v/v) glutaraldehyde solution in 0.1 M, pH 7.8 potassium phosphate for 1 hr, followed by enzyme conjugation in 1000 μg/mL α-chymotrypsin (0.1M, pH 7.8 potassium phosphate buffer) for 1 hr. All conjugation solutions were prepared at 1 mL/cm^2 nanofiber mat.

4.3.2.3 Protein Quantification on Nylon 6,6 supports

The amide bonds of nylon 6,6 interfere with the BCA protein assay reagents, therefore the TNBS primary amine assay was used to indirectly quantify protein content of chymotrypsin immobilized on planar and nanofiber nylon 6,6 supports, with glutaraldehyde activated supports as controls. NF-CT mats were incubated at 37°C in 0.5 mL of 0.1M, pH 8.5 sodium bicarbonate buffer with 0.01% (v/v) TNBS while shaking. The reaction was stopped after 2 hrs with 0.25 mL 10% SDS, and absorbances were read at 410 nm. Film-CT was characterized using the same method, but with increased assay volume. All assay substrate concentrations and volume ratios in relation to each other remained the same. Films were submerged in 2 mL buffer, 1 mL TNBS, and 1 mL SDS to accommodate the film shape. The primary amine concentration determined by TNBS was converted to estimated total protein content using values of available primary amines per enzyme and enzyme molecular mass provided by the BRENDA database (BRENDA *Bos taurus* UniProt P00767 pBLAST, E.C. 3.4.21.1).

4.3.2.4 Chymotrypsin Activity

Activities of free enzyme, NF-CT, Film-CT, and ProteoChem Bead-CT were measured using the synthetic substrate, NSPN, by a modification of the method outlined by DelMar and Kaspar *(160, 161)*. A solution of NSPN was prepared to 20 mg/mL in

DMF and stored at 4°C until use. Samples were submerged in 10 mM, pH 7.8 sodium phosphate buffer to which 30 µL of 7 mg/mL NSPN, diluted from stock in 10 mM, pH 7.8 sodium phosphate buffer, was added. The final activity assay volume was 2 mL. Samples were incubated at 25°C, and absorbances at 420 nm were measured at regularly timed intervals through 60 min to quantify hydrolysis of *p*-nitroanilide from the synthetic substrate. Activity in µmol/min/g protein was calculated using only the linear change in absorbance. All activities were normalized to their respective maximum activities as activity per gram of protein for comparison.

Temperature and pH activity profiles and optima were determined by varying either temperature (every 5°C from 20°C to 60°C, constant pH value of 7.8) or pH (3-10, constant temperature of 25 °C). Buffers for pH activity profiles were prepared at 10 mM according to the target buffering pH ranges including sodium citrate (pH 3-5), potassium phosphate (pH 7-8), sodium phosphate (pH 7.8), and sodium carbonate (pH 9-10). The thermostability for immobilized chymotrypsin was determined by evaluating enzyme activity retention after 12 hrs incubation at 30, 40, 50, and 60ºC in 10mM, pH 7.8 sodium phosphate buffer.

Michaelis-Menten Kinetic constants were determined at the optimum temperature and pH established for free enzyme (pH 7.8, 25°C) using the synthetic substrate, NSPN, at concentrations of 1, 2, 4, 6, 8, and 10 µg/mL prepared from the 20 µg/mL stock solution. Measurements were taken at regular intervals over 30 min at 420 nm.

4.3.2.5 Scanning Electron Microscopy (SEM)

Scanning electron micrographs were captured on a benchtop SEM (JEOL Neoscope JCM 6000) operating at 10 kV (Nikon Instruments, Inc. Melville, NY). To

prevent surface charging, samples were coated with 20 nm of gold utilizing argon gas by a Cressington Sputter Coater 108auto (Watford, UK) prior to microscopy. Nanofiber diameter was determined by image analysis of electron micrographs, using ImageJ (NIH). A total of 75 diameters were measured, representing 25 diameters from each of 3 independent micrographs, acquired under the same magnification.

4.3.2.6 Surface Area (Quantachrome Autosorb iQ)

Total surface area of the nanofiber mats was calculated using Brunauer-Emmett-Teller Theory *(162-164)*. Up to 10 mg of nanofiber mat were outgassed in multiple steps; 90 min at 35°C, 90 min at 60°C, 180 min at 90°C, and finally 110°C for 240 min to drive off residual solvent without heat damage to the nanofiber mat. Adsorption and desorption isotherms were created using liquid and gaseous nitrogen, with helium backfill on a Quantachrome Autosorb iQ (Florida, U.S.A.). A multipoint analysis was composed of up to 20 relative pressures between 0 and 0.2 p/p_0 and Brunauer-Emmett-Teller calculations were applied by Quantachrome software.

4.3.2.7 Statistical Analysis

Unless otherwise noted, all determinations were performed in quadruplicate, and values are representative of independent experiments performed on two separate days. One-Way Analysis of Variance (ANOVA) with Tukey's pairwise comparison post-test ($p<0.05$) and Michaelis-Menten kinetic constants were calculated using GraphPad Prism (v. 5.04, GraphPad Software, La Jolla, CA).

4.4 Results

4.4.1 Surface Area and Morphology of Solid Supports

Electron microscopy and gas sorption surface area quantification were performed to characterize the morphology of immobilized enzyme systems. Electron micrographs revealed a smooth, uniform surface for clean nylon 6,6 film. Nylon 6,6 nanofibers were produced in a non-woven mat of 0.177 ± 0.012 mm thickness with smooth and cylindrical morphology, with an average diameter of 164 ± 73 nm **(Fig. 4.3)**. Surface modification and enzyme immobilization caused loss of distinctive fiber shape due to chymotrypsin coating, with fiber junctions appearing to join the mat into a cohesive network. ProteoChem Bead-CT exhibited a typical spherical morphology with a smooth, uniform surface **(Fig. 4.4)**. Surface area of ProteoChem Bead-CT was variable due to the range of bead diameters, with up to 3468 cm^2/g surface area compared to 23.05 cm^2/g of the planar film. In contrast, nanofiber mats presented up to 81.23 m^2/g total surface area by gas sorption, an increase in available surface area of ~ 40,000 times that of the planar film, and ~ 250 times that of the commercial agarose bead.

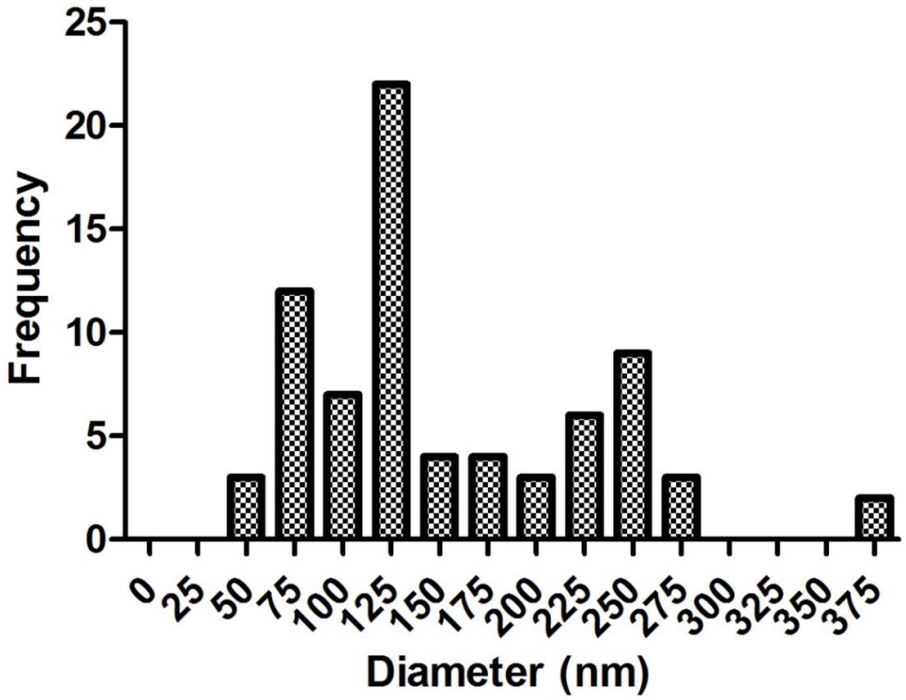

Figure 4.3. Diameter distribution of electrospun nylon 6,6 nanofiber mats. Diameter data was determined by ImageJ analysis of SEM images at 5000x magnification. Twenty-five measurements were collected from each of three images, n = 75. The average diameter was calculated as 164±73 nm.

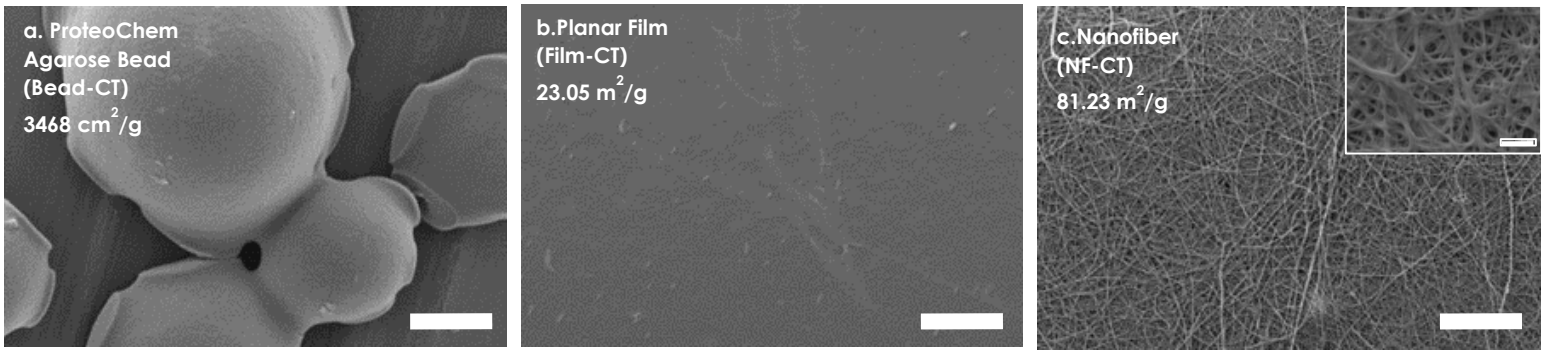

Figure 4.4. Morphology of immobilized chymotrypsin systems [a) ProteoChem Bead-CT, b) planar nylon 6,6 film, c) electrospun nylon 6,6 nanofibers] as determined by scanning electron micrographs (1000× magnification) where scale bars represent 20 µm. Inset of functionalized nanofiber material (NF-CT) with scale bar representing 2 µm at 10000× magnification. Reported values of surface area per mass solid support were determined by BET theory on nitrogen adsorption isotherm.

4.4.2 Protein Loading on Macro and Nanoscale Supports

Protein loading on nylon supports was quantified by the TNBS primary amine assay, using numbers of primary amines per enzyme and enzyme molecular weight reported in the BRENDA database (*Bos taurus* UniProt P00767 pBLAST, E.C. 3.4.21.1). Protein content was used to compare enzyme activity retention per mass protein, as well as to demonstrate the influence on material morphology on protein loading capacity. Film-CT presented 0.005 µg protein/mg solid support, while NF-CT had 1.63 µg protein / mg solid support. This 326 fold increase in protein per unit mass of solid support is not directly proportional to the increase in surface area achieved by introducing the nanoscale as would be expected from surface analysis data. The assay develops color by losing a sulfonic acid group and attaching onto primary amines, producing a chromatic response. However, TNBS is hydrophilic and may not have fully disassociated from the immobilized enzyme material which may account for lower than expected protein increase at the nanoscale *(33, 165, 166)*. As expected, the ProteoChem Bead-CT had the most conjugated protein at 18.7 µg/mg solid support. The observed differences in order of magnitude of protein content compared to the nylon 6,6 supports are due to differences in material synthesis. The reported nylon 6,6 immobilized enzyme system is prepared by immobilization of chymotrypsin on the surface of a solid support, whereas ProteoChem Bead-CT is prepared by crosslinking enzyme throughout the bulk of agarose beads

4.4.3 Activity Retention of Immobilized Chymotrypsin

The influence of solid support size and morphology on retention of enzyme activity after immobilization was determined by quantifying activity with a synthetic substrate (NSPN) at optimum parameters outlined by the supplier for free enzyme (25°,

pH 7.8) **(Fig. 4.5)**. Data are reported as percentage activity retention, by comparison to activity of free enzyme under the same conditions. ProteoChem Bead-CT exhibited and activity retention of 29.2% compared to free chymotrypsin. To enable parallel comparison to chymotrypsin on nylon immobilized enzyme systems, all activity retention assays were performed at 25°C, while the optimum temperature for ProteoChem Bead-CT is reported to be 35°C, likely influencing the observed retention of activity. Nevertheless, results from the temperature activity profile assays **(Fig. 4.5)** suggest that the general trend of enzyme activity retention between the three systems (NF-CT>Bead-CT>Film-CT) are expected to be the same regardless of temperature at which activity assays are performed. Immobilization of chymotrypsin on planar nylon films (Film-CT) resulted in a 96.5% reduction in activity (3.50% retained activity). Such a significant loss is similar to other reports of enzyme activity retention after immobilization on a planar polymer support. Wong *et al.* found lactase lost activity with increased protein mass through Layer-by-Layer deposition *(32)*. Rodrigues *et al.* proposed that loss of cellulase and alcohol dehydrogenase activity on Langmuir-Blodgett films was due to enzyme packing patterns and the surface environment, not denaturation *(167-169)*. In contrast, despite use of the same solid support (nylon 6,6) and the same bioconjugation chemistries (amine to amine conjugation by glutaraldehyde cross-linker), NF-CT retained 55.6% of free chymotrypsin activity. These results support our hypothesis that immobilization on nano-scale solid supports improves retention of enzyme activity.

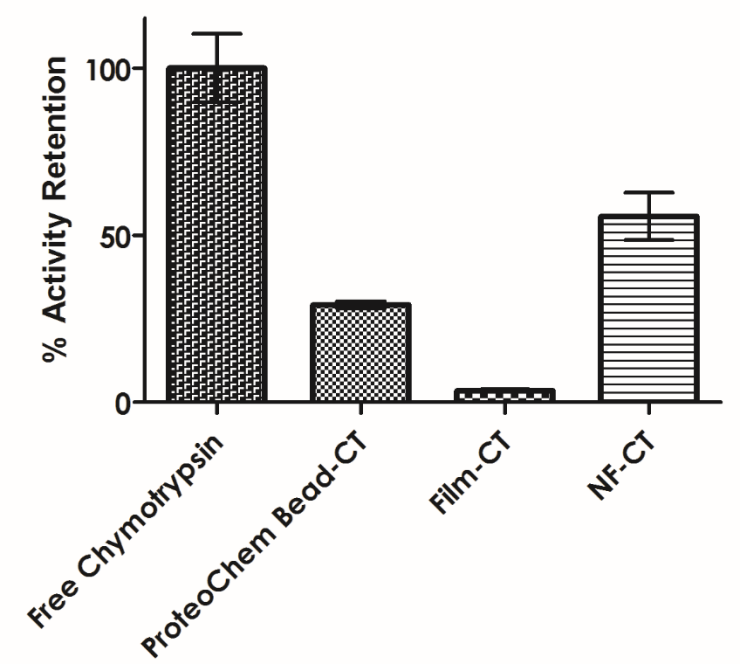

Figure 4.5. Percent activity retention compared to free chymotrypsin at 25ºC and pH 7.8. Values represent means ± standard deviations of n=8 determinations (quadruplicate determinations on each of two independent days).

4.4.4 Immobilization Shifts pH and Temperature Activity Profiles

To characterize the influence of enzyme immobilization on performance at varying pH values and temperatures, pH and temperature activity profiles were created by varying pH at constant temperature (25°C, **Fig. 4.6**) or varying temperature at constant pH (pH 7.8, **Fig. 4.7**). Data are presented as relative activity, normalized to maximum activity at the optimum pH for each immobilized enzyme system. All immobilized enzyme systems experienced shifts in the optimum pH compared to free enzyme. Free chymotrypsin presented the sharpest activity profile, with the highest activity at the established pH 7.8 and relative activities below 0.5 at all other pH values. ProteoChem Bead-CT retained relative activities above 0.5 at pH 6 and above with its optimum matching that of free chymotrypsin at pH 7.8 and pH 8.0. Immobilization of chymotrypsin on the modified nylon supports resulted in a left-skewed pH activity profile, suggesting that the reported bioconjugation chemistry (amine to amine via

glutaraldehyde) shifted the working range of chymotrypsin to more basic conditions. Film-CT presented a pH optimum at pH 8.0 with significant activity retention at pH 9.0-10 and below 50% activity below pH 7.0. The observed increase in pH optimum was more pronounced for NF-CT, with an optimum pH between pH 9.0 and pH 10. These results are in agreement with prior reports where pH optima of immobilized enzymes shift towards higher, basic, values. For example, chymotrypsin immobilized with trypsin onto microspheres had its optimal pH shifted to pH 8.2 *(170).*

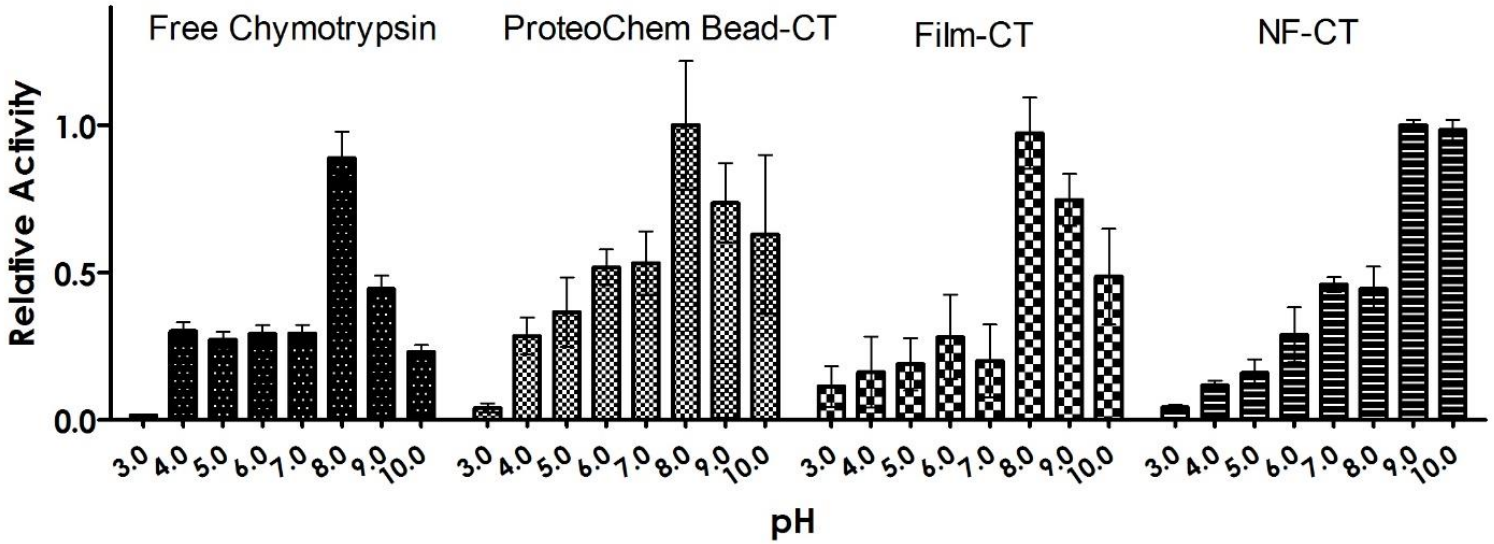

Figure 4.6. pH activity profiles of free and immobilized chymotrypsin. Activities have been normalized to maximum activity values of each immobilized enzyme system. Values represent means ± standard deviations of n=8 determinations (four sample determinations on each of two independent days).

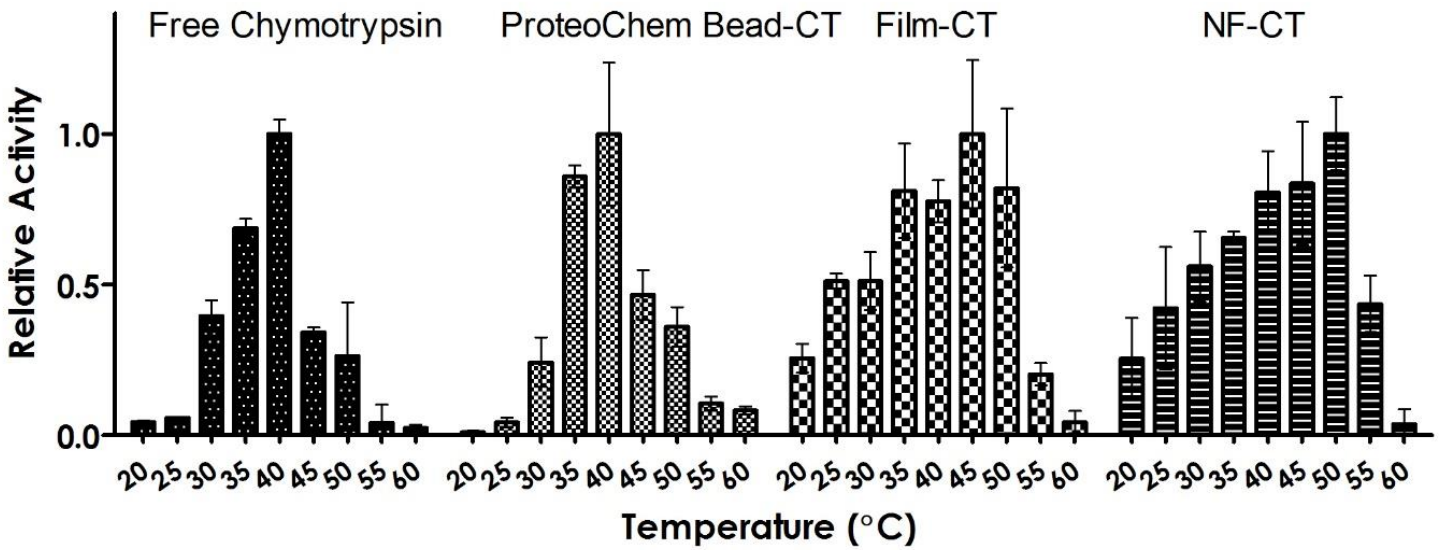

Figure 4.7. Temperature activity profiles of free and immobilized chymotrypsin. Activities have been normalized to maximum activity values of each immobilized enzyme system. Values represent means ± standard deviations of n=8 determinations (four sample determinations on each of two independent days).

Temperature activity profiles of immobilized enzyme systems were compared to that of free chymotrypsin by plotting relative activity (normalized to maximum activity values for each system) against temperature **(Fig. 4.7)**. It is interesting to note that despite the manufacturer supplied temperature optimum of 25°C, our results indicated that free chymotrypsin had an optimal temperature of 40°C, likely a result of differences in synthetic substrate. Both optimum and activity profiles of ProteoChem Bead-CT were similar to free enzyme, in support of ProteoChem recommended optima. Enzyme immobilization has been reported to shift temperature optima as well as enable overall activity retention over a broader range of working temperatures *(145, 146)*. Both Film-CT and NF-CT systems yielded similar temperature optima of 45-50 °C, with NF-CT exhibiting a slight increase in temperature optimum. Likewise, temperature activity profiles were similar for Film-CT and NF-CT systems, with at or above 0.5 relative activity values at temperatures of 30-50 °C. These results suggest that immobilization onto nylon supports by glutaraldehyde cross-linking improves the temperature working range, most notably for NF-CT, for which the percent activity retention was significantly higher than for Film-CT.

In addition to altering optimum working temperatures, enzyme immobilization can influence, stabilizing and often enhancing, thermostability by modification of its tertiary structure *(171-173)*. Such resistance to denaturation under extreme conditions such as extended exposure to elevated temperatures supports the utilization of immobilized enzyme systems in industrial bioprocessing applications. Here, the thermostabilities of free and immobilized chymotrypsin systems were determined by quantifying relative activity (by normalization to maximum activity for each system) at

times points up to 12 hrs during incubated at 30, 40, 50, and 60ºC **(Fig. 4.8)**. Free Chymotrypsin exhibited poor thermostability, with only 16.67% activity retention after 12 hrs at 30 °C, and 99.99% activity loss at 60ºC **(Fig. 4.8a.)**. ProteoChem Bead-CT also exhibited poor thermostability, with less than 10% retained activity after 4 hours incubation at any of the temperatures tested. Other reports note denaturation as a cause for thermal instability, but cross-linked alginate beads may influence autoproteolysis in solution *(174, 175)*. In contrast, Film-CT retained 68.03% activity after 2 hrs at 30ºC and maintained 23.41% after 12 hrs (Fig. 6c.). At further elevated temperatures of 40, 50, and 60ºC, Film-CT did not retain observable activity after incubation. It is worth noting that while Film-CT had an apparent improvement in thermostability at 30 °C compared to Bead-CT, the overall loss of activity (reported in **Fig. 4.5**) was higher for Film-CT, so the apparent improvement in thermostability is likely not of practical significance. In contrast, NF-CT retained over 30% activity after 12 hrs at 30, 40, and 50ºC. After 2 hrs at 30ºC, NF-CT retained 94.22% activity, and 88.05% after 12 hrs of incubation. NF-CT maintained 64.84% activity at 40ºC and 30.25% at 50ºC after 12 hrs **(Fig. 4.8d.)**. Only at 60ºC did NF-CT lose activity (98.65%) similar to that of free chymotrypsin, ProteoChem Bead-CT, and Film-CT. The observed higher standard deviation for NF-CT values is likely a result of the variability of fiber diameters.

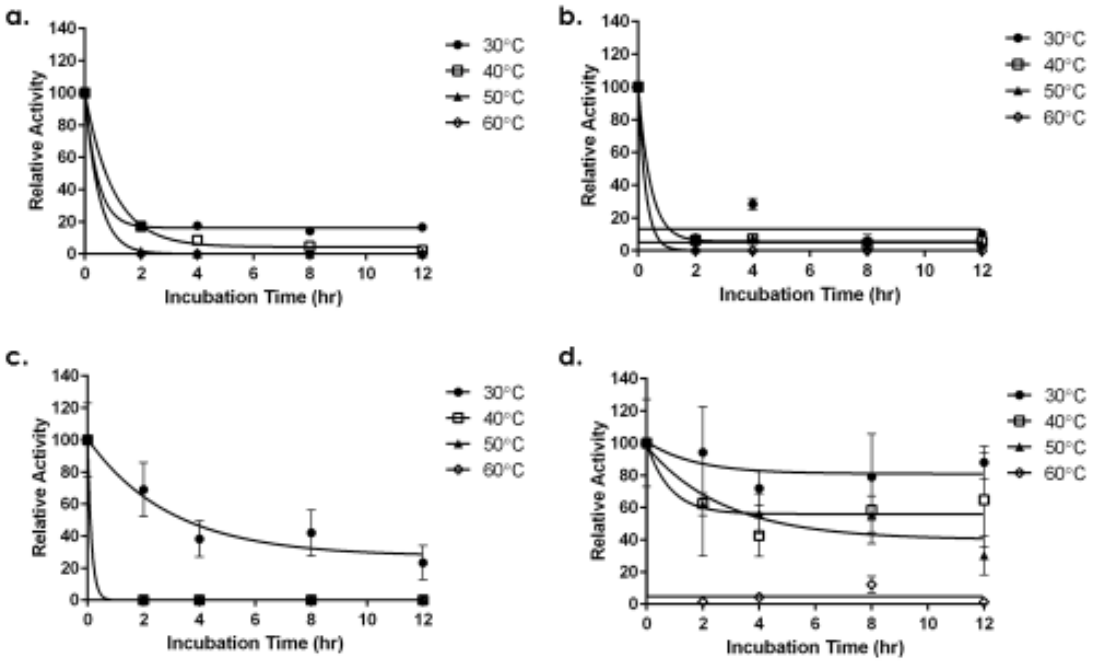

Figure 4.8. Thermostability of a. free chymotrypsin, b. Bead-Ct, c. Film-CT, and d. NF-CT. Activities have been normalized to the maximum activity of each enzyme system observed, and were assayed against controls of solid support and glutaraldehyde. Values represent means ± standard deviation of n=4 determinations and are representative of experiments performed on two independent trials. Models of inactivation (one-phase exponential decay) have been fitted to the values.

These results suggest that the activity retention of the macroscale solid support, Film-CT, performed similarly to the industry standard, ProteoChem Bead-CT, and did not retain more activity after incubation than free chymotrypsin. As noted previously, the nanofiber mat support for NF-CT has about 40,000 times more surface area due to its nanoscale than the planar film. Both macroscale supports lost enzymatic activity similarly to that of free chymotrypsin, most lost after 2 hrs at all temperatures. Chymotrypsin immobilized on the nanoscale material retained more activity at higher temperatures.

4.4.5 Michaelis-Menten Kinetics

Michaelis-Menten kinetic constants were calculated for each immobilized chymotrypsin system by determining the amount of product produced over time for a

range of synthetic substrate concentrations. First, it must be assumed the enzyme system is saturated with substrate and that there is only one active site available for catalysis. The amount of product released over time, or enzyme velocity, was graphed versus substrate concentration for Michaelis-Menten constant calculation. All constants were compared to those determined for free chymotrypsin **(Table 4.1)**.

Table 4.1. Michaelis-Menten kinetic constants of free and immobilized chymotrypsin determined at 25°C and pH 7.8 with NSPN concentrations ranging from 1 – 20 mg/mL. Different superscript letters indicate significant differences at p<0.05.

	Relative Activity (%)	V_{max} **(mM/s)**	K_m **(mM)**	k_{cat} **(1/s)**	k_{cat}/K_m **(1/mM s)**
Free Chymotrypsin	100	5.92e-4 ± 7.0e-5 [a]	4.10 ± 1.5 [a]	1.48e4 ± 5.3e2 [a]	3611 ± 130 [a]
ProteoChem Bead-CT	29.2	4.01e-4 ± 1.6e-3 [a]	190 ± 48 [b]	2.00e3 ± 11 [b]	342.4 ± 0.014 [b]
Film-CT	3.50	6.57e-6 ± 2.0e-6 [b]	16.2 ± 6.5 [a]	1.99 ± 0.56 [c]	0.1230 ± 0.333 [c]
NF-CT	55.6	8.00e-4 ± 1.3e-4 [a]	5.84 ± 2.4 [a]	2.90e3 ± 70 [d]	496.2 ± 28.5 [d]

There were no significant differences in maximum velocity, V_{max}, for each immobilized enzyme system compared to free enzyme. Velocity was proportional to substrate concentration until V_{max} was reached. V_{max} was used to derive the constant, K_m, that represented the inverse relationship to substrate affinity. Substrate affinity is dependent on the substrate type itself as well as the immobilization method. In this case, ProteoChem Bead-CT had a K_m, significantly higher than the other systems, or lower affinity for the synthetic substrate was experienced during catalysis. It should be noted that low K_m, or high substrate affinity, can also hinder catalytic efficiency such that the enzyme-substrate complex will not disassociate quickly enough to create product efficiently.

The turnover number, k_{cat}, relates V_{max} to the enzyme concentration in the system. All immobilized chymotrypsin systems were significantly different from free chymotrypsin. This value represents the amount of substrate each active site was able to convert to product over time, and was therefore dependent on enzyme concentration. Increasing enzyme concentration increases the number of active sites available for catalysis. NF-CT had the highest k_{cat} relative to free chymotrypsin and Film-CT had the lowest k_{cat} relative to free chymotrypsin. Therefore NF-CT was able to create more product over time when compared to macro-scale supports which was supported by the large differences in protein content per unit mass of solid support. The catalytic efficiency, k_{cat}/K_m, tells of substrate specificity in combination with the speed at which the enzyme and substrate can form a complex for catalysis, and is limited by diffusion. Therefore, k_{cat}/K_m speaks to the number of collisions with substrate the enzyme experiences. All k_{cat}/K_m values were significantly different from free chymotrypsin. NF-

CT had the highest k_{cat}/K_m when compared to free chymotrypsin and Film-CT had the lowest k_{cat}/K_m, which indicated the support size and morphology affected the collision frequency and diffusion of substrate to immobilized enzyme. This may be in part to enzyme packing on the various solid supports.

These results are in support of prior works which demonstrate improved performance of enzymes after immobilization on nanoscale solid supports due to high interconnectivity and decreased mass transfer hindrance in the microenvironment *(176, 177)*. The observed increased catalytic efficiency may be due to the microenvironment created around the enzyme during immobilization. The smaller support may increase protein loading, but may make the enzyme believe it is in an environment similar to free enzyme. This influences overall substrate affinity and can reduce diffusion limitations taken into account during catalytic efficiency calculations.

4.5 Conclusions

In this work, chymotrypsin was immobilized onto nylon 6,6 supports in two size formats: as macroscale planar films and as electrospun nanofiber mats. Performance, pH and temperature activity profiles, and kinetics were characterized and compared to that of free and commercially available immobilized chymotrypsin. Nylon 6,6 nanofibers exhibited about 40,000 times more surface area per gram than planar film and about 250 times more surface area agarose beads. More potential sites for surface immobilization enabled an increase in enzyme activity retention. Previous works have shown immobilization can shift an enzyme's pH and temperature working ranges of an enzyme. The pH activity profile of chymotrypsin immobilized onto nylon supports was left skewed to higher pH optima values, and maintained more activity over a wider pH range.

Immobilization onto the nylon nanofiber resulted in increased thermostability with higher retained activity over a wider temperature range, and an increased temperature optimum of 50°C when compared to free chymotrypsin and chymotrypsin immobilized to macro-scale planar films and ProteoChem Bead-CT. NF-CT had an increased pH optimum, with the highest absolute activity at pH 9, and maintained 97% of that activity at pH 10. Chymotrypsin immobilized to macro-scale supports had similar pH activity profile as free enzyme. The determination of Michaelis-Menten kinetic constants showed NF-CT had similar maximum velocity and turnover rate compared to free chymotrypsin. The catalytic efficiency was higher for NF-CT than Film-CT and ProteoChem Bead-CT indicating chymotrypsin immobilized to the nanoscale supports experienced more diffusion related collisions with substrate that produced product than chymotrypsin immobilized to the other macro-scale materials. These results suggest that while the chymotrypsin was bound to a solid support, the nanoscale material may create a micro-environment that mimics free enzyme. Immobilized chymotrypsin was able to maintain the most activity and expand its working range while attached to nanofibers. Immobilization to nanoscale polymer materials effectively increases the surface area to volume ratio of a solid support, and may allow enzymes to experience reduced lateral interaction with neighboring proteins, in effect creating a microenvironment that is similar to that of free native enzyme. Utilization of hierarchically assembled solid supports for enzyme immobilization, as demonstrated here, may leverage benefits of both nano- and macroscale size regimes. Nanofibers improve enzyme performance in extreme environments similar to that observed after immobilization on nanoparticles, yet

assembly into a larger, macroscale mat enables handling and recovery to facility use in food and bioprocessing applications.

CHAPTER 5

CHYMOTRYPSIN ENCAPSULATION IN EMULSION ELECTROSPUN POLYCAPROLACTONE/POLY(VINYL ALCOHOL) FIBERS

5.1 Abstract

Enzyme immobilization by electrospinning into polymer nanofibers and surface immobilization of enzymes onto electrospun solid supports has increased protein loading, but not addressed activity loss due to bio-incompatibility. Even after subjection to high voltages, enzymes have withstood exposure to rapid drying techniques. Emulsion electrospinning allows enzyme introduction into water insoluble materials with a one-step process by bringing two immiscible phases together at various ratios to protect enzymatic activity and to create material with high surface area rapidly. Here, chymotrypsin is introduced to a polycaprolactone and poly(vinyl alcohol) emulsion (PCL/PVA) with the addition of a stabilizing emulsifier, Span 80, for electrospinning. Emulsion electrospinning quickly immobilizes enzymes and creates a multifunctional environment where protein is protected and easily incorporated into water insoluble materials. Chymotrypsin in PCL/PVA retained activity, had high protein loading compared to traditional immobilization to planar surfaces, and had stable kinetic efficiency and enhanced stability.

5.2 Introduction

Enzyme immobilization can extend activity in extreme environments, increase stability, and improve recovery and reuse which are all ideal traits for food processing and bioactive packaging. Enzyme processing systems in the food industry are marred by inefficiencies in material use, product throughput, time consumption, and cost – and

enzyme immobilization must overcome the limitations of low activity and low catalytic efficiency in order to benefit the food industry. There are many influences on immobilized enzyme retained activity like surface modification technique, temperature, and pH. Current technologies in enzyme immobilization including adsorption, embedding, and crosslinking which simplify dosing methods, have high loading efficiency, and expand working environments. However, these immobilized enzymes often suffer from limits of diffusion, denaturation, disadvantageous enzyme orientation, incompatibilities with the solid support, and deactivation by cross-linking procedures.

Embedding and encapsulation are successful immobilization means for enzyme delivery. Enzyme encapsulation methods have been widely used to protect catalytic activity and introduce proteins for various processes *(78, 178, 179)*. These materials often suffer from high solubility and low overall mechanical stability. Hydrophilic solid supports are often crosslinked in order to increase enzyme retention within the solid support and prevent material dissolution during catalysis in aqueous environments. To this effect, encapsulation has been widely studied for controlled release and time-lapse release of drugs *(180, 181)*. Examples of enzyme encapsulation include microcapsules composed of sol-gel, alginate, and Layer-by-Layer polymer assembly for timed release *(77, 179, 182, 183)*. Although, direct encapsulation can prevent important interactions at the material interface.

Enzyme immobilization success is in part dependent on bulk material properties and characteristics of the applied system. One material development method, electrospinning, produces non-woven fiber mats by employing a high positive voltage to draw fluid polymer through a capillary, from which an elongation allows the jet to dry as

it travels to a grounded collector. The changes in surface charge and surface tension at the tip of the capillary creates a stream of fibers stemming from the formation of a Taylor Cone *(84, 86, 184)*. Control of spinning parameters such as humidity, polymer concentration, solvent type, voltage, fluid flow rate, and distance allows for the production of versatile nanoscale fibers. Methods to produce electrospun nanofibers are advantageous for protein attachment and delivery in that nanoscale materials allow for increased surface area available for immobilization. Introduction of bioactive components to nanofibers are aimed at ease of production and ease of use. Nanofibers have been successfully explored as emulsion, drug, and protein carriers such that enzyme immobilization is a natural advancement in electrospinning *(94, 96, 185)*. The immobilization of enzymes onto nanofibers with traditional enzyme immobilization techniques has shown to improve catalytic efficiency and broaden the working pH and temperature optimum ranges of enzymes, and have increased control over bioactive material use *(96, 97)*, such that the formation of core/shell electrospun nanofibers and emulsion electrospinning has further increased studies of carrying bioactive ingredients.

Enzymes are water soluble proteins, and with a few exceptions, lose activity on hydrophobic surfaces. However, most successful inedible packaging and processing materials are composed of hydrophobic polymers and are water insoluble. Increasing biocompatibility of the material can in turn increase enzyme efficiency. Biocompatible polymers, like gelatin and chitosan, have served as components of electrospun fibers for targeted protein and drug delivery *(186-189)*. In order to incorporate water soluble proteins with hydrophobic polymers, non-woven fiber mats developed by emulsion/dual-phase electrospinning was employed.

An emulsion should contain two traditionally immiscible phases (continuous and dispersed) that when mixed form a solution of dispersed droplets of one phase in the other. Often the assistance of an emulsifier under the appropriate physical agitation is necessary to stabilize the emulsion from the natural drive to separate. Emulsion electrospinning combines the benefits of quick material production, scale-up, ease of preparation, and multifunctional material characteristics. Forming an emulsion for encapsulation can protect the enzyme and create a nanoenvironment that enhances enzyme usability, and can introduce alternative material strength and physical properties that may limit diffusion hindrances *(84, 142, 190)*. Other works have used emulsion electrospinning as a mechanism of physical enzyme protection that eases recovery and reuse. Li *et al.* emulsion electrospun proteinase K into poly(ethylene glycol)-poly(L-lactide) without the assistance of a dispersed polymer phase to observe retained activity, but also timed *in vitro* protein release *(191)*. Laccase emulsion electrospun in polylactide and PEO had a porous and core/shell morphology maintained over 50% of its original activity after 10 cycles of reuse *(192)*. Additionally, trypsin entrapped in PCL by emulsion electrospinning, also without polymer in the dispersed phase retained 66% activity with increased reusability *(193)*. Not only do these fiber mats protect protein, but also are designed for efficient *in situ* immobilization and recovery.

In this case, a dual-phase polymer preparation, will incorporate and protect immobilized chymotrypsin (**Fig. 5.1**). Poly(vinyl alcohol) (PVA), a food contact approved linear polymer composed of a carbon backbone containing alcohol group functionality, served as the "aqueous" polymer phase *(194-196)*. PVA can be electrospun at appropriate molecular weights, and has benefitted from the addition of cross-linkers

like glutaraldehyde to prevent solubility in water. Additionally, PVA can form gels at the appropriate temperature and water content. Polycaprolactone (PCL) formed the largest portion of emulsion, and was chosen for its biocompatibility that has been shown to support bioactive agents *(197-199)*. PCL is soluble in organic solvents that are not miscible with aqueous solutions which is appropriate for emulsion formation and encapsulation.

This work incorporated chymotrypsin with a water-soluble polymer, PVA, through an emulsion to increase the success of activity retention within a water-insoluble polymer, PCL. Both the compatibility of the enzyme with the polymer and possible microenvironment changes were considered for their influence on stability. Some benefits of enzyme immobilization which have included increased pH stability, thermostability, and storage stability have been outlined in previous chapters. Embedding the chymotrypsin in an aqueous phase will increase the biocompatibility and therefore activity retention of the enzyme. The materials are appropriate for food contact and mechanically stable with potential for functionalization.

This emulsion electrospun fiber for chymotrypsin immobilization aimed to increase retained activity of immobilized chymotrypsin in comparison to other immobilized enzymes and free chymotrypsin due to low protein loading and incompatibility with the solid support. The combination of nanoscale support and "aqueous" polymer phase should decrease detrimental protein-protein and protein-material interactions, allowing enzymes to behave more closely to free enzymes.

5.3 Materials and Methods

5.3.1 Materials

Polycaprolactone (PCL) [MW = 150,000] was purchased from Scientific Polymer. Poly(vinyl alcohol) (PVA) [MW = 130,000], Type II lyophilized α-chymotrypsin (BRENDA *Bos taurus* UniProt P00767 pBLAST, E.C. 3.4.21.1) from bovine pancreas (40 units/mg) and N-Succinyl-Ala-Ala-Pro-Phe *p*-nitroanilide (NSPN), p-anilide, nile red, fluorescein isothiocyanate isomer I (FITC), and Span 80 (sorbitane monooleate) were purchased from Sigma-Aldrich (St. Louis, Mo., U.S.A.). Sodium phosphate monobasic monohydrate, sodium phosphate dibasic heptahydrate, potassium phosphate monobasic, sodium carbonate, sodium bicarbonate, potassium phosphate dibasic, chloroform, methanol, PTFE syringe filters (0.22 µm), and dimethylformamide were purchased from Fisher Scientific (Fairlawn, N.J., U.S.A.). The Pierce BCA Protein Kit and Pierce MicroBCA Protein Kit were purchased from Thermo Scientific (Waltham, MA., U.S.A.).

5.3.2 Methods

5.3.2.1 Polymer Emulsion Fiber Preparation

The electrospinning polymer solution was prepared from solubilized PCL and PVA. PCL was solubilized overnight at room temperature to 12% (w/v) in an 80:20 solution of chloroform and DMF respectively. PVA was solubilized by heating to 80°C in DI water while stirring. PVA solutions were corrected for water loss during heating to form 12% (w/v) solutions. A polymer mixture was emulsified by adding Span 80 to PCL while stirring at 700 rpm, to which PVA was added drop-wise **(Fig. 5.1)**. After 15 min the final emulsion was further incorporated by subjection to a sonicator (Branson, CT,

U.S.A.) for 30 min. Emulsion stability was determined by visual inspection and optical microscopy for aggregation, ripening, and creaming instabilities. PCL/PVA and PCL/PVA-CT were made before use and electrospun immediately after preparation. The final emulsion was composed of 72% PCL, 8% Span 80, and 20% PVA with chymotrypsin (v/v). Fibers electrospun from this solution, herein referred to as PCL/PVA, served as controls for all following characterizations.

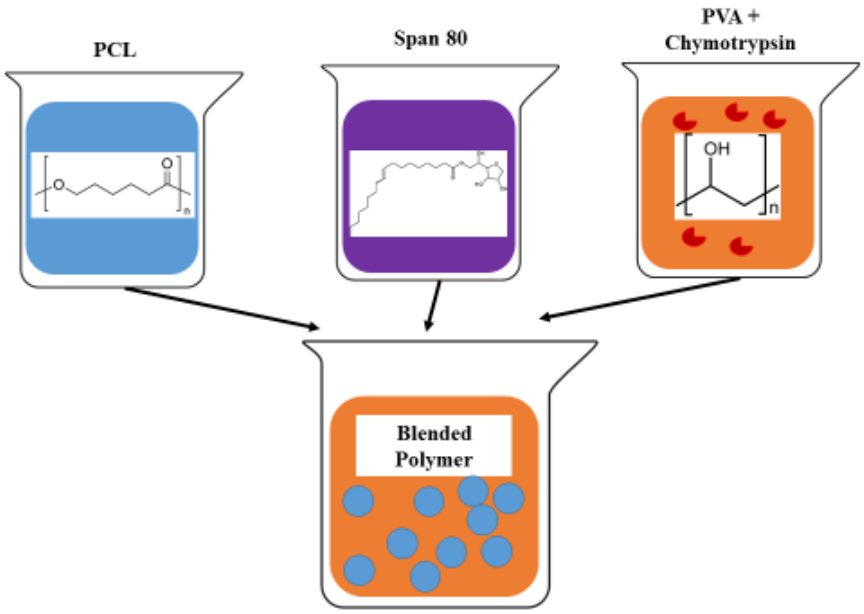

Figure 5.1. Components of blended polymer solution for electrospinning.

Chymotrypsin was purified before use by passing enzyme solubilized in 0.1 M, pH 7.8 potassium phosphate buffer through a 0.22 µm PTFE syringe filter. Purified enzyme was stored for further use at 4ºC. Protein concentration was determined by the BCA assay where a colorimetric response from the reduction of copper by peptide bonds was read at 562 nm after incubation at pH 7.8, 37°C for 30min. The protein concentration was calculated against a standard curve of BSA ranging from 0 to 2000 µg/mL.

Electrospun fibers containing chymotrypsin (PCL/PVA-CT) were prepared as above **(Fig. 5.2)**, except the 12% PVA polymer was prepared with purified chymotrypsin to achieve a buffered concentration of 1000 µg/mL before addition to PCL in water.

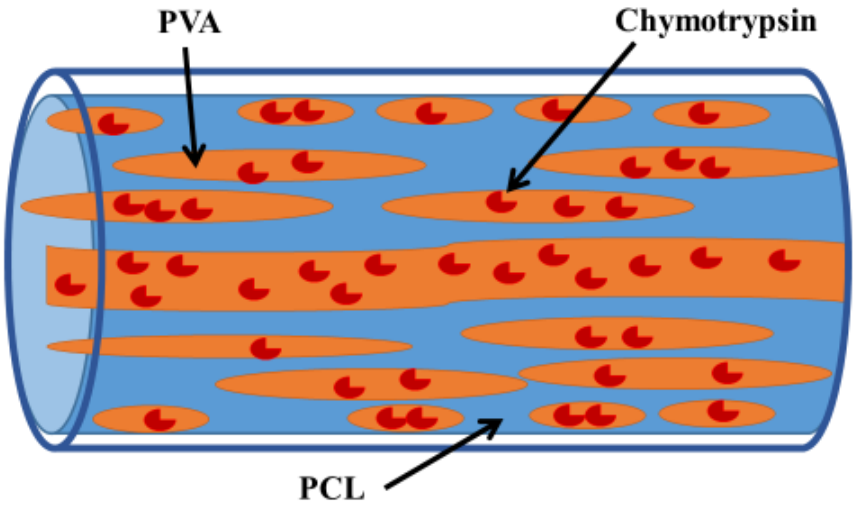

Figure 5.2. Proposed cross-section of chymotrypsin incorporated into dual-phase nanofiber. The dispersed phase experience elongation.

PCL/PVA solutions were passed through 22 gauge blunt needles at 1 mL/hr for electrospinning. Up to 20 kV were passed through the solution where dried fibers were collected on a grounded copper plate covered in aluminum foil 18 cm from the needle tip. Fibers were collected for 5 min, and normalized for all assays described by mass of nanofiber material.

5.3.2.2 Fiber Characterization

General fiber morphology was analyzed by electron microscopy. Fiber mats were sputter coated with 15 nm gold to prevent surface charging. Scanning Electron Micrographs were captured and the diameter distribution was created by ImageJ analysis of SEM micrographs from 20 measurements taken from each of 3 micrographs totaling

60 data points. Fibers were assessed for uniformity and morphology by Scanning Electron Microscopy (SEM). SEM micrographs were captured on both JEOL JCM 6000 (Neoscope) operating at (Nikon Instruments, Inc. Melville, NY) and FEI Magellan 400 XHR-SEM instruments. Samples were affixed to aluminum stubs with carbon tape and sputter coated with 10 nm of gold with argon gas by a Cressington Sputter Coater 108auto (Watford, UK) sputter coater. The JEOL 6000 operated at 10 kV and the Magellan operated at 5 kV. Micrographs were taken by the JEOL 6000 at 500, 1000, and 5000× magnification. Micrographs from the Magellan were captured at 10000, 20000, and 80000× magnification.

Additional imaging for verifying the stability of emulsion before electrospinning was performed by optical microscopy (images not shown), and by Confocal Laser Scanning Microscopy (CLSM). Fiber mat samples for CLSM were prepared prior to electrospinning. Nile red was prepared at 1 mg/mL in DMF in an amber vial and added to PCL prior to emulsification. For fluorescent tagging, chymotrypsin was purified in 0.1 M, pH 9 sodium carbonate buffer. A solution of FITC (1 mg/mL) was prepared in methanol and added at 1:1 molar ratio to free lysine attributed to the primary amino acid sequence of chymotrypsin by the BRENDA enzyme database (BRENDA *Bos taurus* UniProt P00767 pBLAST, E.C. 3.4.21.1). Tagged chymotrypsin was washed and recovered two times to remove excess dye. FITC tagged chymotrypsin was added to PVA prior to emulsification with PCL. CLSM micrographs shown were representative of samples at 40× and 60× magnification with oil immersion. All materials were stored in aluminum foil covered amber vials at 4°C to prevent premature quenching. Emulsions for

electrospinning and fibers were prepared in concentrations and methods stated previously.

5.3.2.3 Chymotrypsin Characterization

The protein content was imperative to assess the efficiency of the electrospinning process. The total protein content of the electrospun nanofiber mat can be compared to the concentration of protein introduced to the polymer emulsion for electrospinning as a ratio. BCA produces a color change indicative of protein in a system when copper in the working reagent is reduced by a peptide bond. The total immobilized protein content of fiber mats was determined by a modified MicroBCA assay and compared to a standard created by BSA within the detection range of 0.5 – 20 µg/mL. Nanofiber mats were submerged in 1 mL of 0.1 M, pH 7.8 potassium phosphate buffer and mixed with 1 mL of MicroBCA working reagent. Samples were incubated for 1 hr at 60ºC and read at 562 nm. Protein content is expressed as µg protein per mg of nanofiber material.

Protein leaching was monitored over 3 weeks of storage at 37°C. The storage method was altered from methods outlined for drug delivery and protein migration in materials *(94, 200, 201)*. Fiber mats (10 mg) were stored in closed clean vials 2 mL of 0.1M, pH 7.8 potassium phosphate buffer. At time of measurement, 1 mL of storage buffer was removed and assayed for protein content. Every sample was an independent vial, and samples were evaluated at weeks 0, 1, 2, 3.

Activity was expressed as the amount of *p*-nitroaniline produced from the hydrolysis of NSPN by CT per unit time and mass of protein present in a 2 mL reaction, where one *p*-nitroaniline is produced for every NSPN reacted. NSPN stock substrate was prepared at 20 mg/mL in DMF and diluted to necessary concentrations for activity and

kinetics with 10 mM, pH 7.8 sodium phosphate buffer. Nanofiber mats were submersed in 10 mM, pH 7.8 sodium phosphate buffer and reacted with 30 µL of 7 mg/mL NSPN at 25ºC. Activity was monitored over 20 min with measurements taken at regular intervals at 410 nm. All calculations utilized an empirically determined extinction coefficient (ε) of 4701 $mM^{-1}cm^{-1}$ from a standard curve of *p*-nitroaniline at concentrations of 0 to 0.5 mM in 10 mM, pH 7.8 sodium phosphate buffer. This extinction coefficient is in the same magnitude as previously reported extinction coefficients for *p*-nitroaniline and chymotrypsin at pH 7-8 (Chapter 4).

Thermostability of CT in PCL/PVA-CT was evaluated over 8 hrs where mats were stored at varying temperatures or pHs. Thermostability was determined at pH 7.8 in 10 mM sodium phosphate buffer and pH stability was determined at 25ºC. Samples were evaluated for activity at 0, 1, 2, 4, and 8 hrs using the 2 mL NSPN assay previously described for thermostability at 30, 40, 50, and 60°C. Additionally, long term stability in pH 3, 5, 7, and 9 was determined. Buffers for pH stability include 10mM buffers of sodium citrate (pH 3,5), potassium phosphate (pH 7), and sodium carbonate (pH 9). Measurements for pH stability were taken at 0, 1, 2, and 4 hrs. The optimum temperature and pH of CT in PCL/PVA-CT were evaluated at pH 7.8 and 25ºC respectively in the same manner described above.

Michaelis-Menten Kinetic constants were calculated from activity measurements performed at 0, 1, 2, 4, 8, 10, and 20 mg/mL NSPN. Velocities from activity measurements at 25ºC were used to calculate V_{max}, K_m, k_{cat}, and k_{cat}/K_m constants for comparison to previously published free and immobilized chymotrypsin kinetic data.

5.3.2.4 Statistical Analysis

All data sets are representative of 2 independent days of fiber mat production unless otherwise noted. Michaelis-Menton Kinetics and statistical significances were calculated in whole or in part by Prism GraphPad (v. 6.07, GraphPad Software, La Jolla, CA).

5.4 Results and Discussion

5.4.1 Fiber Characterization

The proposed fiber morphology **(Fig. 5.2)** indicated PCL as the continuous phase and PVA as the dispersed phase carrying chymotrypsin where enzyme would be encapsulated by the continuous phase. It was expected that electrospinning would cause stretching and elongation of the polymer components in order to pass through the capillary. With stretching characteristic of all electrospinning, the dispersed phases may experience the most deformation and elongation at the geometric center of the fiber cross-section due to the formation of the Taylor Cone *(202)*. Enzyme stability to shear has been documented in support of its retained activity in physical stress.

CLSM on the emulsion prior to electrospinning indicated the FITC tagged chymotrypsin in PVA formed the continuous phase even with though the emulsion contained 72% PCL in solution **(Fig. 5.5a)**. As PCL composed 72% of the polymer mixture prior to electrospinning, it was expected to form the continuous phase of the emulsion; however, CLSM revealed PCL to be the dispersed phase. Both the composition and the HLB value determine the stability and the phase orientation of the emulsion. PCL established itself as the continuous phase during electrospinning, composing the bulk of the fiber. The dual phase polymer mixture contained Span 80 in order to stabilize the

resulting emulsion and was selected for its ability to stabilize water in oil emulsions which have low HLB values. The Hydrophile-Lipophile Balance, or HLB, is accepted as a numeric system that assigns values to solution mixtures in order to choose appropriate emulsifiers *(203, 204)*. This emulsion was formed using low-energy emulsification (stirring and sonicator), and therefore had a large emulsifier requirement. Although this solution contained 8% Span 80, low-energy emulsifications have required up to 20% emulsifier for stabilization. As emulsifier concentrations increase, Ostwald Ripening destabilization decreases *(205)*. This emulsion composition was optimized for protein content and spinnability, where surfactants and emulsifiers vary viscosity that becomes an important parameter for successful fiber formation by electrospinning.

Electrospun fibers had an average diameters within the range of 117 nm and 1 μm **(Fig. 5.3)**. Fiber surface morphology was uniform, but the diameter distribution was wide. Diameter was consequential to the emulsion viscosity, voltage, and environment humidity. These electrospinning parameters can introduce variations in material that affect the enzyme characterization. SEM micrographs showed the fibers were cylindrical and contained no diameter variations along individual fibers. On further observation with the Magellan SEM at 10,000 × (inset) and 20,000× magnification, micrographs revealed rippled surfaces and cracking that were a result of rapid drying **(Fig. 5.4a)**. At 80,000× magnification, fiber surface contained dimples and pores. The surface pore characteristics support emulsion electrospinning as a success. PCL and PVA formed an emulsion, whose immiscibility allowed the creation of pockets or recesses in the fiber surface during solvent evaporation **(Fig. 5.4b)**. These recesses may have allowed substrate and product

to interact with chymotrypsin within the fiber. Both PVA/PCL and PVA/PCL-CT contained porous surface morphology.

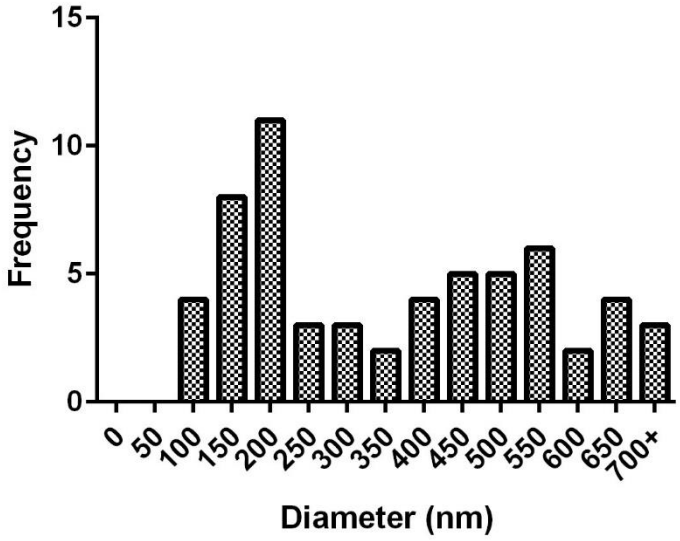

Figure 5.3. Diameter distribution of emulsion electrospun fibers from 3 micrographs captured at 1000x magnification and 5 kV. Diameter. Distribution was determined by 20 measurements taken from each micrograph, n = 60.

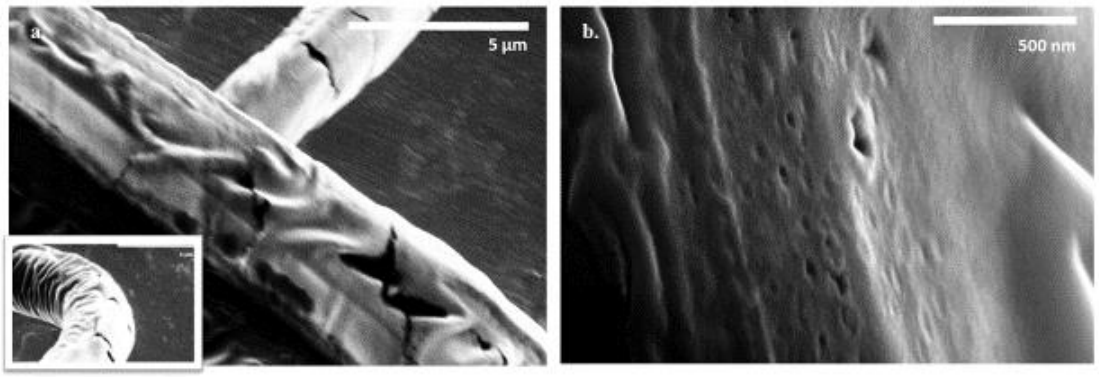

Figure 5.4. Micrographs of fiber surface captured at 5 kV a. 20,000× magnification, inset at 10,000× magnification, and b. 80,000× magnification.

CLSM micrographs were taken before and after electrospinning to observe chymotrypsin location throughout the solid support. The scale bar was representative of 2 µm and 1 µm **(Fig. 5.5)**. The PCL dispersed phase was not uniform in size distribution, but remained circular **(Fig. 5.5a)**. After electrospinning **(Fig. 5.5b)**, the phases appeared to switch, with PCL forming the bulk of the fiber as observed with nile red. FITC tagged chymotrypsin appeared on the surface of overlay images of electrospun fiber **(Fig. 5.5c)**. This indicated chymotrypsin availability for activity at the surface and the immiscibility of phases provided for chymotrypsin encapsulation.

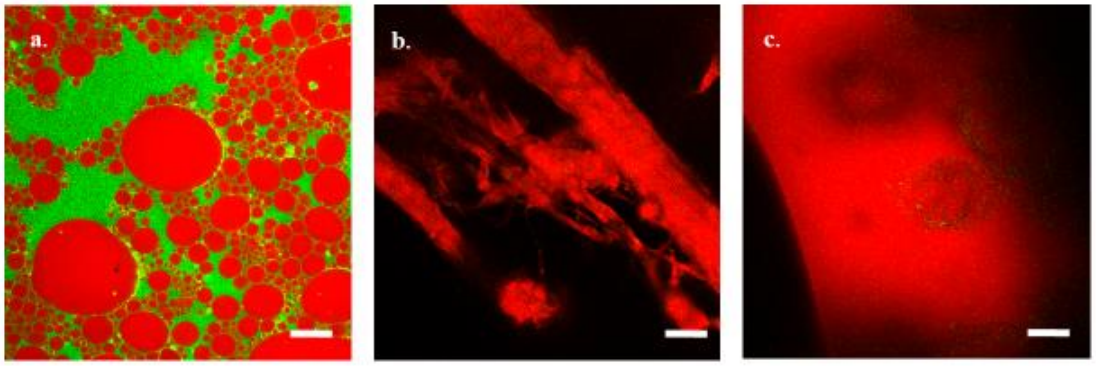

Figure 5.5. CLSM micrographs of emulsion at 40 × and 60× magnification a. prior to electrospinning at 40× where scale bar represents 2 µm , b. at 40× of electrospun fiber where scale bar represents 2 µm, and c. at 60× of electrospun fiber where scale bar represents 1 µm.

The amount of emulsifier present was reduced to increase polymer concentrations to achieve appropriate bead free fiber material. Various emulsifiers with low HLB values, like polyglycerol polyricinoleate, were tested in this emulsion system, but were found to create large dispersed phases or were not able to electrospin. Porras *et al.* suggest that water in oil stabilization is dependent on HLB value and ratio to solvents in nanoemulsions *(206)*. Here, emulsion stability was necessary only up until electrospinning to create dual-phase fibers. It has been suggested that shear force influences emulsion composition and stability when creating water in oil nanoemulsions *(207, 208)*. Under these conditions, low-energy emulsification created an oil in water emulsion with chymotrypsin and PVA as the continuous phase that under shear force from passing through a narrow capillary during electrospinning influenced a shift to a fiber of PCL continuous phase when forming PCL/PVA-CT

5.4.2 Immobilized Chymotrypsin Characterization

The total protein loading determined by the MicroBCA assay was 1.33 ± 0.243 µg/mg nanofiber. This is up to six times the protein content of surface immobilized planar nylon and on the same order of magnitude of surface functionalized nylon nanofiber. The emulsion nanofiber retained 32.5% activity of native chymotrypsin, or 58.45% activity retained by surface immobilized nanofiber chymotrypsin. Although encapsulated chymotrypsin experienced large activity loss, PCL/PVA-CT retained the activity of chymotrypsin immobilized onto a planar surface tenfold (Chapter 4).

Protein migration was monitored over 3 wks of storage at 37°C. Each sample contained 10 mg of fiber mat, equivalent to 13.3 µg protein. After 3 wks, no detectable

protein was found in the buffered storage solution where the detectable range of the MicroBCA assay is 0.5-20 µg/mL.

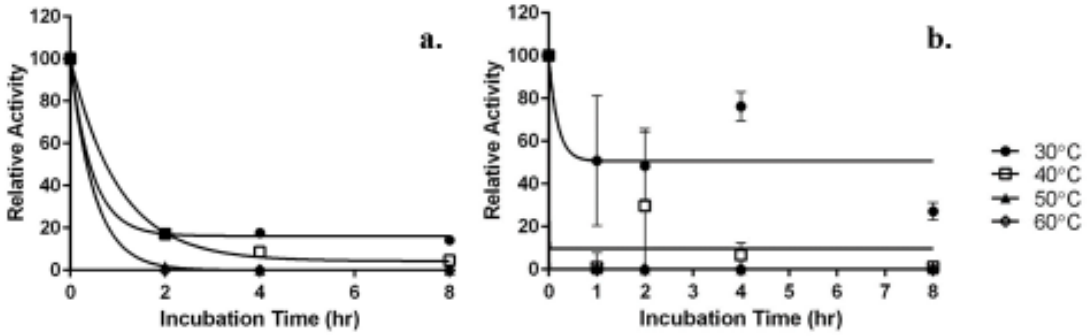

Figure 5.6. Thermostability of a. free chymotrypsin and b. PCL/PVA-CT at pH 7.8 for 30, 40, 50, and 60°C. Data is of n = 4 from one sample preparation, representative of samples prepared on two independent days. Models of one-phase decay have been fitted in order to discern differences between activity loss.

Thermostability was measured at the published optimum pH of free chymotrypsin of pH 7.8. Data shown was of 8 samples total from 2 data sets collected from independent days. Regression models of one-phase decay were fitted to the data **(Fig. 5.6)** in order to discern differences in activity behavior between temperatures. Free chymotrypsin was not thermostable outside of normal biological temperatures (37-39°C) for humans or bovine species (enzyme source). After 2 hrs at 40°C, 82% of free chymotrypsin activity was lost **(Fig. 5.6a)**. Encapsulated chymotrypsin in PCL/PVA-CT had increased thermostability at lower incubation temperatures of 30°C and 40°C, where PCL/PVA-CT had detectable activity through 8 hrs and 4 hrs of incubation respectively **(Fig. 5.6b)**. Having increased thermostability can introduce opportunities for extended use in food processing, especially where temperature is used for the overall safety of a product. Enzyme thermostability depends on the means of immobilization and active environment, and as emulsion electrospinning is versatile can lead to tailorable enzyme systems *(37, 129, 176).*

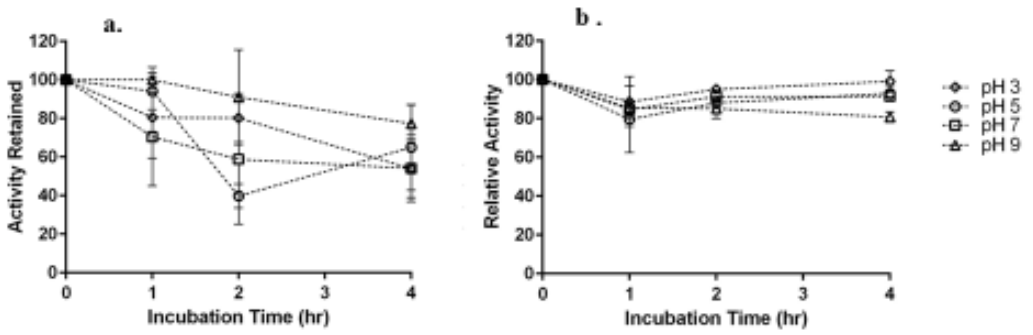

Figure 5.7. pH Stability of a. free chymotrypsin and b. PCL/PVA-CT at 25°C
For pH 3, 5, 7, 9. Data is of n = 4 from one sample preparation, representative of samples prepared on two independent days.

Alternatively, pH stability also allows for extended enzymatic use in processing environments, especially in the processing of acidic foods like fruit juices which generally have a pH below 4.5 *(6, 8).* Exponential non-linear regression models of decay were fitted to the data to compare differences in activity loss. Each figure depicts data from 4 samples of one trial whose trend is representative of trials over 2 independent days. Free chymotrypsin was stable for up to 4 hrs of incubation at the entire range of pHs between 3 and 10. PCL/PVA-CT retained more than 38.56% activity at all tested pH's after 2 hrs incubation, with most activities remaining greater than 54.03% of its maximum velocity at time 0, after 4 hrs of incubation.

PVA contains functional alcohol groups along its carbon backbone which can be protonated at high pH. Protonation, and retention of these alcohol groups may have created a nanoenvironment around the encapsulated chymotrypsin that caused higher activity losses than that of free chymotrypsin at non-optimal pHs especially at the solid and aqueous assay interface *(209, 210).*

5.4.3 Michaelis-Menten Kinetics

Michaelis-Menten Kinetic Constants, V_{max}, K_m, k_{cat}, k_{cat}/K_m, were calculated from chymotrypsin activity measured at NSPN concentrations of 1, 2, 4, 8, 10, 20 mg/mL. Michaelis-Menten constants are comparable to previously published constants **(Table 5.1)**. Data for surface immobilized chymotrypsin has been reprinted from Chapter 4 on surface functionalized nylon 6,6 nanofibers. It is assumed that the enzyme system is saturated with substrate and that there is only one active site available for catalysis in order for apparent constants to be comparable. The amount of product released over time, or enzyme velocity, was graphed versus substrate concentration for Michaelis-Menten constant calculations.

There were no significant differences in maximum velocity, V_{max}, for each immobilized enzyme system compared to free enzyme. Velocity was proportional to substrate concentration until V_{max} was reached. V_{max} was used to derive the constant, K_m. K_m of free chymotrypsin and PCL/PVA-CT were statistically similar, and indicated that encapsulation did not hinder substrate affinity such that substrate capture was not more favored by one enzyme system over the other.

The turnover number, k_{cat}, was determined by relating V_{max} to the enzyme concentration in the system. The surface immobilized chymotrypsin (Chapter 4) and PCL/PVA-CT system k_{cat} were significantly different from free chymotrypsin and each other. k_{cat} represented the amount of substrate each active site was able to convert to product over time, and was therefore dependent on enzyme concentration. PCL/PVA-CT had the highest k_{cat} relative to free chymotrypsin. PCL/PVA-CT was able to create more product over time when compared to free chymotrypsin, but not as readily as surface

immobilized chymotrypsin which may have been influenced by enzyme availability at the material/aqueous interface during activity assays. The catalytic efficiency, k_{cat}/K_m, speaks to the substrate specificity with the speed at which the enzyme and substrate can form a complex for catalysis, and is limited by substrate diffusion. Therefore, k_{cat}/K_m represents collisions between substrate the enzyme. k_{cat}/K_m for PCL/PVA-CT was significantly different from free chymotrypsin. Much of the chymotrypsin exists encapsulated within the emulsion fiber, and access to this enzyme for protein and activity quantification rely on fluid flow through the polymer network (assisted by pores and gel behavior). Synthetic substrates, like NSPN, are smaller than native proteins in food processing which may also affect kinetic data.

Table 5.1. Michaelis-Menten Kinetic Constants for free chymotrypsin, surface immobilized chymotrypsin (Chapter 4), and emulsion electrospun chymotrypsin. Constants were calculated from n = 8 samples, representative of two sets of n = 4 produced on independent days.

	V_{max} (mM/s)	K_m (mM)	k_{cat} (1/s)	k_{cat}/K_m (1/mM s)
Free Chymotrypsin	5.92e-4 ± 7.0e-5	4.10 ± 1.5	1.48e4 ± 5.3e2	3611 ± 130
Surface Immobilized (Nylon NF)	8.00e-4 ± 1.3e-4	5.84 ± 2.4	2.90e3 ± 70	496.2 ± 28.5
Emulsion Encapsulated (PCL/PVA NF)	1.81e-2 ± 1.6e-3	3.06 ± 1.9	1.91e4 ± 25	6226 ± 13.2

5.5 Conclusions

Chymotrypsin was embedded by incorporation into a polymer emulsion where enzyme and PVA were stabilized within a PCL continuous phase. Microscopy revealed that the two phases remained separate after electrospinning, and that surface tears and pores formed aid in increased access between substrate and enzyme as well as release of colorimetric products. The emulsion nanofiber retained activity when assayed at free chymotrypsin's optimum temperature and pH. The range of retained activity at low temperatures compared to the thermostability of free enzyme and surface immobilized chymotrypsin showed promise for tailorable immobilized enzyme systems. Native chymotrypsin is relatively pH stable, and as immobilized is pH stable too. Michaelis-Menten Kinetic data showed that encapsulation by emulsion electrospinning did not hinder catalytic efficiency compared to free enzyme, and had similar substrate affinity to that of surface immobilized chymotrypsin. Although, encapsulated protein may be subjected to diffusion limitations, substrate size, and ease of solid support preparation by single step processes can enhance the promise of scaling enzyme immobilization systems in food and agricultural processing.

CHAPTER 6

FINAL CONCLUSIONS

This work was in pursuit of benefiting the retained activity and catalytic efficiency of immobilized enzyme systems for food and agricultural applications. Enzymes are capable of increasing product yield, quickly while decreasing material losses and are therefore a ubiquitous component of food processing. Although enzymology and native enzyme characterization has been well documented, the application and precision of material development and protein characterization on these particular solid supports has been inconsistent. Advancements in material synthesis and enzyme stabilization continue, and the progress made, particularly in the previous chapters, are parts of the greater understanding of enzymes on hierarchical materials.

Layer-by-layer immobilization originated to increase bioactive loading on surfaces. Here, multiple layers were conjugated with lactase onto planar LDPE. It was found that immobilization of lactase onto LDPE, in effect increased surface area for binding and therefore increased protein loading, but did not increase material activity due to diffusion limitations and decreased access with additional layers (Chapter 2) *(30, 32)*. Attaching proteins to hydrophobic materials required vigorous surface functionalization methods and the assistance of a homobifunctional cross-linker (glutaraldehyde) which may have contributed to activity loss *(211-214)*.

To overcome negative interactions between enzymes and the hydrophobic polymer surface, lactase was encapsulated in water soluble PEO by electrospinning. Blending enzymes into water soluble polymers demonstrated the validity of the electrospinning techniques in enzyme immobilization in the protective environment of

the water-soluble polymer and surfactant. Direct incorporation of the enzyme with polymer and electrospinning facilitated quick material production, and high maintained relative activity of up to 92% *(38, 104)*. Electrospinning did not adversely affect retained enzyme activity when compared to free enzyme (Chapter 3).

As the retained activity of enzyme in nanofiber was high, surface modification of nanofiber was considered too. To establish the nanoscale as beneficial to enzyme immobilization – Nylon 6,6 was chosen due to its previous uses in packaging and polyamide backbone (Chapter 4). Covalent immobilization on a non-water soluble material should allow for storage, recovery, and reuse. The nanofiber structure added a hierarchical element to material removal in comparison to nanoparticles and cross-linked beads available commercially. Immobilization was successful in increasing pH stability and thermostability compared to free chymotrypsin and chymotrypsin immobilized to macroscale supports further showing immobilization can extend enzyme use. Previous studies have shown that the overall protein loading was influenced by the characteristics of the solid support. Nanoscale supports have higher surface area than both planar and spherical macroscale solid supports, and therefore have more surface available for functionalization *(38, 84, 101)*. Hierarchical structuring of the large mat composed of nanofibers facilitates higher activity retention while provides for a means of recovery faster than magnetic nanoparticles while extending enzyme stability.

Immobilized enzymes on nanoscale supports behave as free enzymes, where curvature and size play a role in reducing protein-protein and protein-material interactions. Even with immobilized protein, hydrophobic solid supports may cause diffusion limitations due to changes in fluid flow and substrate availability near its

surface. Emulsion electrospinning incorporated the material benefits of both water-soluble and water insoluble polymers for enzyme encapsulation. Varying the solid support composition assisted in creating nanostructures with porous morphology. Chymotrypsin was incorporated into PCL with the assistance of PVA, and retained activity while maintaining high protein loading characteristic of nanoscale materials (Chapter 5).

Enzymes are naturally robust, but can have increased stability and wider uses in severe environments by stabilization and immobilization. To assess the benefits immobilized enzyme systems bring to food contact materials, both material and protein characterization were employed. Food and agriculture have recently turned to hierarchical materials in processing and packaging due to the increased surface area to volume ratio, ease of manufacturing scale-up, and maintained or even improved mechanical stability of nanomaterials. A combination of the scale and curvature provided allows enzymes to behave like their free enzyme counterparts. Integrating biocatalysts into food packaging also allows for extended use and clean-labeling when non-migratory which may enable "in-package processing" where food constituents undergo changes to improve quality or shelf-life while in transport and storage. Immobilized enzymes are more readily recovered, regenerated, and reused – decreasing overall energy, material, and environment costs. Introducing biocatalytic materials to solid polymeric supports requires varied techniques in order to maintain activity. These techniques developed for bioconjugation further the usability of immobilized enzymes.

CHAPTER 7

THE FUTURE OF ENZYME STABILIZATION AND IMMOBILIZATION FOR FOOD PACKAGING AND PROCESSING

This work has explored variations in surface functionalization and enzyme immobilization techniques in order to improve protein loading, retained activity, expanded working ranges, stability, and overall robustness. These findings have drawn conclusions based off of projects that have opened doors for further exploration based on these results. Areas of interest for further investigative consideration in the realm of increasing enzyme efficiency in biocatalytic materials are outlined below.

7.1 Native Enzyme Variability

Parameters by which enzymes are used are in part determined by their source and production method. Their natural environment for catalysis influences each enzyme's optimal working ranges. As an increasing number of studies evaluate extending the working ranges of enzymes in harsh environments by direct modification, immobilization, and stabilization, having a more robust native enzyme may further affect the overall changes experienced. For example, whether stabilization methods can further increase the thermostability and optimal working temperature of a thermophilic enzyme.

7.2 Stabilizer Additives

This work has focused mainly on solid support enhancements and functionalization to increase enzyme activity retention. Other publications have noted the benefits short chain sugars have on enzyme stability. Many have stated the addition of sugar and trehalose may protect enzymes during freeze drying and storage, yet certain salts have been detrimental. The next frontier in enzyme immobilization explores how

solid supports and stabilizers can change the micro/nanoenvironment to benefit catalytic efficiency. Explorations into adding stabilizers as released in encapsulations or as attached to immobilized enzyme systems can further tailorable enzyme technologies.

7.3 Enzyme Modification

Increasing biocompatibility was an important consideration in the previously discussed encapsulation procedures. Without direct enzyme modification, increasing biocompatibility with water insoluble polymer materials was dependent on variations made to the solid support composition and surface functionalization techniques. However, direct enzyme modification prior to immobilization may influence catalysis due to changes in interactions at the solid/enzyme interface (Appendix C). Changing the hydrophilicity and hydrophobicity of an enzyme allows the protein to be further tailorable to certain solid supports that are used in food and agriculture. Modification to active sites and potential attachment amino acid residues are alternatives as well.

7.4 Cross-linker Compatibility and Characterization

Preliminary work on increasing biocompatibility of cross-linker for covalent conjugation has combined many of the suggested benefits of sugar stabilization on enzymes (Appendix B). Although glutaraldehyde and epoxides readily crosslink materials and proteins, studies have shown their detrimental effects on enzyme activity as well as the processing environment. Finding food-safe cross-linkers for processing materials is important for influencing the enzyme microenvironment, support biocompatibility, and protein loading. This avenue of exploration also expands the possibility of increasing value-added materials and processes agriculture by converting materials previously deemed as waste to usable chemical compounds.

7.5 Scale-up Technology

Material scale-up is a common hurdle for applying advanced bioactive materials and packaging to continuous food processing. Bench-top proof-of-concept work verifies the efficacy of the bioactive and can help to ascertain changes in behavior due to modifications and interactions with solid supports and aqueous interfaces. However, applying material to better quality and safety is left as an afterthought. Translating technologies through scale-up to large batches presents its own challenges as material uniformity and production processes change.

These biocatalytic materials benefit from hierarchical design. Many material morphologies can be produced by the methods described above. Introducing gradations in size and surface morphology can further demonstrate enzyme stabilization.

APPENDIX A

IMPACT OF ACTIVE FOOD PACKAGING MATERIALS ON FLUID MILK QUALITY AND SHELF-LIFE

A.1 Abstract

Active packaging, in which active agents are embedded into or on the surface of food packaging materials, can enhance the nutritive value, economics, and stability of food as well as enable in-package processing. In one embodiment of active food packaging lactase was covalently immobilized onto packaging films for in-package lactose hydrolysis. In prior work, lactase was covalently bound to low-density polyethylene (LDPE) using polyethyleneimine (PEI) and glutaraldehyde (GL) cross-linkers to form the packaging film. Because of the potential contaminants of proteases, lipases, and spoilage organisms in typical enzyme preparations, the goal of the current work was to determine the impact of immobilized-lactase active packaging technology on unanticipated side effects such as shortened shelf-life and reduced product quality. Results suggested that there was no evidence of lipase or protease activity on the active packaging films, indicating that such active packaging films could enable in-package lactose hydrolysis without adversely impacting product quality in terms of dairy protein or lipid stability. Storage stability studies indicated that lactase did not migrate from the film over a 49 day period, and that dry storage resulted in 13.41% retained activity while wet storage conditions enabled retention of 62.52% activity. Results of a Standard Plate Count indicated that the film modification reagents introduced minor microbial contamination; however, the microbial population remained under the 20,000 CFU/mL limit through the manufacturer's suggested 14 day storage period for all film samples.

This suggests that commercially produced immobilized lactase active packaging should utilize purified cross-linkers and enzyme. Characterization of unanticipated effects of active packaging on food quality reported here is important in demonstrating the commercial potential of such technologies.

A.2 Introduction

Lactose intolerance can produce uncomfortable intestinal symptoms, which can be prevented by consuming lactose-free products *(43-45)*. Traditionally lactose-free fluid milk is produced by the addition of β-galactosidase to fluid pasteurized milk in a batch operation which requires a secondary heat treatment to deactivate the enzyme, and to inactivate any microbial or enzymatic contamination from the enzyme preparation. This method results in a characteristic 'cooked' milk flavor which can be dissatisfying to consumers *(46, 215)*. Immobilized enzyme reactors have been investigated as a continuous processing alternative *(216-218)*. Despite the potential for reuse and recovery of the immobilized enzymes, fouling and stability concerns have limited their commercial application.

Active packaging, in which an active component is embedded into or onto a packaging material with the goal of improving the safety, economics, and shelf life of packaged foods may offer an alternative means to produce lactose free fluid milk products *(1, 219)*. Developments in active packaging with immobilized enzymes for dairy products are aimed at reducing the negative sensory characteristics of batch processing *(30, 31)*. One such active package was created by layer by layer (LbL) deposition of lactase, in which lactase is covalently immobilized onto a UV functionalized low-density

polyethylene (LDPE) surface between layers of repeated depositions of polyethyleneimine (PEI) and glutaraldehyde (GL) cross-linking layers *(32)*.

Some researchers have evaluated the intended effects of active packaging in terms of product quality, consistency, and consumer acceptance in dairy products whereas separate comprehensive fluid milk quality studies have evaluated bacterial counts, sensory acceptance, and shelf-life of the final product *(56, 220, 221)*. However, reports on novel active packaging technologies typically do not evaluate their potential unanticipated adverse effects on dairy quality. As there are additional steps in the manufacture of active packaging materials, there is a potential for introduction of microbial and enzymatic contaminants (e.g. lipases and proteases from the enzyme preparations) which can directly affect the quality and shelf stability of the packaged food products. Therefore the overall goal of this work was to evaluate the effect of an immobilized lactase active packaging material on the quality and shelf stability of fluid milk. Ultra-high temperature pasteurized (UHT) skim milk was subjected to storage studies in contact with the active packaging material, and was evaluated for protease and lipase activity, as well as microbial growth by Standard Plate Count (SPC). Migration studies and activity studies were also performed.

A.3 Materials and Methods

Additive-free LDPE pellets were purchased from Scientific Polymer Products (Ontario, NY). Anhydrous potassium phosphate dibasic, anhydrous potassium phosphate monobasic, anhydrous sodium bicarbonate, anhydrous sodium carbonate, anhydrous sodium acetate trihydrate, glacial acetic acid, hydrochloric acid, sodium hydroxide, acetone (99.8%), iso-propanol (99.9%), methanol (99.9%), peptone, and

polytetrafluoroethylene (PTFE) filter units (0.2 μm) were purchased from Fisher Scientific (Fairlawn, NJ). 1-Ethyl-3-(3-dimethylaminopropyl) carbodiimide hydrochloride (EDC - HCl) was purchased from Proteo-Chem (Denver, CO). N-hydroxysuccinimide (NHS), sodium phosphate tribasic dodecahydrate (98%), ortho-Nitrophenol (ONP), para-Nitrophenyl acetate (pNPA), and 2-(N-morpholino) ethanesulfonic acid (MES) were purchased from Acros Organics (Geel, Antwerp, Belgium). Glutaraldehyde (25%) was purchased from Alfa Aesar (Ward Hill, MA). Protazyme OL tablets were purchased from Megazyme International (Bray, Ireland). Aerobic Count Plate Petrifilm were purchased from 3M (Two Harbors, MN). *o*-Nitrophenol-β-D-galactopyranoside (ONPG), bicinchoninic acid (BCA) assay reagents, and bovine serum albumin (BSA) were purchased from Thermo Scientific (Rockford, IL). Branched polyethylenimine (PEI, M_w 25 kDa) and para-Nitrophenol (pNP) were purchased from Sigma-Aldrich (St. Louis, MO). ‘‘Amicon Ultra’’ (50k MWCO) centrifugal filter devices were purchased from Millipore Ireland (Carrigtwohill, Co. Cork, Ireland). Syringe filters were purchased from Whatman (Florham Park, NJ). Hershey’s UHT skim milk was purchased from Diversified Foods Inc. (Metairie, LA). Dried lactase preparation from *Aspergillus oryzae* was donated by Enzyme Development Corporation (New York, NY).

A.3.1 Preparation, Functionalization, and Analysis of LDPE Films

The lactase was purified in a 0.1 M, pH 5.0 acetate buffer and filtered through a 0.2 μm PTFE syringe filter before centrifugal filtration (50k MWCO) at 6500 rpm for 30 min. Lactase purification is performed to remove contaminating enzymes and microorganisms from the enzyme preparation, and to create a stock solution for ease of

film preparation. Lactase trapped in the membrane filter was flushed out with 0.1M, pH 5.0 sodium acetate buffer and stored at 4°C for further use. The purified solution is heretofore referred to as the "free lactase enzyme solution".

The immobilized lactase active packaging films analyzed in this study were prepared using a layer by layer lactase immobilization method on functionalized polyethylene as previously reported for the development of multilayer films *(32)*. Briefly, acetone and iso-propanol cleaned films (2 × 1 cm) pressed from LDPE pellets on a Carver Laboratory Press (Fred S. Carver Inc., Summit, Summit, N.J.) to 294 ± 17 μm were exposed to 28 mW/cm^2 ultraviolet light at 254nm to generate carboxylic acid groups to which branched PEI was bound using water soluble cabodiimide chemistry to produce LDPE-PEI films. Purified lactase was covalently linked to the amine-functionalized polyethylene using reductive animation chemistry through a GL cross-linker (LDPE-GL films). The resulting film represented a single multilayer (LDPE-LAC films). All quality and stability tests described herein were done on individual multilayer films.

The total protein content of the free lactase enzyme solution and LDPE-LAC was quantified using an altered BCA assay for film surfaces against buffer and LDPE controls. An aliquot of 10 μL free lactase enzyme solution was reacted in 2 mL of BCA working reagent for 30 minutes at 37°C to determine free enzyme protein content while each (2 × 1 cm) sample film was shaken in 3 mL of BCA working reagent for 1 hr at 60°C *(31)*. Samples were read at 562 nm on a Synergy 2 with Gen5 Software (BioTek Instruments, Inc., Winooski, V.T.), and compared against a standard curve of known concentrations of BSA. Protein migration was measured by quantifying and comparing

the total protein content of blank MES buffer, MES film storage buffer, LDPE films, and LDPE-LAC films following the methods for free enzyme and film content BCA assays respectively.

Lactase activity was determined using the ONPG assay as outlined in the Foods Chemical Codex for *A.oryzae (74).* Assay conditions followed conditions for free lactase from *A.oryzae* with an optimum activity at 50°C and pH 5.0. The lactase activity was calculated using an experimentally determined extinction coefficient (ε) of 4.05 μmol/mL produced by a standard curve of o-Nitrophenol (99%) and 1% (wt/vol) sodium carbonate aqueous solution *(38)*. The resulting activity calculations in acid lactase units (ALU) represent the cleaved ONPG in μmol/min. To measure the activity of lactase, individual films of LDPE-LAC and LDPE (2 × 1 cm) were placed in 3 mL of 3.7 mg/mL ONPG in 0.1 M, pH 5.0 acetate buffer for 1 hr (films) or 15 min (free enzyme solution) of shaking at 50°C. The reaction was stopped with 4 mL of 10% (wt / vol) sodium carbonate solution in water. DI water was added to make the final sample volume 10 mL. Activity of films after storage for up to eight weeks under wet (4°C) and dry conditions was also quantified. To evaluate activity under wet storage conditions, films were stored in individual sterile glass tubes containing 1 mL/cm^2 0.1 M, pH 5.0 MES buffer. For dry storage films, dried films were stored in a covered petri dish over calcium sulfate desiccant (<98%) at room temperature and 15% relative humidity.

Standard Plate Counts (SPC) were used to determine the effect of film preparation on product spoilage. Each sample of LDPE and LDPE-LAC film (2 × 1 cm) was stored in individual sterile glass test tubes containing 1 mL/cm^2 UHT skim milk at 4°C with all components assembled using aseptic methods. After 0, 7, 14, and 21 days of storage,

samples were diluted accordingly in 1% peptone water, plated on 3M Aerobic Count Plate Petrifilm, and discarded. Petrifilms were incubated at 32°C for 48 hrs and counted for colonies as outlined by the AOAC methods 986.33 and 989.10 for milk and dairy products *(222)*. UHT skim milk and LDPE films in UHT skim milk stored at the same conditions as the LDPE-LAC films in milk were plated as controls. The countable range for 3M Petrifilm is 25 to 250 colony forming units (CFU).

The presence of lipase was determined by assessing the overall activity of potential lipase contaminants in film storage solution (0.1 M, pH 5.0 MES and milk), from films stored at 4°C for 21 days in sterile tubes (1 mL/cm2160). The p-Nitrophenyl acetate (pNPA) assay was prepared and performed as outlined by Bier for lipases *(223)* (Bier, 1955). The assay was performed at 50°C and pH 5.0 as to follow the optimum conditions of the purified lactase. The samples from milk and MES storage solution were compared to a blank of storage buffer from LDPE. Activity was calculated from an experimentally determined extinction coefficient (ε) of 0.147 μmol/mL produced by a standard curve of p-Nitrophenol (99%) and 0.1 M, pH 5.0 MES buffer. The resulting activity in Units/mL represents one μmol pNPA cleaved per minute per mL total assay. Lipase activity of films stored in both 0.1 M, pH 5.0 MES buffer and UHT skim milk was measured against LDPE as a negative control and 10% (wt/vol) lipase from Candida *rugosa* (Sigma Aldrich) as a positive control.

Assessment of protease contamination of final dairy product from film preparation was completed with the Protozyme OL reagent tablet from Megazyme. Protozyme OL tablets are used for the assay of endo-proteases that are active on collagen. Megazyme Protazyme OL tablets utilize an azurine-crosslinked collagen unit as a

substrate that when cleaved produces a blue color. LDPE was the negative control and 0.5% (wt/vol) α-chymotrypsin from bovine pancreas (Sigma Aldrich) was the positive control. For each sample, one tablet was hydrated in 1 mL of 0.1 M, pH 5.0 sodium acetate buffer and stirred for 5 min at 40°C. Once hydrated, 1 mL of milk or MES buffer from the modified films stored at 4°C for 21 days (1 mL/cm^2) was added to the tablet and stirred for 10 min. The reaction was stopped by the addition of 10 mL of $Na_3PO_4 \cdot 12H_2O$ (2% wt/vol, pH 11), and vortexed. The sample was allowed to stand for 5 min at room temperature and then centrifuged to separate the tablet from supernatant. The supernatant was measured at 590 nm, and was compared to a standard curve provided by Megazyme based on the same assay conditions for a Bioprotease A endo-protease from *Aspergillus niger*.

A.3.2 Statistical Analysis

All statistical analysis was done on Graphpad Prism software (v. 5.04, Graphpad Software, La Jolla, CA., U.S.A.). One-way analysis of variance (ANOVA) with Tukey's pairwise comparison was done for calculation of statistical difference between samples with a 95% confidence interval ($p < 0.05$).

A.4 Results and Discussion

A.4.1 Standard Plate Count

The microbial growth in UHT skim milk alone and in contact with film treatments (LDPE, LDPE-GL, LDPE-LAC) was quantified by SPC to determine if our active packaging films influenced the spoilage rate for UHT skim milk. SPCs were performed as indicators over a typical 21 day consumption period for milk (**Fig. A.1**). Notable growth was observed after 7 days of storage for LDPE-GL and LDPE-LAC film variants

at 1.33 Log_{10}CFU/mL and 1.55 Log_{10}CFU/mL respectively, with microbial growth rates analogous for both film variants through 14 days at 3.44 Log_{10}CFU/mL and 3.46 Log_{10}CFU/mL respectively. These results suggest that any contamination in the film preparation method was due to the cross-linking step rather than by introduction of microbial contaminants in the enzyme preparation. Purification of the cross-linking reagents (in the current work, cross-linking reagents were used 'as received' without further purification) may prevent the observed microbial growth. Preparation of an active package often requires more procedural steps that can lead to unexpected changes in food stability and quality. After 21 days of storage, microbial growth was observed in fluid milk stored without any films. Native PE, the negative control, showed no growth or change in CFU/mL after 21 days of storage, further suggesting that any microbial contamination of the active packaging film was introduced by the cross-linking reagent. No differences were seen between growth for LDPE-GL and LDPE-LAC until day 21. It should be noted that the aerobic SPC method used here cannot differentiate between spoilage or pathogenic microorganisms, so results represent total microbial growth over the storage period. Microbial growth in milk stored with LDPE-LAC and LDPE-GL films remained under the limit defined by the Pasteurized Milk Ordinance (PMO) for Grade "A" pasteurized and ultra-pasteurized milk (20,000 CFU/mL or 4.301 Log_{10}CFU/mL) *(224)* through 14 days of storage. These results suggest that the active packaging films developed herein would not increase microbial populations in milk over 14 days post packaging, and that purification of cross-linking reagents would likely improve this shelf life. Commercial manufacturing of the reported films should consider use of purified cross-linking reagents to further improve microbial stability.

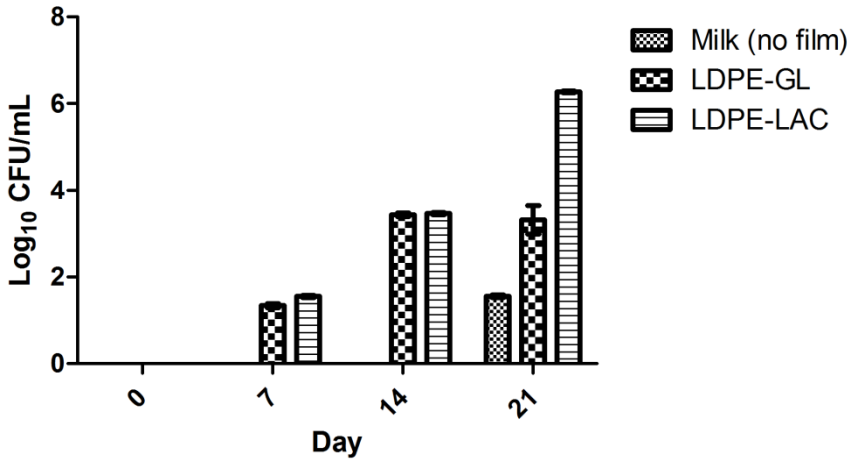

Figure A.1. Microbial growth in UHT skim milk stored at 4°C alone, in contact with cross-linker modified PE (LDPE-GL), and in contact with active packaging film (LDPE-LAC) where n = 3. Milk stored in contact with native PE exhibited no growth over the course of the study (data not shown).

A.4.2 Lipase Determination

Commercial enzyme preparations often contain enzymatic impurities (e.g. lipases, proteases) that can adversely impact milk quality. Lipases have been known to produce off-flavors and off-odors decreasing fluid milk shelf-life and negatively affecting consumer acceptance of dairy products *(225)*. Lipase activity in milk or buffer after storage in contact with LDPE-LAC active packaging films was determined using the substrate, p-Nitrophenyl acetate (pNPA), as an overall indicator of lipase. Lipase activity is reported in Units/mL representing one μmol cleaved pNPA per minute for every mL under the conditions of the assay. The positive control (10% lipase from *Candida rugosa*) exhibited an expected lipase activity of 0.026 Units/ml, while neither milk nor buffer exhibited any significant lipase activity after storage with LDPE-LAC films. Further, there was no statistically significant difference between the lipase activity of native LDPE (negative control) or LDPE-LAC stored in MES buffer or milk (**Fig. A.2**). Lipase activity measurements were taken from both storage buffer and from milk to verify that lipase activity reported was a result of the film preparation and not from lipase naturally

occurring in milk. These results suggest that the immobilized lactase active packaging film reported here would not introduce any additional lipase contamination from the film preparation into packaged fluid milk.

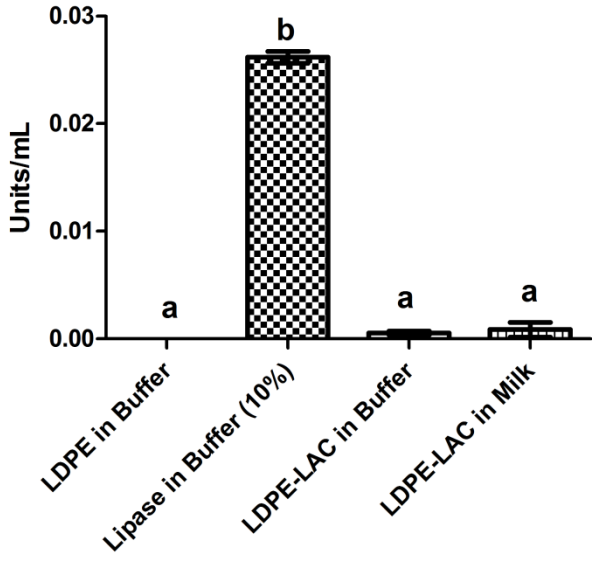

Figure A.2. Lipase activity in milk or buffer after storage in contact with LDPE-LAC active packaging films at 4°C for 21 days as determined by p-Nitrophenyl acetate assay where n = 4. Native PE and 10% lipase from Candida rugosa in 0.1M, pH 5.0 MES buffer served as negative and positive controls.

A.4.3 Protease Determination

Peptides produced by proteolysis of casein from the introduction of protease contaminants, have been reported to impart bitterness and astringency in dairy products *(225, 226)*. Protease activity in milk or buffer after storage in contact with LDPE-LAC films was measured using Megazyme Protazyme OL tablets. Protease activity is reported in Units/mL representing one μmol soluble tyrosine produced per minute for every ml under the conditions of the assay. The positive control, chymotrypsin, exhibited an expected protease activity of 43.252 Units/ml. The protease activities of native LDPE, as well as that of MES buffer and milk stored in contact with LDPE-LAC films were equivalent at 12.500, 12.250, and 13.500 Units/ml, respectively (**Fig. A.3**). These results

suggest that the LDPE-LAC films did not introduce protease contamination to the fluid milk.

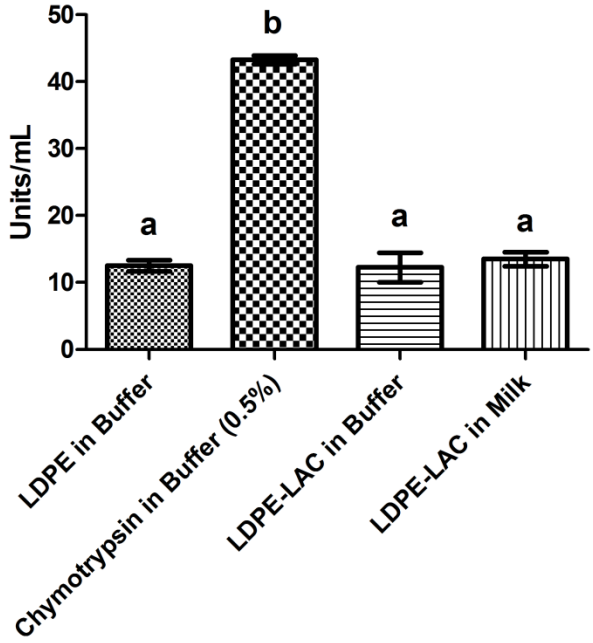

Figure A.3. Protease activity in UHT milk or buffer after storage in contact with LDPE-LAC active packaging films at 4°C for 21 days as determined by Megazyme Protazyme assay where n = 4. Native PE and 10% protease (chymotrypsin) in 0.1M, pH 5.0 MES buffer served as negative and positive controls, respectively.

A.4.4 Protein Migration

The goal of the reported immobilized lactase active packaging technology is to link the lactase to LDPE via a covalent cross-linking chemistry *(30, 32)*. Protein migration was measured by the comparison of the protein contents of the storage solution and LDPE-LAC film as indicators of the stability of the covalent immobilization chemistry. Protein migration was reported as the total protein mass in storage buffers and on films at day 0 and after 49 days of storage (**Fig. A.4**). No significant difference was observed in the protein contents of the MES storage buffer between days 0 and 49. Likewise, there was no significant difference in protein content on the LDPE-LAC films at day 0 and day 49 (**Fig. A.4**). These results indicate that the lactase immobilization

chemistry was covalent and that no protein migrated from the film over the 49 day long term storage period. Establishing that active agents and cross-linking reagents are unlikely to migrate to the food, such reagents would require regulatory approval as indirect additives rather than as direct additives, a potential labeling and regulatory advantage.

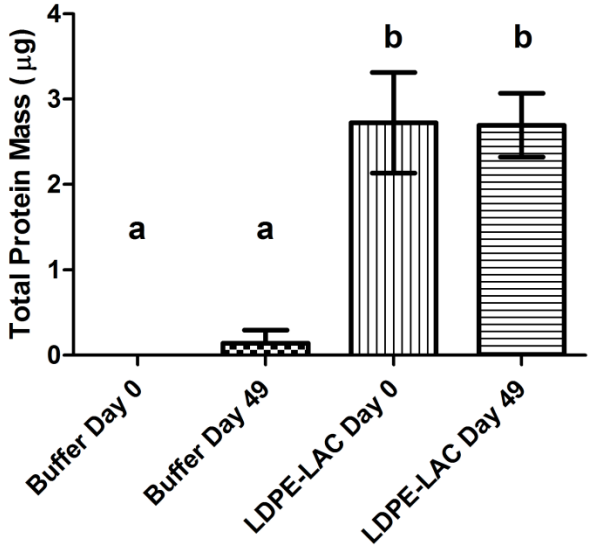

Figure A.4. Stability of lactase immobilized on active packaging films. Migration of protein after storage of LDPE-LAC films in MES buffer for 49 days at 4°C as determined by BCA assay where n = 4. Buffer results (left) represent protein content in MES storage buffer initially and after 49 days storage with films. LDPE-LAC results (right) represent amount of immobilized protein on LDPE-LAC films initially and after 49 days storage.

A.4.5 Activity Retention

The retention of lactase activity of the immobilized lactase active packaging films was measured using the ONPG assay after 8 weeks of storage in both wet (MES buffer at 4°C) and dry (15% Relative Humidity at 25°C) storage conditions. Activity measurements are expressed as % activity retention normalized to the activity of freshly prepared LDPE-LAC films (**Fig. A.5**). There was an initial decrease in activity for films stored in both dry and wet conditions after one week of storage. Films stored in MES buffer retained up to 78.57% of original film activity while films in dry conditions

dropped to 63.24% activity. Retained activity of films stored in dry conditions was at 13.41% of the original activity after 8 weeks of storage, about one fourth of the activity of films stored in contact with buffer (62.52%) after 8 weeks of storage. Although some activity was retained after dry film storage, these results indicated that storage in the presence of buffer helped to maintain the structural integrity of the enzyme immobilized on the modified film. Alternative storage conditions such as higher relative humidity, use of freeze dried enzyme preparations, or highly hydrophilic cross-linking reagents may improve activity retention of immobilized enzyme active packaging films stored in dry conditions.

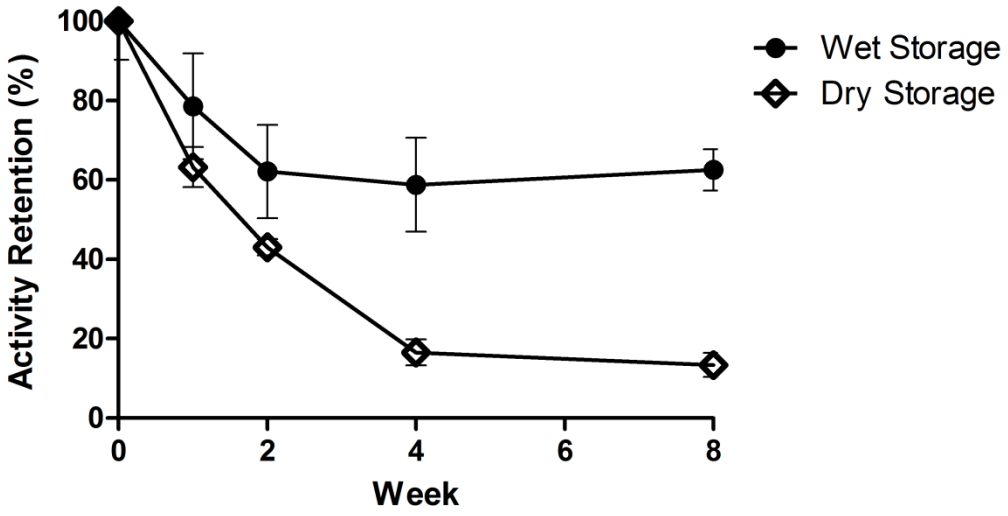

Figure A.5. Activity retention of immobilized lactase active packaging films under wet (MES and dry storage conditions. Lactase activities are reported as percent retained activity, normalized to lactase activity of freshly prepared LDPE-LAC films where n = 4.

A.5 Conclusions

Active food packaging technologies offer the ability to achieve a desired technical effect on a packaged food. A hurdle in demonstrating the commercial potential of active packaging materials is the often overlooked potential for unanticipated technical effects by the material on the packaged food due to the extra preparation required. In this work,

we analyzed the stability and quality of UHT skim milk after storage in contact with an immobilized lactase active packaging film using standard protease, lipase, and lactase activity measurements, as well as SPC and protein migration assays. Standard Plate Counts indicated that microbial growth occurred in the samples in contact with the immobilized lactase films after 7 days of storage, but remained under the PMO regulation for the CFU spoilage threshold until after 14 days of storage. It was determined that the cross-linkers were the primary source of microbial contamination, suggesting that film preparation should use purified reagents and cross-linkers. Protease and lipase activity assays indicated that no additional protease or lipase was added to the food system. Protein migration assays indicated that no protein migrated from the film into the storage buffer over the course of the storage study, suggesting that the lactase was covalently bound to the active packaging film. Demonstrating that an active agent is unlikely to migrate to the food product is a potential regulatory benefit, as the cross-linkers and active agents used in non-migratory active packaging technologies require Food Contact Notification as indirect additives whereas those used in migratory active packaging technologies require approval as a direct additive *(12)*. Films stored under wet conditions retained up to 62.52 % activity whereas those stored in dry conditions retained only 13.41% activity after 8 weeks of storage, indicating that alternative immobilization chemistries or storage conditions should be considered to improve dry storage stability. Overall, the immobilized lactase active packaging films exhibited significant retained activity after up to 8 weeks of storage, in which the active agent (lactase) was found to be non-migratory and did not significantly affect microbial growth. Formal sensory evaluations would need to be performed prior to commercial adoption of the film.

APPENDIX B

CARBOHYDRATE POLYALDEHYDES FOR CROSS-LINKED ENZYME AGGREGATES

B.1 Introductions

Traditional covalent enzyme immobilization techniques often employ anchors with functional end group ligands that tether the enzyme to a support. Crosslinked immobilized enzymes similarly utilize crosslinkers with functional end group ligands to entangle enzymes. Crosslinkers are often mid-length carbohydrate chains with aldehyde and epoxy ends; however, the ligands that deem crosslinkers functional can cause large enzymatic activity losses. Environmental and health safety have become a concern for highly reactive crosslinkers as well in agricultural and food processing.

Glutaraldehyde is one of the most utilized protein cross-linkers for protein immobilization. Glutaraldehyde is a homobifunctional tether, a five carbon backbone with a carbonyl on each end (**Fig. B.1**). Glutaraldehyde produces a strong covalent amide bond with primary amines, and will cross-link itself *(227-229).* However, enzymes immobilized with glutaraldehyde have experienced up to 95% activity loss *(132, 211, 213, 214).* Along with activity loss, glutaraldehyde has been associated with toxicity in mammals *(212, 230-232).* Although glutaraldehyde has exhibited polymer and protein stabilization capabilities, especially in synthetic tissues and implants, its use in food and agriculture have been limited as a result. The Code of Federal Regulations, Title 21, which outlines allowable materials for consumption and use in food and drugs has only provided glutaraldehyde be used as indirect food additives from adhesives and packaging, or as secondary direct additives as parts of preparation and processing controls *(194).* The

enzyme activity loss coupled with toxicity concerns provides an opportunity to establish alternative cross-linkers for enzyme immobilization and polymer stabilization for food processing.

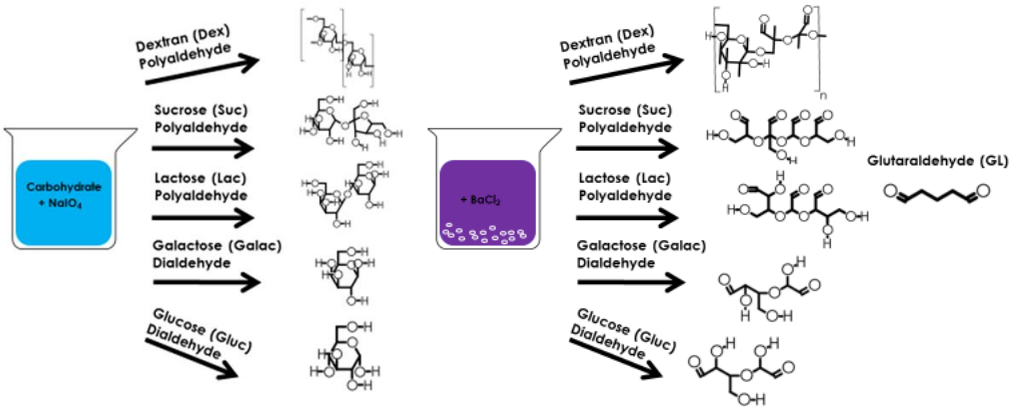

Figure B.1. Periodate oxidation of carbohydrates.

Here Cross-Linked Enzyme Aggregates (CLEA) were made using crosslinking alternatives and compared to that of CLEA produced with glutaraldehyde. CLEA from aggregated enzyme serve as a simple immobilized enzyme method as proof of concept of alternative crosslinker efficacy.

As glutaraldehyde has a simple carbon backbone, carbohydrates available from food and agricultural waste streams were a natural starting material. By transitioning unwanted byproducts from processing and providing the components with new functionality, these cross-linker analogs create a value-added product. If these carbohydrate components were gathered from byproduct off-streams, the cross-linkers should be better for use in food than glutaraldehyde in terms of protein compatibility and human toxicity.

B.2 Materials and Methods

Type II lyophilized α-chymotrypsin (BRENDA *Bos taurus* UniProt P00767 pBLAST, E.C. 3.4.21.1) from bovine pancreas (40 units/mg) and N-Succinyl-Ala-Ala-Pro-Phe *p*-nitroanilide (NSPN), and *p*-anilide were purchased from Sigma-Aldrich (St. Louis, Mo., U.S.A.). Sodium phosphate monobasic monohydrate, sodium phosphate dibasic heptahydrate, potassium phosphate monobasic, sodium carbonate, sodium bicarbonate, potassium phosphate dibasic, chloroform, acetone, PTFE syringe filters (0.22 µm), lutaraldehyde, sucrose, lactose, dextran, glucose and galactose were purchased from Fisher Scientific (Fairlawn, N.J., U.S.A.). The Pierce BCA Protein Kit was purchased from Thermo Scientific (Waltham, MA., U.S.A.).

B.3 Results and Discussion

B.3.1 Carbohydrate Polyaldehyde Synthesis and Characterization

Carbohydrate cross-linkers were formed by periodate oxidation of materials found in agriculture and food processing (**Fig. B.1**). The success of the carbohydrate polyaldehydes were determined by structure and crosslinking. Glutaraldehyde served as the positive control, and is purchased and stored as a known concentration containing a known amount of aldehyde groups. Titration by standardized NaOH to the end point of methyl orange at pH 4.4 was used to calculate the total available aldehyde concentration of each converted carbohydrate. Glutaraldehyde had the highest available aldehyde concentration of the cross-linkers. Significant difference was determined for each group, and dextran and sucrose had the most available aldehydes in solution (**Fig. B.2**). Dextran was a long carbohydrate chain, with a molecular mass higher than the other sugars. The branched dextran has more free ends at which conversion to aldehydes may occur.

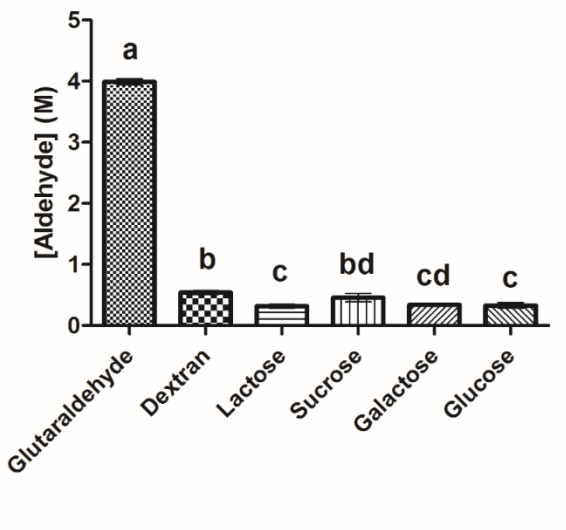

Figure B.2. Aldehyde content of oxidized carbohydrates. Data represents n = 8 from two independent days where letters indicate statistical significance of ($p<0.05$).

B.3.2 CLEA Protein and Activity Characterization

The protein content was determined for each CLEA type produced (data not shown). As each immobilized enzyme system was prepared with the same starting protein concentration, the yield was calculated. These calculations were incorporated into retained activity such that activity was demonstrated as per unit mass of immobilized protein.

CLEA activity at various temperatures was compared to Aggregate Chymotrypsin activity at various temperatures (**Fig. B.3**). The amount of product was measured calorimetrically of the activity assay incubated temperatures between 25ºC (optimum) and 50ºC at pH 7.8. The relative activity was represented as parts of the CLEA activity with its optimum as 100%. All activities were compared to the activities of Aggregated Chymotrypsin which remained constant through each temperature change. CLEA-GL as an industry standard retained over 59.4% of its maximum activity at 45ºC at all temperatures tested. CLEA-Gluc retained over 68.7% of its maximum activity at 40ºC at

temperatures between 25ºC and 45ºC, and only lost 51.5% of its maximum activity at 50ºC. CLEA-Gal similarly retained over 58.8% of its maximum activity at 40ºC at temperatures between 25ºC and 45ºC, and only lost 51.3% of its maximum activity at 50ºC. The CLEA-Lac behaved like the CLEA made with its monosaccharide counterparts. CLEA-Lac retained over 64.2% of its maximum activity at 40ºC at temperatures between 25ºC and 45ºC, and only lost 50.6% of its maximum activity at 50ºC. Although CLEA-Suc was expected to have similar activity retention to CLEA-Lac, it retained below 48.6% of its maximum activity at 40ºC for all temperatures in the tested range except at 45ºC where the CLEA-Lac had 87.6% of its maximum activity. The dextran polyaldehyde had the highest aldehyde content as determined by titration, and had the highest protein content of the CLEA. However, the high protein content did not correlate to higher activity retention. CLEA-Dex had the highest activity at 35ºC and lost up to 99.1% of its maximum activity at all other temperatures. The next highest activity for CLEA-Dex was at 30ºC. The standard deviation was large for all CLEA-Dex activity measurements, which may be attributed to the aggregation of CLEA caused by the dextran length and degree of branching. Introducing the appropriate amount of CLEA-Dex protein to each activity measurement could have caused the variation in activity.

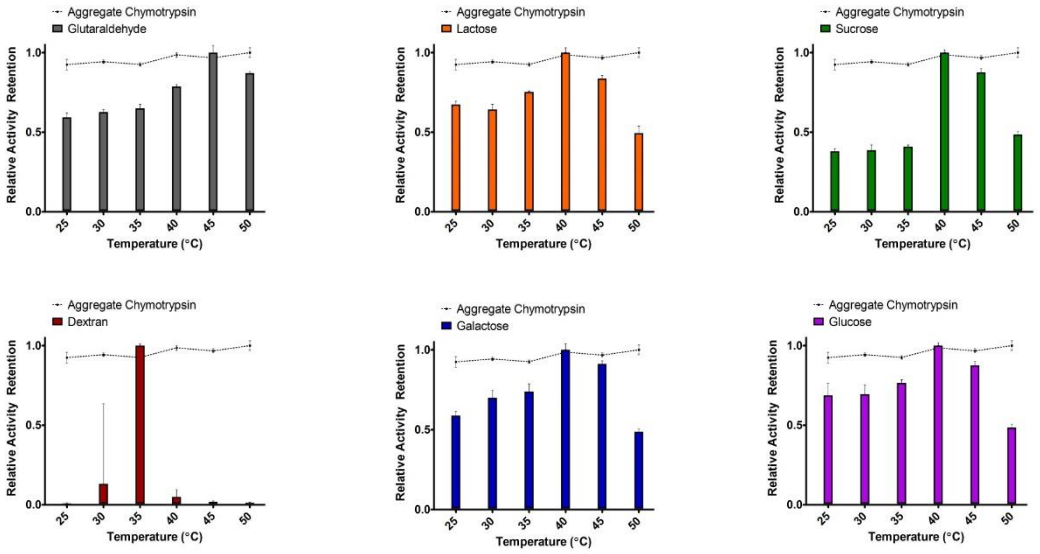

Figure B.3. CLEA activity at pH 7.8 over various temperatures. Optimal temperatures were calculated from n = 8 of two independent days. Relative activity for aggregated chymotrypsin remained unchanged.

Activity was also measured at various pH values for each CLEA type at a steady 25ºC to assess the possible effect of cross-linker length in extreme environments. Activity data at various pH values was compiled in **Figure B.4**. Aggregate chymotrypsin served as the control, with its activities compared to the maximum activity at pH 9 are displayed as a curved line with the lowest activity at pH 3. The published pH maximum for free chymotrypsin was pH 7.8, and for chymotrypsin it was expected that increased pH would lead to increased activity. The relative activity was represented as parts of the CLEA activity with its optimum as 100%. Glutaraldehyde was used as the standard cross-linker, and CLEA-GL had activity increase incrementally to its maximum at pH 10. CLEA made with the monosaccharide polyaldehydes, glucose and galactose, shared similar activity retention and loss at the various pH's. CLEA-Gluc had the highest activity at pH 6 where pH 5 through pH 9 retained over 57.9% of the maximum activity. CLEA-Gal had the highest activity at pH 6, also losing activity at the extremes of pH 3, pH 4, and pH 10. CLEA formed with disaccharide polyaldehyde cross-linkers, sucrose and lactose, had

extended use at high pH. CLEA-Lac had the highest activity at pH 8, but had activity below 10.0% only at pH 3. The maximum activity of CLEA-Suc was at pH 10. The activity increased with increasing pH, and only fell below 71.4% at the lowest pH's, pH 3 through pH 5.

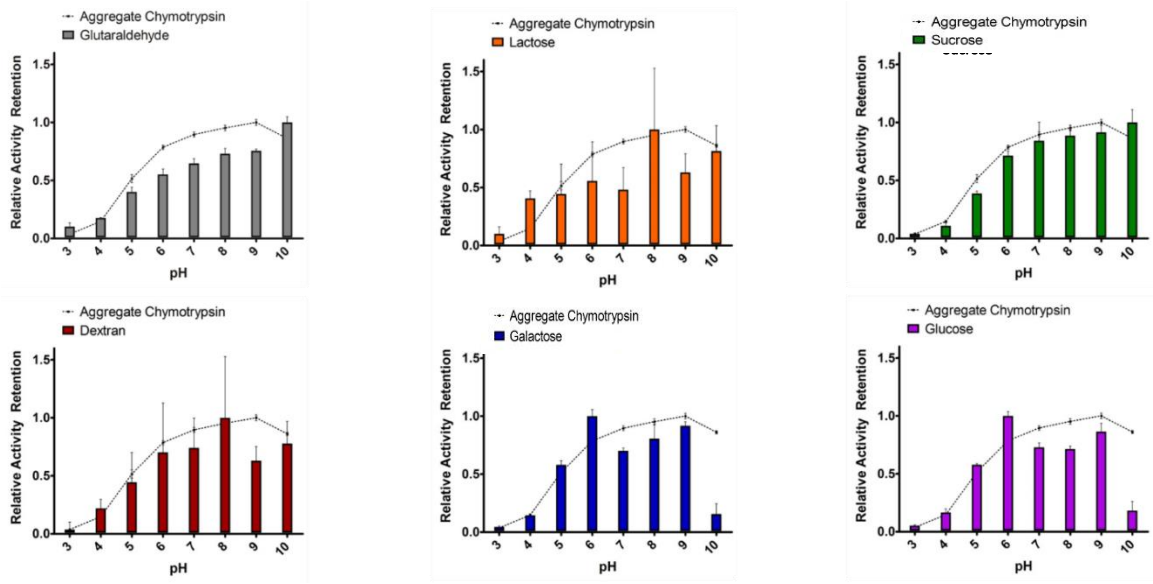

Figure B.4. CLEA activity at 25C at various pH values. Optimal temperatures were calculated from n = 8 of two independent days. Relative activity for aggregated chymotrypsin remained unchanged.

From this preliminary study of carbohydrate polyaldehydes as cross-linkers of carrier-free immobilized chymotrypsin, it was found that the cross-linkers influence enzyme use in extreme environments. Data on cross-linker length and chemical composition will move to make enzyme immobilization tailorable to the final application.

B.3 Conclusions

Immobilization can improve enzyme optimal working conditions and environmental tolerance, while aiding in their recovery and reuse after processing. Many traditional enzyme immobilization methods utilize the cross-linker glutaraldehyde to covalently attach enzymes by their terminal amine group amino acids. Glutaraldehyde is not an ideal material due to its known environmental toxicity, and has been associated

with most activity loss in immobilized enzyme systems. This work aims to synthesize homobifunctional aldehydes produced by periodate oxidation of carbohydrates commonly found in food production and agricultural waste streams that act as cross-linker analogues to replace the need for glutaraldehyde in the stabilization of biopolymers and immobilized enzymes. Glucose, galactose, sucrose, lactose, starch, and dextran were oxidized to convert the ringed diols to multiple aldehyde groups. The cross-linking ability of the modified carbohydrates was determined by reaction and titration with N-hydroxylamine hydrochloride and sodium hydroxide in comparison to glutaraldehyde. The cross-linker analogues were first utilized in preparing carrier-free immobilized enzymes, or cross-linked enzyme aggregates (CLEA) of chymotrypsin. Protein yield and chymotrypsin activity were measured to verify the effectiveness of the cross-linker analogues when compared to glutaraldehyde. CLEA produced from dextran aldehyde had a 64.4% protein yield, and chymotrypsin retained up to 65.8% activity as CLEA produced with the sucrose aldehyde. Cross-linkers prepared from food grade and waste stream carbohydrates represent an alternative to glutaraldehyde that can maintain activity, and may create a system of tailorable biocatalytic materials. Future explorations for these carbohydrate cross-linkers include enzyme immobilization to modified surfaces and stabilization of biopolymers for use in bioprocessing, and create a value-added process to the food and agriculture industries.

APPENDIX C

OXYGEN SCAVENGING POLYMER COATING PREPARED BY HYDROPHOBIC MODIFICATION OF GLUCOSE OXIDASE

C.1 Abstract

Trace oxygen in packaged foods, beverages, and pharmaceuticals can promote a range of oxidative degradation reactions and support microbial growth, ultimately impacting product quality and shelf-life. Oxygen scavenging active packaging systems have therefore been explored to control headspace oxygen content. Herein we report on a hydrophobic ion pairing method to render glucose oxidase hydrophobic and thus soluble in organic solvents. Hydrophobic modified glucose oxidase was blended with ethylene vinyl acetate and cast on the interior of glass vials to demonstrate potential as a commercially translatable coating method for enzyme immobilization. The resulting oxygen scavenging polymer coatings were topographically uniform and presented 0.553 $\mu g/cm^2$ enzyme at the coating interface. The coatings effectively reduced headspace oxygen by 2% in a closed vial system filled 50 vol% with citrate buffer, pH 3.5. Less than 25% protein migrated from the coating over an 8 week leaching study, with no detectable protein leached in the first 4 weeks. Hydrophobic ion pairing of glucose oxidase enabled a facile, high-throughput enzyme immobilization technique without use of complicated, time consuming surface modification chemistries and reagents. Such oxygen scavenging polymer coatings can support controlling headspace oxygen in packaged goods, and thus retaining stability of oxygen sensitive components such as colors, flavors, and nutrients.

This chapter has been submitted for publication – Wong, D.E.; Andler, S.M.; Lincoln, C.; Goddard, J.M.; Talbert, J.N. Oxygen scavenging polymer coating prepared by hydrophobic modification of glucose oxidase . *J. Coating. Tech. Res.* **2016**.

C.2 Introduction

Controlling headspace oxygen in packaged goods (e.g. foods, beverages, pharmaceuticals) is key to the quality and shelf-life of many products. Trace oxygen can promote a number of degradative reactions including color loss, lipid oxidation, loss of nutrient/drug stability, as well as support growth of spoilage organisms. Indeed, lipids have been found to oxidize quickly even when oxygen levels are reduced by half from that of the atmospheric norms (21%) *(233, 234)*. Growth of spoilage microorganisms is also possible at low oxygen levels *(235-237)*. Oxygen sensitive nutrients, like ascorbic acid/Vitamin C, are often dosed at higher than labeled amounts to account for losses due to oxidative degradation during transport and storage. Indeed, ascorbic acid has been found to degrade in the presence of as little as 0.41 g/L dissolved oxygen *(238, 239)*. Vacuum packaging, headspace flushing, and modified atmosphere packaging approaches can reduce initial headspace oxygen, yet even low levels of residual oxygen, as well as oxygen that permeates through the package during storage, can be sufficient to promote degradative reactions that ultimately result in shortened shelf-life and product loss *(10, 199, 233, 240)*.

Oxygen scavenging technologies have been explored to control residual oxygen in oxygen-sensitive packaged goods, by incorporation of oxidation sensitive compounds (e.g. iron, ascorbic acid, photosensitive dyes) into films, sachets, labels, or closures. The wine and brewing industries have employed oxygen scavenging caps, in which a sacrificial reducing agent (e.g. ascorbic acid, sulphite) is embedded in a coating in the crown cap to prevent oxidation of aromatic and bitter compounds *(219, 241-244)*.

Oxidation of photosensitive dyes embedded in polymer films has been explored as a strategy to control color change and off-flavor production in meats *(245, 246)*. The most common commercial oxygen scavenging technology is iron sachets like those manufactured by Multisorb Technologies, Mitsubishi Gas Chemical America, and Nanobiomatters for use in foods *(247-249)*. While effective in controlling oxygen in dry product packaging *(250)*, such sachets are not suitable for liquid food products and beverages, harmful if consumed, and are not visually appealing to consumers.

Incorporation of oxygen-consuming enzymes into or onto the food contact surface of polymer packaging materials has been explored as an alternative oxygen scavenging technology *(219, 251)*. Such enzymatic oxygen scavenging systems could perform in liquid products and have the benefit of continual performance over time, whereas the oxidation sensitive compounds identified above lose oxygen scavenging capacity after they are oxidized. There are two major hurdles to commercial translation of enzymatic active packaging technologies (oxygen scavenging or otherwise). First, there must be sufficient retention of enzyme activity upon immobilization and after exposure to conditions (e.g. pH, temperature) typical of packaged food systems. Enzyme modification and stabilization in polymer matrices can be tailored to promote activity retention*(10, 14, 178)*. Second, the process for introducing enzymes onto a material surface has to be translatable to high throughput, roll-to-roll processing to be economically viable. Adapting enzyme immobilization technologies to a roll-to-roll processing scheme is a significant hurdle, as immobilization chemistries often involve multi-step, reagent and time intensive surface modification techniques *(15, 26, 252,*

253). Rendering enzymes soluble in organic solvents used in coating and printing applications would enable high throughput coating of polymer packaging films.

Herein we report on the hydrophobic modification of glucose oxidase for incorporation into an oxygen scavenging polymer coating. Glucose oxidase is an oxidoreductase that consumes oxygen during conversion of glucose into gluconolactone and hydrogen peroxide*(27)* and has been explored in enzymatic oxygen scavenging systems. In this work, glucose oxidase is modified by hydrophobic ion pairing, a previously reported method *(27, 254, 255)* in which charged surfactants associate with free amine groups on the enzymes surface, rendering it hydrophobic and thus soluble in the nonpolar organic solvent, toluene. The hydrophobic modified glucose oxidase in toluene is blended with ethylene vinyl acetate to produce an enzymatic oxygen scavenging polymer coating. Such coatings were characterized for enzyme content and activity and performance as an oxygen scavenging system.

C.3 Materials and Methods

C.3.1 Materials

Didodecyldimethylammonium bromide (DDAB), glucose oxidase (EC 1.1.3.4), *Aspergillus niger*; Type X-S, 100,000 - 250,000 units/g solid, ascorbic acid, horse radish peroxidase (EC 1.11.1.7) , and dichloroindolphenol, were purchased from Sigma Aldrich (Saint Louis, MO). Ethylene-vinyl acetate (EVA; 28% vinyl acetate) was obtained from Scientific Polymer Products (Ontario, NY). Bicinchoninic acid (BCA) assay reagents, Micro BCA assay reagents, D-glucose, buffer salts, and bovine serum albumin (BSA) were purchased from Thermo Scientific (Rockford, IL, U.S.A.). HPLC grade water and solvents were purchased from Fisher Scientific (Fairlawn, NJ, U.S.A.).

C.3.2 Methods

C.3.2.1 Hydrophobic Modification of Glucose Oxidase

Glucose oxidase (*Aspergillus niger*; Type X-S) was dissolved in 20mM sodium acetate buffer, pH 5.5, at a protein concentration of 1000 µg/ml. The resulting solution was passed through a 0.22 µM cellulose filter. The filtrate was then centrifuged at 14,000 x g for 15 minutes in a 10K MWCO centrifugal filter (Amicon Ultra, Millipore). Protein content of the retentate was characterized using the bicinchoninic acid (BCA) by comparison to a bovine serum albumin (BSA) standard curve. Purified enzyme was diluted to 650 µg/ml in 20 mM sodium acetate buffer, pH 5.5, and immediately subjected to hydrophobic ion pairing (HIP). HIP has previously been described as a means to render enzymes hydrophobic and thus soluble in organic solvents such as toluene *(256)*.

HIP was performed as follows. Purified glucose oxidase was added dropwise to a 2 mM solution of DDAB in toluene. The solution was stirred for three minutes then centrifuged for three minutes (12,000 x g). The organic layer was removed, and then filtered through a 0.22 µM syringe filter. The filtrate was centrifuged for three minutes (12,000 x g), and the resulting organic layer, containing glucose oxidase rendered hydrophobic by DDAB in toluene, was stored at 4 ºC until solvent casting. Protein concentration was determined through BCA, using 2 mM DDAB in toluene as a control and a standard curve of BSA.

C.3.2.2 Preparation and characterization of glucose oxidase embedded polymer coatings

Polymer coatings composed of hydrophobic modified glucose oxidase in ethylene vinyl acetate (EVA) were prepared by solvent casting. EVA pellets were cleaned by

sonication in isopropanol, acetone, and deionized water (two cycles of 10 minutes per solvent). A solution of 8% EVA in toluene (w/v) was prepared by stirring clean EVA pellets in toluene at 40 ºC until all polymer had dissolved. Hydrophobic modified glucose oxidase in toluene was blended with EVA in toluene (8% w/v EVA) at a ratio of 1:10, and stirred for one minute. Solvent cast coatings were prepared by coating the interior of screw cap glass vials (22.5 x 46 mm, Supelco). After addition of 1 ml of hydrophobic modified glucose oxidase/EVA in toluene solution, vials were rotated on a roller until all solvent evaporated, approximately 8 hours. Dried, coated vials were stored at 4 ºC until used in further experiments. The coated surface area was calculated as 16.92 cm^2 per vial manufacturers provided dimensions. Coatings are hereafter referred to as EVA (control coating), EVA+DDAB (EVA coating containing equivalent DDAB surfactant), and EVA+DDAB+GOx (EVA coating containing embedded hydrophobic modified glucose oxidase).

Protein content of the polymer coatings was quantified by a modified micro BCA assay. Briefly, working reagent was added into coated vials and rotated at 60°C for one hour. Absorbance was measured at 562 nm and protein content (expressed as $\mu g/cm^2$) was quantified from a standard curve prepared with BSA with EVA+DDAB coatings serving as control.

To measure coating thickness, coatings were delaminated from the vials using forceps and 300 µl of water. Calipers (CD-6”CSX, Mitutoyo Corp., Kawasaki, Japan) were used to measure coating thickness at six different locations; three at the top, and three at the bottom of the cylindrically shaped coating.

Coating hydrophobicity was determined by dynamic water contact angle of coatings prepared on glass slides using a direct dosing system (DO3210, Kruss, Hamburg, Germany) attached to a Kruss DSA100 Drop Shape Analyzer (Hamburg, Germany). Advancing and receding angles were obtained using HPLC grade water for four samples of each coating type. A total volume of 5 µl of water was dispensed at a flow rate of 25 µl/minute and analyzed using the Tangent Method 2 in the Drop Shape Analysis software (version 1.91.0.2).

Coating morphology and uniformity was characterized by Scanning Electron Microscopy. Micrographs were taken on a JEOL Neoscope JCM 6000 Benchtop SEM from Nikon Instruments, Inc. (Melville, NY), operation at 10 kV. Coatings were solvent cast onto glass microscope slide cover slips (2.2 x 2.2 cm) and coated in 20 nm of gold using a Cressington Sputter Coater 108auto (Watford, UK) with the assistance of argon gas. Micrographs are representative of at least four images acquired from each of three independently prepared samples for each treatment.

C.3.2.3 Oxygen scavenging capacity of glucose oxidase embedded polymer coatings

The potential application of the glucose oxidase embedded EVA coatings as active packaging materials was demonstrated by characterizing their ability to scavenge headspace oxygen as well as the stability of the hydrophobic modified glucose oxidase against migration from the polymer coating. Glass vials in which glucose oxidase embedded EVA coatings had been cast (EVA+DDAB+GOx) were filled with 5 mL of 50 mM sodium citrate buffer, pH 3.5 containing 10% (wt/vol) β-D-glucose. An acidic pH was selected to simulate conditions typical of many bottled beverages and salad dressings, which represents a target application for the reported active packaging coating.

Vials were capped with PTFE septum topped screw caps and stored at room temperature for up to 8 wks. The headspace oxygen was measured at 0, 1, 2, 4, and 8 weeks using a Model 902D DualTrak Oxygen/Carbon Dioxide Analyzer from Quantek Instruments (Grafton, MA), calibrated against ambient air and nitrogen. Glass vials in which EVA+DDAB coatings had been cast served as controls.

The migration of protein from the polymer coatings was determined by adding 10 ml of 50 mM citrate buffer, pH 3.5, to cover the coatings cast on the interior of the glass vials. Coated vials were stored at approximately 22 ºC and protein content of the storage buffer was determined at weeks 0, 1, 2, 4, and 8 using the micro BCA assay, by comparison to a BSA standard curve prepared in 50mM citrate buffer, pH 3.5 (limit of detection: 0.5 µg protein/ml).

C.3.2.4 Statistical Analysis

All measurements were conducted in quadruplicate and results are representative of experiments performed on two independent days. Results are expressed as mean ± standard deviation. Significant differences were determined through analysis of variance followed by Tukey's post-test with a 95% confidence interval using GraphPad Prism 5 version 5.04 (GraphPad Software Inc., La Jolla, CA, USA).

C.4 Results and Discussion

C.4.1 Characterization of Glucose Oxidase Embedded Polymer Coatings

Hydrophobic ion pairing (HIP) has been shown to increase the dispersibility of proteins in organic solvents *(257)*. This technique allows for the creation of a single-phase solution of hydrophobic modified enzyme in polymer for solvent cast coating applications. The protein content of the hydrophobic modified GOx in toluene was

determined to be 332±28 µg protein/ml, representing 51% enzyme recovery in the hydrophobic phase. After casting on the interior of glass vials, protein content of EVA+DDAB+GOx coatings was determined by BCA assay to be 0.553±0.0.051 µg protein/cm^2. Theoretical protein content of the cast coatings was expected to be 1.96 □g protein/cm^2. The observed ~72% reduction in apparent protein content can be attributed to the embedding of enzyme within the polymer coating, limiting accessibility of BCA assay reagent to the surface of the coating **(Fig. C.1)**.

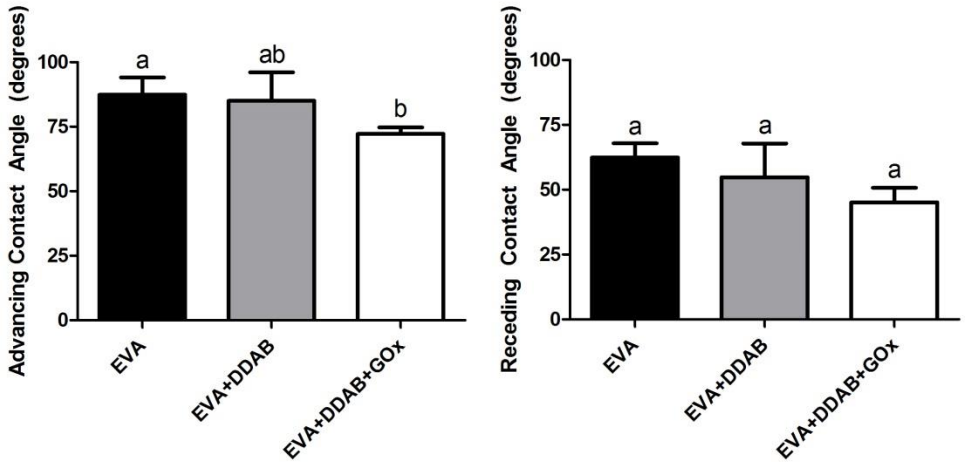

Figure C.1. Dynamic contact angle of EVA, EVA+DDAB, and EVA+DDAB+Glucose oxidase coatings. Values represent means of n=4 measurements ± standard deviation. Letters indicate statistical significance at $p<0.05$.

Coatings prepared on glass vials had thickness ranging from 120 ± 20 □m to 200 ± 30 □m, on the top and bottom edge of the vial, respectively. Overall, thickness was uniform at each end of the vial, represented by the low standard deviation. The observed difference in thickness between the top and bottom edges of the coating was likely a result of the pitch of the roller used in the coating operation. Electron microscopy of cast polymer coatings was performed to characterize coating morphology **(Fig. C.2)**. Control EVA coatings exhibited uniform morphology with no notable topographical features.

Presence of ca. 2 micrometer sized features in EVA+DDAB and EVA+DDAB+GOx coatings suggests formation of DDAB micelles and incomplete separation of aqueous phase during hydrophobic ion pairing. Introduction of hydrophobic modified glucose oxidase in EVA+DDAB+GOx coatings resulted in a uniform coating with no cracks, supporting potential application of the coatings in packaging applications.

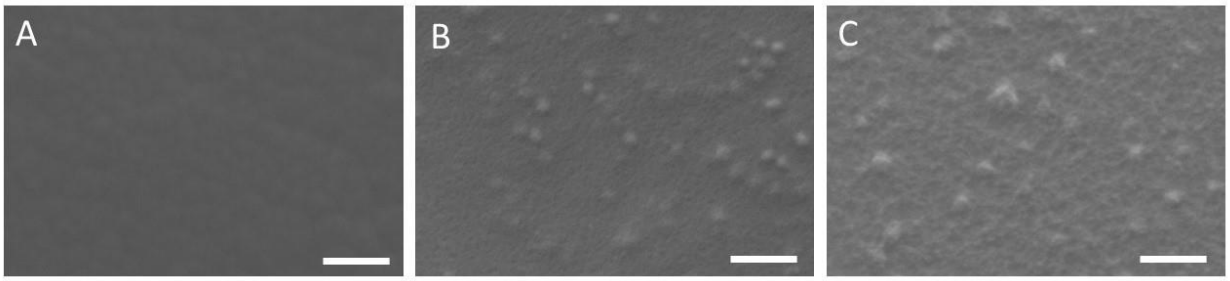

Figure C.2. Electron micrographs of A) EVA, B) EVA+DDAB, and C) EVA+DDAB+GOx cast polymer coatings. Micrographs were captured at 10 kV and 1000x magnification where scale bars represent 20 µm. Images are representative of 4 images acquired across 3 independently prepared coatings.

Native EVA coatings presented an advancing contact angle value of 87.4 ± 6.6°, in agreement with prior reports *(258, 259)*. Introduction of DDAB surfactant in the EVA coating had no significant influence on contact angle, while incorporation of hydrophobic modified glucose oxidase (ie: EVA+DDAB+GOx) reduced advancing contact angle to 72.2 ± 2.5°. The observed increase in hydrophilicity is likely a result of both the surfactant, DDAB, and the glucose oxidase, which despite being rendered soluble in hydrophobic solvents retains hydrophilic residues. Such increase in hydrophilicity may support improved substrate-active site interactions by reducing diffusion limitations often resulting from hydrophobic surfaces, thus improving oxygen scavenging capacity in industrial coating applications.

C.4.2 Protein Migration

Stability of the hydrophobic modified enzyme against leaching from the polymer coating is important for industrial coating applications, for which migration of functional components (e.g. enzymes) can have adverse regulatory implications *(12, 17, 260)* as well as practical limitations in long term coating performance *(30, 32, 214, 217)*. To demonstrate stability of the hydrophobic modified glucose oxidase in cast EVA coatings, a leaching study was performed in which 50 mM citrate buffer, pH 3.5, was added to EVA+DDAB+GOx coated glass vials. Protein content of the buffer was monitored over 8 weeks during static storage at room temperature **(Fig. C.3)**. An acidic buffer was selected to characterize coating performance in beverage or other acidic packaged goods application, for which oxygen control yields enhanced shelf life benefits. Over the course of the 8 week study, more than 75% of protein was retained in the cast coating, with no detectable protein in the leaching solution for the first 4 weeks of the study (limit of detection: 0.5 µg/mL). The observed low levels of protein migration support that hydrophobic modified glucose oxidase was confined within the polymer matrix, without the need for cross-linkers. Cross-linkers are commonly added to enzyme-polymer matrices to increase protein retention and stabilize the enzyme *(261, 262)*. However, these cross-linkers can impact enzyme activity by decreasing substrate accessibility, if the crosslinking density is too high *(263)*. The reported solvent casting method does not rely on chemical cross-linkers to prevent protein leaching, and represents a relatively simple method to produce immobilized enzyme thin films *(262, 263)*.

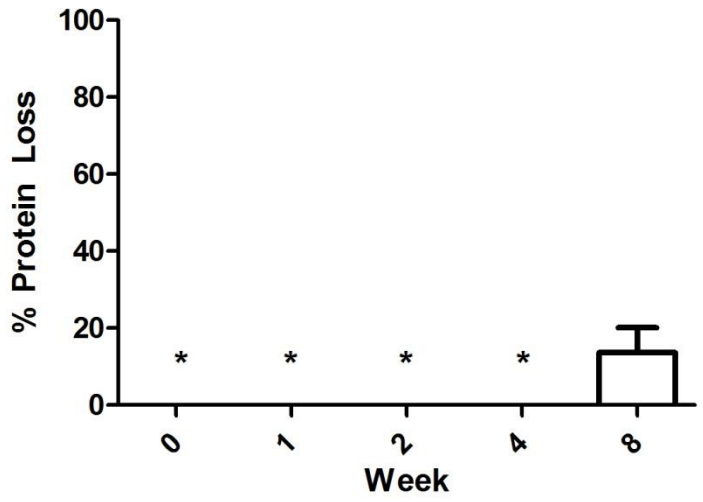

Figure C.3. Protein migration from coating during an 8 week storage study. Asterisk symbols indicate values below the limit of detection for the assay (0.5 µg/ml). Values represent means of n=4 measurements ± standard deviation.

C.4.3 Oxygen scavenging capacity of glucose oxidase embedded polymer coatings

After modification, GOx retained <2% activity of native GOx in reactions of synthetic substrate, O-dianisidine dihydrochloride, when coupled with horseradish peroxidase at pH 5.1. GOx in EVA+DDAB+GOx coatings were found to have an absolute activity of $1.57e^{-9} \pm 1.70e^{-10}$ µmol/s/µg protein or 17.5% of activity compared to modified GOx. To demonstrate the performance of the EVA+DDAB+GOx coating as an oxygen scavenging system, 50 mM citrate buffer, pH 3.5, containing 10% (wt/vol) b-D-glucose, was added to coated glass vials and capped to a final vial system of 50% (v/v) headspace and 50% (v/v) glucose in buffer. Oxygen content of the headspace was monitored over an 8 week storage period. After equilibration, initial headspace oxygen content was 13.7%, and oxygen scavenging was reported as percent reduction in headspace oxygen **(Fig. C.3)**. The headspace oxygen content of the control capped vial, coated with EVA+DDAB, reduced steadily by 0.5% over the 8 weeks. The observed

reduction cast only with 8% EVA and DDAB remained steady, reducing to 13.3% after 8 wks. This is indicative of the enclosed environment and oxygen dissolution into the buffer solution over time. After 8 weeks of storage, headspace oxygen of the EVA+DDAB+GOx coated vials reduced by 1.98%. Regression lines fitted to oxygen percentage values **(Fig. C.4)** indicate the difference in headspace oxygen change between the control and EVA+DDAB+GOx. It is worth noting that the test setup in this proof-of-concept study (in which the vial was 50% headspace) was not typical of packaged goods for which this technology could see application. This large headspace was selected to enable insertion of headspace oxygen instrumentation into the capped vial. It is expected that reducing the percentage headspace by increasing the fill volume and coating surface area to industrially relevant values would enhance the performance of the reported coating. Nevertheless, these results suggest that embedding hydrophobic modified glucose oxidase in EVA results in a polymer coating capable of reducing headspace oxygen without significant leaching of enzyme from the coating.

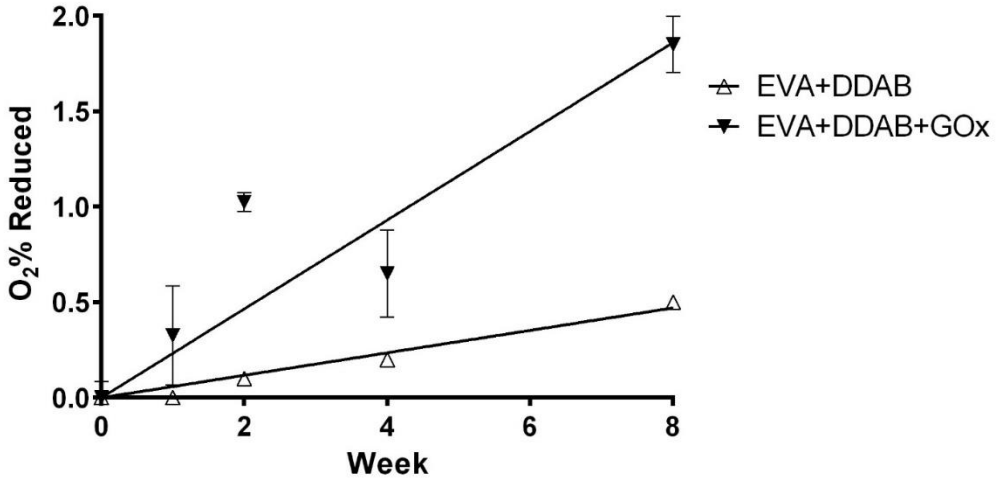

Figure C.4. Reduction in headspace oxygen concentration by EVA+DDAB+GOx coating. Values represent means of n = 4 determinations with error bars indicating standard deviations.

C.5 Conclusions

Oxygen in packaged foods is detrimental to quality, safety, and nutritional value. Methods by which oxygen is reduced in packaged foods is often cumbersome and not designed for food contact. Here, a method established for modifying glucose oxidase to increase solubility in organic solvent is utilized to create an oxygen scavenging active packaging system. Glucose oxidase was rendered hydrophobic by association with the charged surfactant, DDAB, and embedded in EVA cast onto glass vials. The coatings were evaluated for protein content, enzyme activity, and efficacy in reducing headspace oxygen.

Approximately 50% of the glucose oxidase was recovered in the toluene phase after hydrophobic ion pairing, which upon embedding in EVA and solvent casting resulted in a uniform coating with 0.553 μg enzyme/cm^2 available at the coating surface. Introduction of hydrophobic modified glucose oxidase reduced the contact angle of EVA from 87.4° to 72.2°. The oxygen scavenging polymer coatings effectively reduced headspace oxygen by 2% over 8 weeks in the closed-vial system (50 vol% headspace, 50 vol% citrate buffer, pH 3.5). Minimal protein migration was observed over the 8 week study (below limit of detection for first 4 weeks, <25% migration at week 8), suggesting long term durability of the coating without the need for cross-linking reagents commonly used in immobilized enzyme systems. These results suggest that hydrophobic modified glucose oxidase can be incorporated in hydrophobic polymers for application in oxygen scavenging coating applications. Such coatings can be readily adapted to high throughput coating systems, supporting the potential for commercial translation.

REFERENCES

1. Fernández A, Cava D, Ocio MJ, Lagarón JM. Perspectives for biocatalysts in food packaging. *Trends Food Sci Technol.* 2008; 19(4): 198-206.

2. Enzymes in food technology [homepage on the Internet]. West Sussex, U.K.; Ames, Iowa: Wiley-Blackwell. 2010.

3. Paige D, Bayless T, Huang S, Wexler R. Lactose hydrolyzed milk. *Am J Clin Nutr.* 1975; 28(8): 818-822.

4. Horner TW, Dunn M, Eggett D, Ogden L. B-galactosidase activity of commercial lactase samples in raw and pasteurized milk at refrigerated temperatures. *J Dairy Sci.* 2011; 94(7): 3242-3249.

5. Lorenzen PC, Breiter J, Clawin-Rädecker I, Dau A. A novel bi-enzymatic system for lactose conversion. *Int J Food Sci Tech.* 2013; 48(7): 1396-1403.

6. Hsu J, Heatherbell D, Yorgey B. Effects of fruit storage and processing on clarity, proteins, and stability of granny smith apple juice. *J Food Sci.* 1989; 54(3): 660-662.

7. Sandri IG, Fontana RC, Barfknecht DM, da Silveira MM. Clarification of fruit juices by fungal pectinases. *LWT - Food Science and Technology.* 2011 12; 44(10): 2217-2222.

8. Nagar S., Mittal A.,Gupta V.K.,. Enzymatic clarification of fruit juices (apple, pineapple, and tomato) using purified bacillus pumilus SV-85S xylanase. *Biotechnol.Bioprocess Eng.Biotechnology and Bioprocess Engineering.* 2012; 17(6): 1165-1175.

9. Soares N, Hotchkiss J. Naringinase immobilization in packaging films for reducing naringin concentration in grapefruit juice. *J Food Sci.* 1998; 63(1): 61-65.

10. Johansson K, Jönsson LJ, Järnström L. Oxygen scavenging enzymes in coatings: Effect of coating procedures on enzyme activity. *Nordic Pulp & Paper Research Journal.* 2011; 26(2): 197-204.

11. Vermeiren L, Devlieghere F, van Beest M, de Kruijf N, Debevere J. Developments in the active packaging of foods. *Trends Food Sci Technol.* 1999; 10(3): 77-86.

12. Koontz J. Active packaging materials to inhibit lipid oxidation: US regulatory framework. *International news on fats, oils and related materials.* 2012; 23(9): 598-600.

13. Tian F, Decker EA, Goddard JM. Controlling lipid oxidation of food by active packaging technologies. *Food Funct.* 2013; 4(5): 669-680.

14. Brody AL, Budny JA. Enzymes as active packaging agents. In: Rooney ML, editor. Active Food Packaging. New York, NY: Blackie Academic and Professional; 1995. p. 174-192.

15. Goddard JM, Hotchkiss JH. Polymer surface modification for the attachment of bioactive compounds. *Prog Polym Sci.* 2007; 32(7): 698-725.

16. Talbert J, Goddard J. Enzymes on material surfaces. *Colloids Surf , B.* 2012; 93: 8-19.

17. Bastarrachea LJ, Wong DE, Roman MJ, Lin Z, Goddard JM. Active packaging coatings. *Coatings.* 2015; 5(4): 771-791.

18. Ghasemi-Mobarakeh L, Semnani D, Morshed M. A novel method for porosity measurement of various surface layers of nanofibers mat using image analysis for tissue engineering applications. *J Appl Polym Sci.* 2007; 106(4): 2536-2542.

19. Norde W, Zoungrana T. Surface-induced changes in the structure and activity of enzymes physically immobilized at solid/liquid interfaces. *Biotechnol Appl Biochem.* 1998; 28(2): 133-143.

20. Fang F, Szleifer I. Effect of molecular structure on the adsorption of protein on surfaces with grafted polymers. *Langmuir.* 2002 07/01; 18(14): 5497-5510.

21. Novick SJ, Dordick JS. Protein-containing hydrophobic coatings and films. *Biomaterials.* 2002 1; 23(2): 441-448.

22. Betancor L, López-Gallego F, Hidalgo A, Alonso-Morales N, Fuentes M, Fernández-Lafuente R, Guisán JM. Prevention of interfacial inactivation of enzymes by coating the enzyme surface with dextran-aldehyde. *J Biotechnol.* 2004 5/27; 110(2): 201-207.

23. Del Nobile MA, Conte A. Bio-based packaging materials for controlled release of active compounds. In: Packaging for Food Preservation. Springer; 2013. p. 91-107.

24. Kong F, Hu YF. Biomolecule immobilization techniques for bioactive paper fabrication. *Analytical and bioanalytical chemistry.* 2012; 403(1): 7-13.

25. Andersson M, Andersson T, Adlercreutz P, Nielsen T, Hörnsten EG. Toward an enzyme-based oxygen scavenging laminate. influence of industrial lamination conditions on the performance of glucose oxidase. *Biotechnol Bioeng.* 2002; 79(1): 37-42.

26. Johansson K, Kotkamo S, Rotabakk BT, Johansson C, Kuusipalo J, Jönsson LJ, Järnström L. Extruded polymer films for optimal enzyme-catalyzed oxygen scavenging. *Chemical Engineering Science.* 2014; 108: 1-8.

27. Talbert JN, He F, Seto K, Nugen SR, Goddard JM. Modification of glucose oxidase for the development of biocatalytic solvent inks. *Enzyme Microb Technol.* 2014 2/5; 55(0): 21-25.

28. Soares N, Hotchkiss J. Bitterness reduction in grapefruit juice through active packaging. *Packaging technology and science.* 1998; 11(1): 9-18.

29. Nunes MA, Vila-Real H, Fernandes PC, Ribeiro MH. Immobilization of naringinase in PVA–alginate matrix using an innovative technique. *Appl Biochem Biotechnol.* 2010; 160(7): 2129-2147.

30. Goddard JM, Talbert JN, Hotchkiss JH. Covalent attachment of lactase to low-density polyethylene films. *J Food Sci.* 2007; 72(1): E36-E41.

31. Mahoney KW, Talbert JN, Goddard JM. Effect of polyethylene glycol tether size and chemistry on the attachment of lactase to polyethylene films. *J Appl Polym Sci.* 2013; 127(2): 1203-1210.

32. Wong DE, Talbert JN, Goddard JM. Layer by layer assembly of a biocatalytic packaging film: Lactase covalently bound to Low-Density polyethylene. *J Food Sci.* 2013; 78(6): 853-860.

33. Hermanson GT. Bioconjugate techniques. Burlington : Elsevier,; 2008.

34. Wong SS, Wong LC. Chemical crosslinking and the stabilization of proteins and enzymes. *Enzyme Microb Technol.* 1992 11; 14(11): 866-874.

35. Manta C, Ferraz N, Betancor L, Antunes G, Batista-Viera F, Carlsson J, Caldwell K. Polyethylene glycol as a spacer for solid-phase enzyme immobilization. *Enzyme Microb Technol.* 2003 12/2; 33(7): 890-898.

36. Mattson G, Conklin E, Desai S, Nielander G, Savage M, Morgensen S. A practical approach to crosslinking. *Mol Biol Rep.* 1993; 17(3): 167-183.

37. Sheldon RA, van Pelt S. Enzyme immobilisation in biocatalysis: Why, what and how. *Chem Soc Rev.* 2013; 42(15): 6223-6235.

38. Wong DE, Dai M, Talbert JN, Nugen SR, Goddard JM. Biocatalytic polymer nanofibers for stabilization and delivery of enzymes. *J Molec Catal B.* 2014; 110: 16-22.

39. Ge L, Zhao Y, Mo T, Li J, Li P. Immobilization of glucose oxidase in electrospun nanofibrous membranes for food preservation. *Food Control.* 2012; 26(1): 188-193.

40. Heyman MB. Lactose intolerance in infants, children, and adolescents. *Pediatrics.* 2006; 118(3): 1279-1286.

41. Lomer M, Parkes G, Sanderson J. Review article: Lactose intolerance in clinical practice–myths and realities. *Aliment Pharmacol Ther.* 2007; 27(2): 93-103.

42. Savaiano DA, Levitt MD. Milk intolerance and microbe-containing dairy foods. *J Dairy Sci.* 1987 2; 70(2): 397-406.

43. Vesa TH, Marteau P, Korpela R. Lactose intolerance. *J Am Coll Nutr.* 2000; 19(2 Suppl): 165-175S.

44. Swallow D. Genetics of lactase persistence and lactose intolerance. *Annu Rev Genet.* 2003; 37: 197-219.

45. Matthews S, Waud J, Roberts A, Campbell A. Systemic lactose intolerance: A new perspective on an old problem. *Postgrad Med J.* 2005; 81(953): 167-173.

46. Adhikari K, Dooley LM, Chambers E, Bhumiratana N. Sensory characteristics of commercial lactose-free milks manufactured in the united states. *LWT-Food Science and Technology.* 2010; 43(1): 113-118.

47. Chapman KW, Lawless HT, Boor KJ. Quantitative descriptive analysis and principal component analysis for sensory characterization of ultrapasteurized milk. *J Dairy Sci.* 2001 1; 84(1): 12-20.

48. Oupadissakoon G, Chambers DH, Chambers IV E. Comparison of the sensory properties of ultra-high-temperature (UHT) milk from different countries. *J Sens Stud.* 2009; 24(3): 427-440.

49. Jelen P, Tossavainen O. Low lactose and lactose-free milk and dairy products - prospects, technologies and applications. *Aust J Dairy Technol.* 2003; 58(2): 161-166.

50. Haider T, Husain Q. Hydrolysis of milk/whey lactose by beta galactosidase: A comparative study of stirred batch process and packed bed reactor prepared with calcium alginate entrapped enzyme. *Chem Eng Process.* 2009; 48(1): 576-580.

51. Ansari S, Husain Q. Immobilization of kluyveromyces lactis beta galactosidase on concanavalin A layered aluminium oxide nanoparticles-its future aspects in biosensor applications. *J Mol Catal B: Enzym.* 2011; 70(3-4): 119-126.

52. Dahlqvis A, Mattiasson B, Mosbach K. Hydrolysis of beta-galactosides using polymer-entrapped lactase - study towards producing lactose-free milk. *Biotechnol Bioeng.* 1973; 15(2): 395-402.

53. Zhou Q, Chen X, Li X. Kinetics of lactose hydrolysis by beta-galactosidase of kluyveromyces lactis immobilized on cotton fabric. *Biotechnol Bioeng.* 2003; 81(2): 127-133.

54. Yam J. Intelligent packaging: Concepts and applications. *J Food Sci.* 2005; 70(1): 1-R10.

55. Zhang Y, Rochefort D. Activity, conformation and thermal stability of laccase and glucose oxidase in poly(ethyleneimine) microcapsules for immobilization in paper. *Process Biochem.* 2011; 46(4): 993-1000.

56. Grosova Z, Rosenberg M, Rebros M, Sipocz M, Sedlackova B. Entrapment of beta-galactosidase in polyvinylalcohol hydrogel. *Biotechnol Lett.* 2008; 30(4): 763-767.

57. Kong F, Hu Y. Biomolecule immobilization techniques for bioactive paper fabrication. *Anal Bioanal Chem.* 2012; 403(1): 7-13.

58. Feng Y, Chang X, Wang W, Ma R. Stabilities of immobilized beta-galactosidase of aspergillus sp AF for the optimal production of galactooligosaccharides from lactose. *Artif Cells, Blood Substitutes, Immobilization Biotechnol.* 2010; 38(1): 43-51.

59. Kothapalli A, Morgan M, Sadler G. UV polymerization-based surface modification technique for the production of bioactive packaging. *J Appl Polym Sci.* 2008; 107(3): 1647-1654.

60. Decher G, Maclennan J, Reibel J, Sohling U. Highly-ordered ultrathin LC multilayer films on solid substrates. *Adv Mater.* 1991; 3(12): 617-619.

61. Decher G. Fuzzy nanoassemblies: Toward layered polymeric multicomposites. *Science.* 1997; 277(5330): 1232-1237.

62. Decher G, Eckle M, Schmitt J, Struth B. Layer-by-layer assembled multicomposite films. *Curr Opin Colloid Interface Sci.* 1998; 3(1): 32-39.

63. Fu J, Ji J, Yuan W, Shen J. Construction of anti-adhesive and antibacterial multilayer films via layer-by-layer assembly of heparin and chitosan. *Biomaterials.* 2005; 26(33): 6684-6692.

64. Lvov Y, Ariga K, Ichinose I, Kunitake T. Assembly of multicomponent protein films by means of electrostatic layer-by-layer adsorption. *J Am Chem Soc.* 1995; 117(22): 6117-6123.

65. Stewart Clark S, Lvov Y, Mills D. Ultrasonic nebulization-assisted layer-by-layer assembly for spray coating of multilayered, multicomponent, bioactive nanostructures. *JCT Res.* 2011; 8(2): 275-281.

66. Disawal S, Qiu H, Elmore B, Lvov Y. Two-step sequential reaction catalyzed by layer-by-layer assembled urease and arginase multilayers. *Colloids Surf , B.* 2003; 32(2): 145-156.

67. Wang Y, Hong Q, Chen Y, Lian X, Xiong Y. Surface properties of polyurethanes modified by bioactive polysaccharide-based polyelectrolyte multilayers. *Colloids Surf , B.* 2012; 100: 77-83.

68. Barish JA, Goddard JM. Topographical and chemical characterization of polymer surfaces modified by physical and chemical processes. *J Appl Polym Sci.* 2011; 120(5): 2863-2871.

69. Tian F, Decker E, Goddard J. Development of an iron chelating polyethylene film for active packaging applications. *J Agric Food Chem.* 2012; 60(8): 2046-2052.

70. Kretchmer N. Lactose and lactase. *Sci Am.* 1972; 227: 70.

71. Sungur S. Immobilization of beta-galactosidase onto gelatin by glutaraldehyde and chromium (III) acetate. *J Chem Technol Biotechnol.* 1994; 59: 303.

72. Brown RE, Jarvis KL, Hyland KJ. Protein measurement using bicinchoninic acid: Elimination of interfering substances. *Anal Biochem.* 1989; 180(1): 136-139.

73. Wiechelman KJ, Braun RD, Fitzpatrick JD. Investigation of the bicinchoninic acid protein assay: Identification of the groups responsible for color formation. *Anal Biochem.* 1988; 175(1): 231-237.

74. Institute of Medicine (US). Committee on Food Chemicals Codex. Food chemicals codex. V ed. Washington, D.C.: National Academies Press; 2003.

75. Cornish-Bowden A. Fundamentals of enzyme kinetics. Butterworths London; 1979.

76. Jia H. Catalytic behaviors of enzymes attached to nanoparticles: The effect of particle mobility. *Biotechnol Bioeng.* 2003; 84(4): 406-414.

77. Caruso F, Trau D, Möhwald H, Renneberg R. Enzyme encapsulation in layer-by-layer engineered polymer multilayer capsules. *Langmuir.* 2000; 16(4): 1485-1488.

78. Betancor L, Luckarift HR. Bioinspired enzyme encapsulation for biocatalysis. *Trends Biotechnol.* 2008; 26(10): 566-572.

79. Park B, Yoon D, Kim D. Recent progress in bio-sensing techniques with encapsulated enzymes. *Biosens Bioelectron.* 2010; 26(1): 1-10.

80. Gassara-Chatti F, Brar SK, Ajila CM, Verma M, Tyagi RD, Valero JR. Encapsulation of ligninolytic enzymes and its application in clarification of juice. *Food Chem.* 2013 4/15; 137(1–4): 18-24.

81. Wan L, Ke B, Xu Z. Electrospun nanofibrous membranes filled with carbon nanotubes for redox enzyme immobilization. *Enzyme Microb Technol.* 2008 3/4; 42(4): 332-339.

82. Talbert JN, Goddard JM. Characterization of lactase-conjugated magnetic nanoparticles. *Process Biochem.* 2013; 48: 656-662.

83. Megelski S, Stephens JS, Chase DB, Rabolt JF. Micro-and nanostructured surface morphology on electrospun polymer fibers. *Macromolecules.* 2002; 35(22): 8456-8466.

84. Andrady AL. Science and technology of polymer nanofibers. Hoboken, N.J: Wiley-Interscience; 2008.

85. Pham QP, Sharma U, Mikos AG. Electrospun poly (ε-caprolactone) microfiber and multilayer nanofiber/microfiber scaffolds: Characterization of scaffolds and measurement of cellular infiltration. *Biomacromolecules.* 2006; 7(10): 2796-2805.

86. Wendorff JH, Agarwal S, Greiner A. Electrospinning materials, processing, and applications. Hoboken, N.J.: John Wiley & Sons; 2012.

87. Reneker DH, Chun I. Nanometre diameter fibres of polymer, produced by electrospinning. *Nanotechnology.* 1996; 7(3): 216.

88. Deitzel JM, Kleinmeyer J, Harris D, Beck Tan NC. The effect of processing variables on the morphology of electrospun nanofibers and textiles. *Polymer.* 2001; 42(1): 261-272.

89. Huang Z, Zhang Y, Kotaki M, Ramakrishna S. A review on polymer nanofibers by electrospinning and their applications in nanocomposites. *Composites Sci Technol.* 2003; 63(15): 2223-2253.

90. Matthews JA, Wnek GE, Simpson DG, Bowlin GL. Electrospinning of collagen nanofibers. *Biomacromolecules.* 2002; 3(2): 232-238.

91. Lagaron JM, Lopez-Rubio A. Nanotechnology for bioplastics: Opportunities, challenges and strategies. *Trends Food Sci Technol.* 2011; 22(11): 611-617.

92. Ma Z, Kotaki M, Inai R, Ramakrishna S. Potential of nanofiber matrix as tissue-engineering scaffolds. *Tissue Eng.* 2005; 11(1-2): 101-109.

93. Kuan C, Yee-Fung W, Yuen K, Liong M. Nanotech: Propensity in foods and bioactives. *Crit Rev Food Sci Nutr.* 2012; 52(1): 55-71.

94. Ignatious F, Sun L, Lee C, Baldoni J. Electrospun nanofibers in oral drug delivery. *Pharm Res.* 2010; 27(4): 576-588.

95. Zhou C, Chu R, Wu R, Wu Q. Electrospun polyethylene oxide/cellulose nanocrystal composite nanofibrous mats with homogeneous and heterogeneous microstructures. *Biomacromolecules.* 2011; 12(7): 2617-2625.

96. Wang Z, Wan L, Liu Z, Huang X, Xu Z. Enzyme immobilization on electrospun polymer nanofibers: An overview. *J Molec Catal B.* 2009; 56(4): 189-195.

97. Stoilova O, Manolova N, Gabrovska K, Marinov I, Godjevargova T, Mita DG, Rashkov I. Electrospun polyacrylonitrile nanofibrous membranes tailored for acetylcholinesterase immobilization. *J Bioact Compatible Polym.* 2010; 25(1): 40-57.

98. Sathishkumar P, Chae J, Unnithan AR, Palvannan T, Kim HY, Lee K, Cho M, Kamala-Kannan S, Oh B. Laccase-poly (lactic-*co*-glycolic acid)(PLGA) nanofiber: Highly stable, reusable, and efficacious for the transformation of diclofenac. *Enzyme Microb Technol.* 2012; 51(2): 113-118.

99. Zeng J, Aigner A, Czubayko F, Kissel T, Wendorff JH, Greiner A. Poly (vinyl alcohol) nanofibers by electrospinning as a protein delivery system and the retardation of enzyme release by additional polymer coatings. *Biomacromolecules.* 2005; 6(3): 1484-1488.

100. Wang Z, Wang J, Xu Z. Immobilization of lipase from candida rugosa on electrospun polysulfone nanofibrous membranes by adsorption. *J Molec Catal B.* 2006 10/2; 42(1–2): 45-51.

101. El-Aassar MR. Functionalized electrospun nanofibers from poly (AN-co-MMA) for enzyme immobilization. *J Molec Catal B.* 2013 1; 85–86(0): 140-148.

102. Li S, Chen J, Wu W. Electrospun polyacrylonitrile nanofibrous membranes for lipase immobilization. *J Molec Catal B.* 2007 7/2; 47(3–4): 117-124.

103. Li S, Fan Y, Hu R, Wu W. < I> pseudomonas cepacia lipase immobilized onto the electrospun PAN nanofibrous membranes for biodiesel production from soybean oil. *J Molec Catal B.* 2011; 72(1): 40-45.

104. Maretschek S, Greiner A, Kissel T. Electrospun biodegradable nanofiber nonwovens for controlled release of proteins. *J Controlled Release.* 2008; 127(2): 180-187.

105. Qu F, Lin JG, Esterhai JL, Fisher MB, Mauck RL. Biomaterial-mediated delivery of degradative enzymes to improve meniscus integration and repair. *Acta Biomater.* 2013; 9(5): 6393-6402.

106. Cho WJ, Kim JH, Oh SH, Nam HH, Kim JM, Lee JH. Hydrophilized polycaprolactone nanofiber mesh-embedded poly (glycolic-co-lactic acid) membrane for effective guided bone regeneration. *J Biomed Mater Res Part A.* 2009; 91(2): 400-407.

107. Liu Y, Chen J, Anh NT, Too CO, Misoska V, Wallace GG. Nanofiber mats from DNA, SWNTs, and poly (ethylene oxide) and their application in glucose biosensors. *J Electrochem Soc.* 2008; 155(5): K100-K103.

108. Schomburg I, Chang A, Placzek S, Sohngen C, Rother M, Lang M, Munaretto C, Ulas S, Stelzer M, Grote A, Scheer M, Schomburg D. BRENDA in 2013: Integrated reactions, kinetic data, enzyme function data, improved disease classification: New options and contents in BRENDA. *Nucleic Acids Research.* 2012; 41(D1): D764-D772.

109. Mckinney RM, Spillane JT, Pearce GW. Factors affecting the rate of reaction of fluorescein isothiocyanate with serum proteins. *J Immunol.* 1964; 93(2): 232-242.

110. Maggi L, Segale L, Torre M, Ochoa Machiste E, Conte U. Dissolution behaviour of hydrophilic matrix tablets containing two different polyethylene oxides (PEOs) for the controlled release of a water-soluble drug. dimensionality study. *Biomaterials.* 2002; 23(4): 1113-1119.

111. Kazarian SG. Simultaneous FTIR spectroscopic imaging and visible photography to monitor tablet dissolution and drug release. *Pharm Res.* 2008; 25(4): 853.

112. Bradford MM. A rapid and sensitive method for the quantitation of microgram quantities of protein utilizing the principle of protein-dye binding. *Anal Biochem.* 1976 5/7; 72(1–2): 248-254.

113. Chaplin LC, Lyster RL. Effect of temperature on the pH of skim milk. *J Dairy Res.* 1988; 55: 277-280.

114. Amamcharla J, Metzger L. Development of a rapid method for the measurement of lactose in milk using a blood glucose biosensor. *J Dairy Sci.* 2011; 94(10): 4800-4809.

115. Haj-Ahmad RR, Elkordy AA, Chaw CS, Moore A. Compare and contrast the effects of surfactants (pluronic® F-127 and cremophor® EL) and sugars (β-cyclodextrin and inulin) on properties of spray dried and crystallised lysozyme. *Eur J Pharm Sci.* 2013; 49(4): 519-534.

116. Pragatheeswaran AM, Chen SB. Effect of chain length of PEO on the gelation and micellization of the pluronic F127 copolymer aqueous system. *Langmuir.* 2013; 29(31): 9694-9701.

117. Kriegel C, Kit K, McClements D, Weiss J. Influence of surfactant type and concentration on electrospinning of chitosan–poly (ethylene oxide) blend nanofibers. *Food Biophys.* 2009; 4(3): 213-228.

118. Kriegel C, Kit K, McClements D, Weiss J. Electrospinning of chitosan–poly (ethylene oxide) blend nanofibers in the presence of micellar surfactant solutions. *Polymer.* 2009; 50(1): 189-200.

119. Ziani K, Henrist C, Jérôme C, Aqil A, Maté JI, Cloots R. Effect of nonionic surfactant and acidity on chitosan nanofibers with different molecular weights. *Carbohydr Polym.* 2011; 83(2): 470-476.

120. Jia L, Qin X. The effect of different surfactants on the electrospinning poly (vinyl alcohol)(PVA) nanofibers. *J Therm Anal Calorim.* 2013; 112(2): 595-605.

121. Pucić I, Jurkin T. FTIR assessment of poly(ethylene oxide) irradiated in solid state, melt and aqeuous solution. *Radiat Phys Chem.* 2012 9; 81(9): 1426-1429.

122. Kong J, Yu S. Fourier transform infrared spectroscopic analysis of protein secondary structures. *Acta Bioch Bioph Sin.* 2007; 39(8): 549-559.

123. Murphy D, de Pinho MN. An ATR-FTIR study of water in cellulose acetate membranes prepared by phase inversion. *J Membr Sci.* 1995; 106(3): 245-257.

124. Ping ZH, Nguyen QT, Chen SM, Zhou JQ, Ding YD. States of water in different hydrophilic polymers — DSC and FTIR studies. *Polymer.* 2001 9; 42(20): 8461-8467.

125. Trezza MA. Hydration study of ordinary portland cement in the presence of zinc ions. *Materials Research.* 2007; 10(4): 331-334.

126. Pan C, Hu B, Li W, Sun Y, Ye H, Zeng X. Novel and efficient method for immobilization and stabilization of β-d-galactosidase by covalent attachment onto magnetic Fe_3O_4 chitosan nanoparticles. *J Molec Catal B.* 2009; 61(3): 208-215.

127. Mai THA, Tran VN, Le VVM. Biochemical studies on the immobilized lactase in the combined alginate–carboxymethyl cellulose gel. *Biochem Eng J.* 2013 5/15; 74(0): 81-87.

128. Mateo C, Palomo JM, Fernandez-Lorente G, Guisan JM, Fernandez-Lafuente R. Improvement of enzyme activity, stability and selectivity via immobilization techniques. *Enzyme Microb Technol.* 2007 5/2; 40(6): 1451-1463.

129. Sheldon RA. Enzyme immobilization: The quest for optimum performance. *Adv Synth Catal.* 2007; 349(8-9): 1289-1307.

130. Brady D, Jordaan J. Advances in enzyme immobilisation. *Biotechnol Lett.* 2009; 31(11): 1639-1650.

131. Garcia-Galan C, Berenguer-Murcia Á, Fernandez-Lafuente R, Rodrigues RC. Potential of different enzyme immobilization strategies to improve enzyme performance. *Advanced Synthesis & Catalysis.* 2011; 353(16): 2885-2904.

132. Barbosa O, Torres R, Ortiz C, Fernandez-Lafuente R. Versatility of glutaraldehyde to immobilize lipases: Effect of the immobilization protocol on the properties of lipase B from candida antarctica. *Process Biochemistry.* 2012; 47(8): 1220-1227.

133. Santos, Jose Cleiton S dos, Barbosa O, Ortiz C, Berenguer-Murcia A, Rodrigues RC, Fernandez-Lafuente R. Importance of the support properties for immobilization or purification of enzymes. *ChemCatChem.* 2015; 7(16): 2413-2432.

134. Mnyusiwalla A, Daar AS, Singer PA. 'Mind the gap': Science and ethics in nanotechnology. *Nanotechnology.* 2003; 14(3): R9.

135. Vaddiraju S, Tomazos I, Burgess DJ, Jain FC, Papadimitrakopoulos F. Emerging synergy between nanotechnology and implantable biosensors: A review. *Biosensors and Bioelectronics.* 2010; 25(7): 1553-1565.

136. Jianrong C, Yuqing M, Nongyue H, Xiaohua W, Sijiao L. Nanotechnology and biosensors. *Biotechnol Adv.* 2004; 22(7): 505-518.

137. Ferrari M. Cancer nanotechnology: Opportunities and challenges. *Nature Reviews Cancer.* 2005; 5(3): 161-171.

138. Farokhzad OC, Langer R. Impact of nanotechnology on drug delivery. *ACS nano.* 2009; 3(1): 16-20.

139. Weiss J, Takhistov P, McClements DJ. Functional materials in food nanotechnology. *J Food Sci.* 2006; 71(9): R107-R116.

140. Arinstein A, Burman M, Gendelman O, Zussman E. Effect of supramolecular structure on polymer nanofibre elasticity. *Nature nanotechnology.* 2007; 2(1): 59-62.

141. Zussman E, Burman M, Yarin A, Khalfin R, Cohen Y. Tensile deformation of electrospun nylon-6, 6 nanofibers. *Journal of Polymer Science Part B: Polymer Physics.* 2006; 44(10): 1482-1489.

142. Wong S, Baji A, Leng S. Effect of fiber diameter on tensile properties of electrospun poly (ε-caprolactone). *Polymer.* 2008; 49(21): 4713-4722.

143. Stachewicz U, Barber AH. Enhanced wetting behavior at electrospun polyamide nanofiber surfaces. *Langmuir.* 2011; 27(6): 3024-3029.

144. Talbert JN, Goddard JM. Influence of nanoparticle diameter on conjugated enzyme activity. *Food Bioprod Process.* 2013 10; 91(4): 693-699.

145. Ansari SA, Husain Q. Potential applications of enzymes immobilized on/in nano materials: A review. *Biotechnol Adv.* 2012 0; 30(3): 512-523.

146. Cipolatti EP, Silva MJA, Klein M, Feddern V, Feltes MMC, Oliveira JV, Ninow JL, de Oliveira D. Current status and trends in enzymatic nanoimmobilization. *J Molec Catal B.* 2014; 99: 56-67.

147. Klein MP, Nunes MR, Rodrigues RC, Benvenutti EV, Costa TM, Hertz PF, Ninow JL. Effect of the support size on the properties of β-galactosidase immobilized on chitosan: Advantages and disadvantages of macro and nanoparticles. *Biomacromolecules.* 2012; 13(8): 2456-2464.

148. Oldham CJ, Gong B, Spagnola JC, Jur JS, Senecal KJ, Godfrey TA, Parsons GN. Encapsulation and chemical resistance of electrospun nylon nanofibers coated using integrated atomic and molecular layer deposition. *J Electrochem Soc.* 2011; 158(9): D549-D556.

149. Niu H, Wang X, Lin T. Needleless electrospinning: Influences of fibre generator geometry. *Journal of the Textile Institute.* 2012; 103(7): 787-794.

150. Niu H, Lin T. Fiber generators in needleless electrospinning. *Journal of nanomaterials.* 2012; 2012: 12.

151. Han W, Nurwaha D, Li C, Wang X. Free surface electrospun fibers: The combined effect of processing parameters. *Polymer Engineering & Science.* 2014; 54(1): 189-197.

152. Shuakat MN, Lin T. Recent developments in electrospinning of nanofiber yarns. *Journal of nanoscience and nanotechnology.* 2014; 14(2): 1389-1408.

153. Manesh K, Kim HT, Santhosh P, Gopalan A, Lee K. A novel glucose biosensor based on immobilization of glucose oxidase into multiwall carbon nanotubes–polyelectrolyte-loaded electrospun nanofibrous membrane. *Biosensors and Bioelectronics.* 2008; 23(6): 771-779.

154. Yoo HS, Kim TG, Park TG. Surface-functionalized electrospun nanofibers for tissue engineering and drug delivery. *Adv Drug Deliv Rev.* 2009 10/5; 61(12): 1033-1042.

155. Pérez-Esteve E, Bernardos A, Martínez-Máñez R, M Barat J. Nanotechnology in the development of novel functional foods or their package. an overview based in patent analysis. *Recent patents on food, nutrition & agriculture.* 2013; 5(1): 35-43.

156. Hosseinkhani H, Hosseinkhani M, Khademhosseini A, Kobayashi H. Bone regeneration through controlled release of bone morphogenetic protein-2 from 3-D tissue engineered nano-scaffold. *J Controlled Release.* 2007 2/26; 117(3): 380-386.

157. Campbell AS, Dong C, Meng F, Hardinger J, Perhinschi G, Wu N, Dinu CZ. Enzyme catalytic efficiency: A function of bio–nano interface reactions. *ACS applied materials & interfaces.* 2014; 6(8): 5393-5403.

158. Skordoulis CD, Makropoulou M, Serafetinides AA. Ablation of nylon-6,6 with UV and IR lasers. *Appl Surf Sci.* 1995 2; 86(1–4): 239-244.

159. Pantchev I, Farquet P, Surbeck H, Meyer T. Surface modified nylon 6,6 and application for adsorption and detection of uranium in potable water. *React Funct Polym.* 2007 2; 67(2): 127-135.

160. DelMar E, Largman C, Brodrick J, Geokas M. A sensitive new substrate for chymotrypsin. *Anal Biochem.* 1979; 99(2): 316-320.

161. Kaspar P, Moller G, Wahlefeld A. New photometric assay for chymotrypsin in stool. *Clin Chem.* 1984 Nov; 30(11): 1753-1757.

162. Ahn C, Ye Y, Ratnakumar B, Witham C, Bowman Jr R, Fultz B. Hydrogen desorption and adsorption measurements on graphite nanofibers. *Appl Phys Lett.* 1998; 73(23): 3378-3380.

163. Peigney A, Laurent C, Flahaut E, Bacsa R, Rousset A. Specific surface area of carbon nanotubes and bundles of carbon nanotubes. *Carbon.* 2001; 39(4): 507-514.

164. Ji L, Zhang X. Fabrication of porous carbon nanofibers and their application as anode materials for rechargeable lithium-ion batteries. *Nanotechnology.* 2009; 20(15): 155705.

165. Kakade M, Liener IE. Determination of available lysine in proteins. *Anal Biochem.* 1969; 27(2): 273-280.

166. Weber C, Coester C, Kreuter J, Langer K. Desolvation process and surface characterisation of protein nanoparticles. *Int J Pharm.* 2000; 194(1): 91-102.

167. Rodrigues D, Camilo FF, Caseli L. Cellulase and alcohol dehydrogenase immobilized in langmuir and Langmuir–Blodgett films and their molecular-level effects upon contact with cellulose and ethanol. *Langmuir.* 2014; 30(7): 1855-1863.

168. Caseli L, Furriel RPM, de Andrade JF, Leone FA, Zaniquelli MED. Surface density as a significant parameter for the enzymatic activity of two forms of alkaline phosphatase immobilized on phospholipid Langmuir–Blodgett films. *J Colloid Interface Sci.* 2004; 275(1): 123-130.

169. Caseli L, Oliveira RG, Masui DC, Furriel RP, Leone FA, Maggio B, Zaniquelli MED. Effect of molecular surface packing on the enzymatic activity modulation of an anchored protein on phospholipid langmuir monolayers. *Langmuir.* 2005; 21(9): 4090-4095.

170. Li D, Ding H, Zhou T. Covalent immobilization of mixed proteases, trypsin and chymotrypsin, onto modified polyvinyl chloride microspheres. *J Agric Food Chem.* 2013; 61(44): 10447-10453.

171. Torchilin V, Maksimenko A, Smirknov V, Berezin I, Klibanov A, Martinek K. The principles of enzyme stabilization. III. the effect of the length of intra-molecular cross-linkages on thermostability of enzymes. *Biochimica et Biophysica Acta (BBA)-Enzymology.* 1978; 522(2): 277-283.

172. Torchilin V, Maksimenko A, Smirnov V, Berezin I, Klibanov A, Martinek K. The principles of enzyme stabilization IV. modification of 'key'functional groups in the tertiary structure of proteins. *Biochimica et Biophysica Acta (BBA)-Enzymology.* 1979; 567(1): 1-11.

173. Lozano P, Diego T, Iborra JL. Dynamic structure/function relationships in the α-Chymotrypsin deactivation process by heat and pH. *European Journal of Biochemistry.* 1997; 248(1): 80-85.

174. Mohapatra SC, Hsu JT. Immobilization of α-chymotrypsin for use in batch and continuous reactors. *Journal of Chemical Technology and Biotechnology.* 2000; 75(7): 519-525.

175. Ortega N, Perez-Mateos M, Pilar MC, Busto MD. Neutrase immobilization on alginate− glutaraldehyde beads by covalent attachment. *J Agric Food Chem.* 2008; 57(1): 109-115.

176. Iyer PV, Ananthanarayan L. Enzyme stability and stabilization—Aqueous and non-aqueous environment. *Process Biochemistry.* 2008 10; 43(10): 1019-1032.

177. Misson M, Dai S, Jin B, Chen BH, Zhang H. Manipulation of nanofiber-based β-galactosidase nanoenvironment for enhancement of galacto-oligosaccharide production. *J Biotechnol.* 2016 3/20; 222: 56-64.

178. Lopez-Rubio A, Gavara R, Lagaron JM. Bioactive packaging: Turning foods into healthier foods through biomaterials. *Trends Food Sci Technol.* 2006 10; 17(10): 567-575.

179. Pinheiro AC, Bourbon AI, Cerqueira MA, Maricato É, Nunes C, Coimbra MA, Vicente AA. Chitosan/fucoidan multilayer nanocapsules as a vehicle for controlled release of bioactive compounds. *Carbohydr Polym.* 2015 1/22; 115(0): 1-9.

180. Kost J, Langer R. Responsive polymeric delivery systems. *Adv Drug Deliv Rev.* 2012; 64: 327-341.

181. Angelopoulou A, Efthimiadou EK, Boukos N, Kordas G. A new approach for the one-step synthesis of bioactive PS vs. PMMA silica hybrid microspheres as potential drug delivery systems. *Colloids and Surfaces B: Biointerfaces.* 2014 5/1; 117(0): 322-329.

182. Gill I, Ballesteros A. Bioencapsulation within synthetic polymers (part 1): Sol–gel encapsulated biologicals. *Trends Biotechnol.* 2000; 18(7): 282-296.

183. Tiourina OP, Sukhorukov GB. Multilayer alginate/protamine microsized capsules: Encapsulation of α-chymotrypsin and controlled release study. *Int J Pharm.* 2002; 242(1): 155-161.

184. Agarwal S, Wendorff JH, Greiner A. Chemistry on electrospun polymeric nanofibers: Merely routine chemistry or a real challenge? *Macromolecular rapid communications.* 2010; 31(15): 1317-1331.

185. Kriegel C, Arrechi A, Kit K, McClements D, Weiss J. Fabrication, functionalization, and application of electrospun biopolymer nanofibers. *Crit Rev Food Sci Nutr.* 2008; 48(8): 775-797.

186. Miao Y, Zhu H, Chen D, Wang R, Tjiu WW, Liu T. Electrospun fibers of layered double hydroxide/biopolymer nanocomposites as effective drug delivery systems. *Mater Chem Phys.* 2012.

187. Meinel AJ, Germershaus O, Luhmann T, Merkle HP, Meinel L. Electrospun matrices for localized drug delivery: Current technologies and selected biomedical applications. *European Journal of Pharmaceutics and Biopharmaceutics.* 2012 5; 81(1): 1-13.

188. Hu J, Wei J, Liu W, Chen Y. Preparation and characterization of electrospun PLGA/gelatin nanofibers as a drug delivery system by emulsion electrospinning. *Journal of Biomaterials Science, Polymer Edition.* 2013; 24(8): 972-985.

189. Jiang H, Wang L, Zhu K. Coaxial electrospinning for encapsulation and controlled release of fragile water-soluble bioactive agents. *J Controlled Release.* 2014 11/10; 193(0): 296-303.

190. Huang Z, Zhang YZ, Ramakrishna S, Lim CT. Electrospinning and mechanical characterization of gelatin nanofibers. *Polymer.* 2004 7/12; 45(15): 5361-5368.

191. Li X, Zhang H, Li H, Yuan X. Encapsulation of proteinase K in PELA ultrafine fibers by emulsion electrospinning: Preparation and in vitro evaluation. *Colloid Polym Sci.* 2010; 288(10-11): 1113-1119.

192. Dai Y, Niu J, Liu J, Yin L, Xu J. In situ encapsulation of laccase in microfibers by emulsion electrospinning: Preparation, characterization, and application. *Bioresour Technol.* 2010 12; 101(23): 8942-8947.

193. Pinto SC, Rodrigues AR, Saraiva JA, Lopes-da-Silva JA. Catalytic activity of trypsin entrapped in electrospun poly (ϵ-caprolactone) nanofibers. *Enzyme Microb Technol.* 2015; 79: 8-18.

194. Food and Drug Administration. Code of federal regulations (CFR) 21.

195. Mohd Zain NA, Mohd Suardi S, Idris A. Hydrolysis of liquid pineapple waste by invertase immobilized in PVA–alginate matrix. *Biochem Eng J.* 2010 7/15; 50(3): 83-89.

196. Basturk E, Demir S, Danis O, Kahraman M. Covalent immobilization of a-amylase onto thermally crosslinked electrospun PVA/PAA nanofibrous hybrid membranes. *J Appl Polym Sci.* 2013; 127(1): 349-355.

197. Zhang Y, Venugopal J, Huang Z, Lim C, Ramakrishna S. Characterization of the surface biocompatibility of the electrospun PCL-collagen nanofibers using fibroblasts. *Biomacromolecules.* 2005; 6(5): 2583-2589.

198. Song, Jie Song, Derya Kahveci, Menglin Chen, Zheng Guo, Erqing Xie, Xuebing Xu, Flemming Besenbacher,Mingdong Dong. Enhanced catalytic activity of lipase encapsulated in PCL nanofibers. *Langmuir.* 2012; 28(14): 6157-6162.

199. Rhim J, Park H, Ha C. Bio-nanocomposites for food packaging applications. *Progress in Polymer Science.* 2013 0; 38(10–11): 1629-1652.

200. Yang D, Li Y, Nie J. Preparation of gelatin/PVA nanofibers and their potential application in controlled release of drugs. *Carbohydr Polym.* 2007 6/25; 69(3): 538-543.

201. Yang Y, Li X, Qi M, Zhou S, Weng J. Release pattern and structural integrity of lysozyme encapsulated in core–sheath structured poly(dl-lactide) ultrafine fibers prepared by emulsion electrospinning. *European Journal of Pharmaceutics and Biopharmaceutics.* 2008 5; 69(1): 106-116.

202. Huang J, You T. Advances in nanofibers, ed., R. maguire. *InTech, Croatia.* 2013: 35-83.

203. Boyd J, Parkinson C, Sherman P. Factors affecting emulsion stability, and the HLB concept. *J Colloid Interface Sci.* 1972; 41(2): 359-370.

204. Bouchemal K, Briançon S, Perrier E, Fessi H. Nano-emulsion formulation using spontaneous emulsification: Solvent, oil and surfactant optimisation. *Int J Pharm.* 2004; 280(1): 241-251.

205. Liu W, Sun D, Li C, Liu Q, Xu J. Formation and stability of paraffin oil-in-water nano-emulsions prepared by the emulsion inversion point method. *J Colloid Interface Sci.* 2006; 303(2): 557-563.

206. Porras M, Solans C, Gonzalez C, Gutiérrez J. Properties of water-in-oil (W/O) nano-emulsions prepared by a low-energy emulsification method. *Colloids Surf Physicochem Eng Aspects.* 2008; 324(1): 181-188.

207. Sah H, Toddywala R, Chien Y. Biodegradable microcapsules prepared by aw/o/w technique: Effects of shear force to make a primary w/o emulsion on their morphology and protein release. *J Microencapsul.* 1995; 12(1): 59-69.

208. Sinha V, Bansal K, Kaushik R, Kumria R, Trehan A. Poly-ϵ-caprolactone microspheres and nanospheres: An overview. *Int J Pharm.* 2004; 278(1): 1-23.

209. McLaren A, Estermann EF. Influence of pH on the activity of chymotrypsin at a solid-liquid interface. *Arch Biochem Biophys.* 1957; 68(1): 157-160.

210. Son WK, Youk JH, Lee TS, Park WH. Effect of pH on electrospinning of poly (vinyl alcohol). *Mater Lett.* 2005; 59(12): 1571-1575.

211. Jansen EF, Tomimatsu Y, Olson AC. Cross-linking of α-chymotrypsin and other proteins by reaction with glutaraldehyde. *Arch Biochem Biophys.* 1971; 144(1): 394-400.

212. Beauchamp RO, St Clair, Mary Beth G, Fennell TR, Clarke DO, Morgan KT, Karl FW. A critical review of the toxicology of glutaraldehyde. *CRC Crit Rev Toxicol.* 1992; 22(3-4): 143-174.

213. Girardot JM, Girardot MN. Amide cross-linking: An alternative to glutaraldehyde fixation. *J Heart Valve Dis.* 1996 Sep; 5(5): 518-525.

214. Pal A, Khanum F. Covalent immobilization of xylanase on glutaraldehyde activated alginate beads using response surface methodology: Characterization of immobilized enzyme. *Process Biochemistry.* 2011; 46(6): 1315-1322.

215. Chapman K, Lawless H, Boor K. Quantitative descriptive analysis and principal component analysis for sensory characterization of ultrapasteurized milk. *J Dairy Sci.* 2001; 84(1): 12-20.

216. Albayrak N. Production of galacto-oligosaccharides from lactose by aspergillus oryzae β-galactosidase immobilized on cotton cloth. *Biotechnol Bioeng.* 2001; 77(1): 8.

217. Freitas F, Ribeiro G, Brandao G, Cardoso V. A comparison of the kinetic properties of free and immobilized aspergillus oryzae beta-galactosidase. *Biochem Eng J.* 2011; 58-59: 33-38.

218. Husain Q. B galactosidases and their potential applications: A review. *Crit Rev Biotechnol.* 2010; 30(1): 41-62.

219. Vermeiren L, Devlieghere F, Van Beest M, De Kruijf N, Debevere J. Developments in the active packaging of foods. *Trends Food Sci Technol.* 1999; 10(3): 77-86.

220. Martin NH, Carey NR, Murphy SC, Wiedmann M, Boor KJ. A decade of improvement: New york state fluid milk quality. *J Dairy Sci.* 2012; 95(12): 7384-90.

221. Hansen AP, Arora DK. Loss of flavor compounds from aseptically processed food-products packaged in aseptic containers. *ACS Symp Ser.* 1990; 423: 318-332.

222. AOAC International.,. Official methods of analysis of AOAC international. *Official methods of analysis of AOAC International.* 2002.

223. Bier M. **[106] Lipases**: RCOOR′+ H2O→ RCOOH+ R′ OH. *Meth Enzymol.* 1955; 1: 627-642.

224. United States. Public Health Service., United States. Food and Drug Administration., United States. Department of Health and Human Services. Food and Drug Administration. Grade "A" pasteurized milk ordinance. [Washington, D.C.]: U.S. Dept. of Health and Human Services, Public Health Service, Food and Drug Administration; 2011.

225. Santos MV, Ma Y, Caplan Z, Barbano DM. Sensory threshold of off-flavors caused by proteolysis and lipolysis in milk. *J Dairy Sci.* 2003; 86(5): 1601-7.

226. Ma Y, Santos M, Barbano DM. Effect of CO2 addition to raw milk on proteolysis and lipolysis at 4 degrees C. *J Dairy Sci.* 2003; 86(5): 1616-31.

227. López-Gallego F, Betancor L, Mateo C, Hidalgo A, Alonso-Morales N, Dellamora-Ortiz G, Guisán JM, Fernández-Lafuente R. Enzyme stabilization by glutaraldehyde crosslinking of adsorbed proteins on aminated supports. *J Biotechnol.* 2005 9/22; 119(1): 70-75.

228. Betancor L, López-Gallego F, Hidalgo A, Alonso-Morales N, Mateo GDC, Fernández-Lafuente R, Guisán JM. Different mechanisms of protein immobilization on glutaraldehyde activated supports: Effect of support activation and immobilization conditions. *Enzyme Microb Technol.* 2006 8/2; 39(4): 877-882.

229. Barbosa O, Ortiz C, Berenguer-Murcia Á, Torres R, Rodrigues RC, Fernandez-Lafuente R. Glutaraldehyde in bio-catalysts design: A useful crosslinker and a versatile tool in enzyme immobilization. *RSC Advances.* 2014; 4(4): 1583-1600.

230. Sano LL, Krueger AM, Landrum PF. Chronic toxicity of glutaraldehyde: Differential sensitivity of three freshwater organisms. *Aquatic toxicology.* 2005; 71(3): 283-296.

231. Takigawa T, Endo Y. Effects of glutaraldehyde exposure on human health. *Journal of occupational health.* 2006; 48(2): 75-87.

232. Allen HJ, Impellitteri CA, Macke DA, Heckman JL, Poynton HC, Lazorchak JM, Govindaswamy S, Roose DL, Nadagouda MN. Effects from filtration, capping agents, and presence/absence of food on the toxicity of silver nanoparticles to daphnia magna. *Environmental Toxicology and Chemistry.* 2010; 29(12): 2742-2750.

233. Johnson DR, Decker EA. The role of oxygen in lipid oxidation reactions: A review. *Annual review of food science and technology.* 2015; 6: 171-190.

234. Cichello SA. Oxygen absorbers in food preservation: A review. *Journal of food science and technology.* 2015; 52(4): 1889-1895.

235. Johnson MJ. Aerobic microbial growth at low oxygen concentrations. *J Bacteriol.* 1967 Jul; 94(1): 101-108. PMCID: PMC251877.

236. Molz FJ, Widdowson M, Benefield L. Simulation of microbial growth dynamics coupled to nutrient and oxygen transport in porous media. *Water Resour Res.* 1986; 22(8): 1207-1216.

237. Stratford M. Food and beverage spoilage yeasts. In: Yeasts in food and beverages. Springer; 2006. p. 335-379.

238. Robertson G, Samaniego C. Effect of initial dissolved oxygen levels on the degradation of ascorbic acid and the browning of lemon juice during storage. *J Food Sci.* 1986; 51(1): 184-187.

239. Burdurlu HS, Koca N, Karadeniz F. Degradation of vitamin C in citrus juice concentrates during storage. *J Food Eng.* 2006; 74(2): 211-216.

240. Damaj Z, Joly C, Guillon E. Toward new polymeric oxygen scavenging systems: Formation of poly (vinyl alcohol) oxygen scavenger film. *Packaging Technology and Science.* 2015; 28(4): 293-302.

241. Teumac FN. The history of oxygen scavenger bottle closures. In: Active Food Packaging. Springer; 1995. p. 193-202.

242. Kuchel L, Brody AL, Wicker L. Oxygen and its reactions in beer. *Packaging Technology and Science.* 2006; 19(1): 25-32.

243. Del Nobile MA, Conte A. New packaging for food beverage applications. In: Packaging for Food Preservation. Springer; 2013. p. 111-122.

244. Crown: Brand-building packaging [homepage on the Internet]. . Available from: http://www.crowncork.com/.

245. Kuswandi B, Wicaksono Y, Abdullah A, Heng LY, Ahmad M. Smart packaging: Sensors for monitoring of food quality and safety. *Sensing and Instrumentation for Food Quality and Safety.* 2011; 5(3-4): 137-146.

246. Realini CE, Marcos B. Active and intelligent packaging systems for a modern society. *Meat Sci.* 2014; 98(3): 404-419.

247. Multisorb techcnologies: Food and beverage oxygen absorbers [homepage on the Internet]. . Available from: http://www.multisorb.com/products-and-systems/food-and-beverage-products-and-systems/oxygen-absorbers/.

248. Mitsubishi gas chemical america [homepage on the Internet]. . Available from: http://ageless.mgc-a.com/.

249. Nanobiomatters [homepage on the Internet]. . Available from: http://www.nanobiomatters.com/wordpress/products/o2block%C2%AE-oxygen-scavengers.

250. Labuza T. Oxygen scavenger sachets. *Food Research.* 1987; 32: 276-277.

251. Cichello SA. Oxygen absorbers in food preservation: A review. *Journal of food science and technology.* 2015; 52(4): 1889-1895.

252. Winestrand S, Johansson K, Järnström L, Jönsson LJ. Co-immobilization of oxalate oxidase and catalase in films for scavenging of oxygen or oxalic acid. *Biochem Eng J.* 2013; 72: 96-101.

253. Ihalainen P, Hämäläinen T, Matilainen K, Savolainen A, Sipiläinen-Malm T, Kaukoniemi O, Määttänen A, Erho T, Smolander M, Peltonen J. Incorporation of laccase into surface-sized paper. *Journal of Coatings Technology and Research.* 2015; 12(2): 365-373.

254. Meyer JD, Manning MC. Hydrophobic ion pairing: Altering the solubility properties of biomolecules. *Pharm Res.* 1998; 15(2): 188-193.

255. Powers ME, Matsuura J, Brassell J, Manning MC, Shefter E. Enhanced solubility of proteins and peptides in nonpolar solvents through hydrophobic ion pairing. *Biopolymers.* 1993; 33(6): 927-932.

256. Grunert KG, Bech-Larsen T, Bredahl L. Three issues in consumer quality perception and acceptance of dairy products. *Int Dairy J.* 2000; 10(8): 575-584.

257. Drake M. Invited review: Sensory analysis of dairy foods. *J Dairy Sci.* 2007; 90(11): 4925-4937.

258. Ucar I, Doganci M, Cansoy C, Erbil H, Avramova I, Suzer S. Combined XPS and contact angle studies of ethylene vinyl acetate and polyvinyl acetate blends. *Appl Surf Sci.* 2011; 257(22): 9587-9594.

259. Doganci M, Cansoy C, Ucar I, Erbil H, Mielczarski E, Mielczarski J. Combined XPS and contact angle studies of flat and rough ethylene-vinyl acetate copolymer films. *J Appl Polym Sci.* 2012; 124(3): 2100-2109.

260. Cushen M, Kerry J, Morris M, Cruz-Romero M, Cummins E. Nanotechnologies in the food industry – recent developments, risks and regulation. *Trends Food Sci Technol.* 2012 3; 24(1): 30-46.

261. Chapman K, Boor K. Acceptance of 2% ultra-pasteurized milk by consumers, 6 to 11 years old. *J Dairy Sci.* 2001; 84(4): 951-954.

262. Clark S, Costello M, Bodyfelt FFW, Drake M. The sensory evaluation of dairy products. Springer; 2009.

263. Croissant AE, Washburn S, Dean L, Drake M. Chemical properties and consumer perception of fluid milk from conventional and pasture-based production systems. *J Dairy Sci.* 2007; 90(11): 4942-4953.